

THE SURFACE GEOCHEMISTRY
OF THE TLETLETSI AREA,
SOUTHEASTERN BOTSWANA

by

Victor Sibiya
Department of Earth Sciences

Submitted in partial fulfillment of the requirement
for the degree of Master of Science

Faculty of Graduate Studies
University of Manitoba
Winnipeg, Manitoba

August, 1982

THE SURFACE GEOCHEMISTRY
OF THE TLETLETSI AREA,
SOUTHEASTERN BOTSWANA

BY

VICTOR SIBIYA

A thesis submitted to the Faculty of Graduate Studies of
the University of Manitoba in partial fulfillment of the requirements
of the degree of

MASTER OF SCIENCE

© 1982

Permission has been granted to the LIBRARY OF THE UNIVERSITY OF MANITOBA to lend or sell copies of this thesis, to the NATIONAL LIBRARY OF CANADA to microfilm this thesis and to lend or sell copies of the film, and UNIVERSITY MICROFILMS to publish an abstract of this thesis.

The author reserves other publication rights, and neither the thesis nor extensive extracts from it may be printed or otherwise reproduced without the author's written permission.

ABSTRACT

The nature of soils and the downprofile distributions of Fe, Mn, Zn, Co, Ni, Pb and Cu within fifteen profiles occurring in the Tletletsi Area (southeastern Botswana) were investigated by sampling at 15 cm intervals within pits.

The underlying geology consists mainly of Precambrian granites, diabbases and redbeds, all of which are intensely faulted and fractured.

The region is characterized by strong seasonal contrasts of the subtropical subhumid climate. Summers are hot and temperatures are typically above 30°C. Winter temperatures are normally a few degrees celsius. The rainfall is irregular but is confined to the months of October to April.

Shallow and incomplete weathering has resulted in a thin veneer (less than 2.5 m) of overburden which is divisible into residual and transported soils. The residual soils are shallower and are developed on higher ground in contrast to the transported soils. The soils reflect the bedrock geochemistry mineralogically, texturally and chemically.

The geochemical response of Fe, Mn, Zn, Co, Ni, Pb and Cu within the soil profiles depend mainly on the nature of the soil. Transported soils tend to have lower trace element contents, ranges and more alkaline pH values compared to residual soils developed on the same rock type. The residual soils commonly show trace element enrichment in specific subhorizons and have generally higher metal contents and ranges and acid pH values.

Correlations of Zn, Co, Ni, Pb, Cu with Fe and Mn taken at $f = 0.10$ suggest that the secondary dispersion patterns of the trace elements are

determined to a significant extent by the absorptive effects of Fe and Mn compounds within the soils.

An R-mode factor analysis was performed on stream sediment data of the Tletletsi Area and the adjoining Gaborone Area (Marengwa, 1978) using Sn, Ti, V, Mn and Cr. The association V-Mn-Cr is taken to also indicate Mn absorption within the sediments.

TABLE OF CONTENTS

	<u>PAGE</u>
ABSTRACT	i
LIST OF TABLES	viii
LIST OF FIGURES	x
ACKNOWLEDGEMENTS	xii

CHAPTER I

INTRODUCTION

Purpose of Study	1
Location and Access	1
Climate	1
Occupation and Industrial Base	3
Previous Prospecting Work	3
Present Study	4

CHAPTER II

GEOLOGY

Regional Geology	5
Geology of the Tletletsi Area	5
The Transvaal System	7
Basal Conglomerates	8
Black Reef Quartzite	8
Dolomite and Chert	8
Chert Breccia	8
Structural Features	9

	<u>PAGE</u>
The Gaborone Granite	9
Kanye Felsites	11
Ntlhantlhe Granite	12
Kgale Granite	12
Thamaga Granite	13
Evolution and Age of the Gaborone Granite	13
The Waterberg System	14
The Younger Intrusions of the Tletletsisi Area	14
Moshaneng Intrusion	15
Diabases of the Moshaneng Intrusion	15
Syenites, Granodiorites	16
Other Intrusive Rocks	17
Genetic Relationships	17
Structural Geology	18
The Geomorphic-Geochemical Environment	18

CHAPTER III

METHODS OF STUDY

Field Methods	20
Site Selection	20
Sampling Methods	20
Laboratory Methods	21
Sample Preparation and Examination	21
Reagents Used	22
Trial Extractions	22
Final Extraction	24

	<u>PAGE</u>
Partial (hot) Leach (Px)	24
Total Digestion (Tx)	26
Precision and Batch Control	26

CHAPTER IV

DATA TREATMENT

Colloidal Activity and Determination by Correlation Analysis	35
Stream Data	37

CHAPTER V

SOIL PROFILE DESCRIPTIONS

Physical and Chemical Properties of Pit 14	42
Physical and Chemical Properties of Pit 15	47
Physical and Chemical Properties of Pit 18	53
Physical and Chemical Properties of Pit 12	58
Physical and Chemical Properties of Pit 11	63
Physical and Chemical Properties of Pit 9	68
Physical and Chemical Properties of Pit 19	73
Physical and Chemical Properties of Pit 8	77
Physical and Chemical Properties of Pit 7	82
Physical and Chemical Properties of Pit 6	87
Physical and Chemical Properties of Pit 5	92
Physical and Chemical Properties of Pit 3	95
Physical and Chemical Properties of Pit 2	99
Physical and Chemical Properties of Pit 1	104
Physical and Chemical Properties of Pit 13	109

CHAPTER VI

RESULTS AND DISCUSSION

Development of Soil Profiles	114
Residual Soils	114
Transported Soils	117
Chemical Results of Soil Sample Analysis	119
Significance of the Extraction Ratio	119
Geochemical Dispersion Within the Soil Profiles	121
Iron Dispersion	123
Manganese Dispersion	125
Other Trace Element Correlations	129
Zinc Correlations	129
Cobalt Correlations	129
Nickel Correlations	131
Lead Correlations	131
Copper Correlations	131
Chromium Correlations	131
The Effects of Carbonate in the Soils	131
Control of the trace element dispersion by Fe and Mn compounds	134
Stream Sediment Data Examination	137
Factor Analysis Results	138
Factor 1V (Cr-V)	143
Factor 2V, 2Q (Ti-Mn)	143
Factor 3V, 1Q (Mn-V, V-Mn-Cr)	147
Factor 3Q (Sn)	147

PAGE

CHAPTER VII

CONCLUSIONS	150
REFERENCES	154
APPENDIX: Analytical Results of Soil Sample Analyses	158

LIST OF TABLES

<u>TABLE</u>		<u>PAGE</u>
1(a)	Trial Extraction Procedure	23
1(b)	Final Extraction Procedure Partial Leaching (Px)	27
1(c)	Final Extraction Procedure Total Leaching (Tx)	28
2(a-d)	Reproducibility Control for Mn, Zn, Cu and Co	29,30,31,32
2(e)	Batch Control	34
3	Soil Profile Description Pit 14	43
4	Correlation Coefficients Pit 14	45
5	Soil Profile Description Pit 15	48
6	Correlation Coefficients Pit 15	50
7	Soil Profile Description Pit 18	54
8	Correlation Coefficients Pit 18	56
9	Soil Profile Description Pit 12	59
10	Correlation Coefficients Pit 12	61
11	Soil Profile Description Pit 11	64
12	Correlation Coefficients Pit 11	66
13	Soil Profile Description Pit 9	69
14	Correlation Coefficients Pit 9	71
15	Soil Profile Description Pit 19	74
16	Soil Profile Description Pit 8	78
17	Correlation Coefficients Pit 8	80
18	Soil Profile Description Pit 7	83

<u>TABLE</u>		<u>PAGE</u>
19	Correlation Coefficients Pit 7	85
20	Soil Profile Description Pit 6	88
21	Correlation Coefficients Pit 6	90
22	Soil Profile Description Pit 5	93
23	Soil Profile Description Pit 3	96
24	Soil Profile Description Pit 2	100
25	Correlation Coefficients Pit 2	102
26	Soil Profile Description Pit 1	105
27	Correlation Coefficients Pit 1	107
28	Soil Profile Description Pit 13	110
29	Correlation Coefficients Pit 13	112
30	Statistical Parameters of Extraction Ratios	120
31	Carbonate Solubility Products for Fe, Mn, Zn, Co, Ni, Pb and Cr	133
32	V, Cr and Ti Contents of Some Magnetites from Pits 15, 18, 12, 7, 13 and 2	139
33	Factor Analysis Results: Tletletsi Area Subpopulation	140
34	Factor Analysis Results: Gaborone Area Subpopulation	141
35	Element Associations and Statistical Parameters of Factors Scores for the Tletletsi Area Subpopulation	142
36	Comparative Affinities of Zn, Co, Ni, Pb and Cu for Fe and Mn	152

LIST OF FIGURES

<u>FIGURE</u>		<u>PAGE</u>
1	Geology of Southeastern Notwani	2
2	Geology of the Tletletsi Area	6
3	Structural Geology of the Tletletsi Area	10
4	Trial Extractions of Random Samples	25
5(a)	Generalized Soil Profile Characteristics Showing the Principal Subhorizons Typical of Residual Soil Profile in the Tletletsi Area	40
5(b)	Drainage Pattern and Soil Type Distribution in the Tletletsi Area	41
6	Downprofile Trace Element Distribution Pit 14	44
7	Downprofile Trace Element Distribution Pit 15	49
8	Downprofile Trace Element Distribution Pit 18	55
9	Downprofile Trace Element Distribution Pit 12	66
10	Downprofile Trace Element Distribution Pit 11	65
11	Downprofile Trace Element Distribution Pit 9	70
12	Downprofile Trace Element Distribution Pit 19	75
13	Downprofile Trace Element Distribution Pit 8	79
14	Downprofile Trace Element Distribution Pit 7	84
15	Downprofile Trace Element Distribution Pit 6	89
16	Downprofile Trace Element Distribution Pit 5	94
17	Downprofile Trace Element Distribution Pit 3	91
18	Downprofile Trace Element Distribution Pit 2	101
19	Downprofile Trace Element Distribution Pit 1	106
20	Downprofile Trace Element Distribution Pit 13	111
21	Ranges of Trace Element Contents in Profiles	122

<u>FIGURE</u>		<u>PAGE</u>
22	Stability Relationships of Fe, Mn Compounds	124
23	Correlations of Fe:Mn for all Pits and (Fe:Mn)Cr for Pits 1 and 2	128
24	Correlations of (Fe,Mn):Zn, Co, Ni, Pb and Cu	130
25	Stability Relationships of Co, Ni, Pb Carbonates	135
26	Factor Loadings of Stream Sediment Data	144
27	Distribution of Factor IV	145
28	Distribution of Factors 2V, 2Q	146
29	Distribution of Factors 3V, 1Q	148
30	Distribution of Factor 3Q	149

ACKNOWLEDGEMENTS

I acknowledge my deep gratitude to my supervisor Professor G.S. Clark for help and guidance during this study. I also thank Professors B. Last and J.B. Westmore for critically reading this thesis and offering many useful suggestions for its improvement.

I gratefully acknowledge CIDA for the major funding of this work. Partial funding was obtained from the Department of Geology, University College of Botswana, Department of Earth Sciences, University of Manitoba and a National Science and Engineering Research Council grant to Professor G. Clark (A3831).

Thanks are also due to the Geological Survey of Botswana for supplying useful reference material for this study, Dr. Desmond Walton for assisting in the computer data processing and Mr. K. Ramlal for offering instruction in the use of the atomic absorption spectrophotometers.

Debbie Kernaghan and Ron Pryhitko did the drafting and Irene Berta assisted with the rock thin sections. The University of Manitoba "On Campus" typing/copy centre did the typing and reproductions.

Finally I wish to thank Professors J. Cooke and B.J. Vink for their assistance during the early stages of this study.

CHAPTER I

INTRODUCTION

Purpose of Study

The purpose of this study is to investigate the geochemical behaviour of selected trace elements (Fe, Mn, Zn, Co, Ni, Pb and Cu) in the soils of the Tletletsi Area. The idea for such a study was conceived after it had become clear that past soil and stream sediment sampling schemes (Van Straaten, 1952; Laughton, 1964 and Marengwa, 1978) had been undertaken without a basis of geochemical orientation survey type data.

Location and Access

The Tletletsi Area lies north of Kanye (Figure 1) and covers an area of approximately 1,080 km². It is enclosed by longitude 25° 10' to 25° 30' E and latitude 25° 10' to 24° 20' S. It is an easily accessible area and has a network of paths and tracks that link up the small isolated settlements. A tarmac passes through the southern end and joins Kanye with the diamond mining town of Jwaneng. This is a relatively new road and is not shown on most existing maps. Gravel roads exist between the major settlements of Thamaga, Moshupa, Kanye, Ranaka and Mashaneng. The roads are usable during both rainy and dry seasons.

Generally, access to any site by suitable vehicle or foot is possible owing to the moderate topography and thin thorn bush vegetation.

Climate

The climate of southeastern Botswana is subhumid, subtropical. The summers are hot and temperatures are normally above 30°C during the

Figure 1. Southeastern Notwani River
Geology

daytime. Winters are cold and the temperatures normally average a few degrees celsius. Extremes of temperatures (over 40°C in summer and below 0°C) are occasional.

The rainfall is confined to the months of October to April and amounts to 50 cm annually. It is irregular and dry spells are not uncommon.

Compared to the rest of southeastern Botswana, the Tletletsi Area is moderately populated. Major settlements are Moshaneng, Thamaga, Moshupa and Ranaka. These jointly constitute a population of a few thousand. Isolated concentrations such as Kubung and Lotlhakane are made up of a few hundred people. One-family settlements are scattered throughout the area. Kanye, which lies southeast of the map area, has a population of 33,000.

Occupation and Industrial Base

The occupation of the majority of the population is livestock and land farming. Much of the land is used for cultivation and livestock grazing. Asbestos mining in Moshaneng employs a small work force and production has been sporadic owing to unstable markets.

Government employs a small number of people mainly for educational, medical, agricultural and rural area development programs.

Previous Prospecting Work

Marengwa (1978) has given a brief history of prospecting in southeastern Botswana:

Little prospecting has been carried out in the area of the Gaborone Granite. Almond (1925) gave the first account of prospecting activities in the area. A limited amount of prospecting, mainly for fluorspar and partly for lead, has taken place in the Ditshukutswane area near Mayana, some 40 km west of Ramotswa. In 1952, C.J. Van Straaten and G.T. Lamont made a preliminary survey of the area (Van Straaten, 1952) and

C. Boocock subsequently also surveyed the mineralized area and prepared a map (unpublished) at a scale 1":100'. No further work was done until 1963 when Laughton (1964) carried out a geochemical prospecting program over an area in which the Ditshukutswane fluorspar deposit lies. In 1963, Marlime Chrysotile Asbestos Corporation were given a crown grant to prospect for fluorspar in an area approximately 113 square miles in the Bangwaketse Tribal Territory. After disappointing drill results in the mineralized veins, the company ceased work.

A geochemical study of stream sediments derived from the Gaborone Granite, Kanye Metavolcanics and adjacent rocks was carried out by Marengwa between October 1974 and January 1975. The study involved twenty trace element determinations. Cr, Co, Cu, Pb, Mn, Ni, Sn, and V were detected in sufficient quantities to warrant statistical analysis. Marengwa (1978) identified moderate anomalies of Cr, Co, Cu, Mn and V and higher anomalies for Pb, Ni, Sn and Zn. He recommended that future investigations in the area should aim at a more detailed study of the areas where anomalous values of any of the trace elements occurred but that priority should be given to areas with higher anomalies of Pb, Sn and Zn.

Amax Botswana Ltd. has carried out a follow-up survey for tin based on the work of Marengwa, but the results were disappointing.

Present Study

The main purpose of this work is to evaluate the Tletletsi Area soils as an exploration medium. The study focuses on geochemical dispersions within several soil profiles.

The existing geological map (Crockett, 1972) has been upgraded and the stream sediment data has been re-analyzed and interpreted in the light of results drawn from the dispersions within the profiles.

CHAPTER II

GEOLOGY

Regional Geology

An updated account of the geology of southeastern Botswana is given by Key (1979).

The oldest rocks belong to the Basement Complex and consist of granitoid gneisses, amphibolites and mafic schists. They are overlain by the Ventersdorp Volcanic Group which consist of tuffs, agglomerates and breccias.

Overlying the Ventersdorp Volcanic Group is the Transvaal System. It comprises quartzites, dolomites, cherts and chert breccias. The Gaborone Granite Complex is intruded into the Ventersdorp and Transvaal rocks and its presently accepted age is 2300 Ma (key, 1979). The youngest sediments are the redbeds of the Waterberg System. They comprise conglomerates, sandstones, siltstones and claystones. Several intrusions of pre- and post-Waterberg age occur throughout southeastern Botswana. They consist of granites, syenites and diabases.

Mallick and Habgood (1978) have compiled a composite map of several quarter degree sheets. Their map is based on satellite imagery and areal photography. It is an excellent overview of the structural framework of southeastern Botswana. Part of the map is reproduced in Figure 1.

Geology of the Tletletsi Area

The Tletletsi Area is underlain by sedimentary and igneous rocks of early to mid-Precambrian age (Figure 2). The oldest rocks belong to the Transvaal System and consist of quartzites, conglomerates, cherts,

Figure 2. Geology of the Tletletsi Area.

dolomites and chert breccias. Intrusive into the Transvaal System is the Gaborone Granite Complex. At present, the accepted age of the Gaborone Granite is 2300 Ma (Key, 1979). The youngest sedimentary rocks are redbeds of the Waterberg System and comprise conglomerates and sandstones with subordinate shales and clays. Intrusive rocks of post-Gaborone Granite age, referred to in this study as Younger Intrusions, are composed of diabbases, granites, granodiorites and syenites.

Quaternary aeolian sands of the Kalahari mask part of the western area (Figure 2).

The Transvaal System

Rocks of the Transvaal System, consisting of basal conglomerates, dolomites and cherts occupy the southeastern portion of the Tletletsi Area (Figure 2). They overlie the Kanye Felsites and belong to the lower series of the system.

Basal Conglomerates

East of Moshaneng (Figure 2) and elsewhere below the Black Reef Quartzite, the Kanye felsites are overlain by a pebbly conglomerate dominated by black well-rounded and flattened chert pebbles and brecciated vein quartz fragments. The matrix is a black to dark grey silty sandstone. Above this is a green argillaceous quartzite which in turn is overlain by a granule conglomerate with a distinctive greenish-grey matrix. Intercalations of finely laminated silty clay occur in several beds particularly toward the top of the unit.

The older conglomerates are overlain by a coarse heterolithic conglomerate recognized by its felsic clasts, silicified pebbles and brown matrix. The clasts are generally smaller than those of the lowermost conglomerate.

Several green and dark grey sandstone layers are present in this unit. The conglomerate alternates with an orthoconglomerate composed of a white silt matrix and 3-4 mm rounded quartz grains.

Black Reef Quartzite

The Black Reef Quartzite is exposed as a continuous and prominent outcrop broken by faults and younger intrusions (Figure 2). It maintains a uniform thickness of approximately 5 m throughout its outcrop. Three types are recognized: a white to cream coloured quartzite at the top, a grey quartzite, and a greyish green quartzite at the base. The latter contains some black to dark brown chert granules. Primary sedimentary structures such as fine bedding are well marked by small discontinuous wisps of black silt and clay beds.

Dolomite and Chert

Above the Black Reef Quartzite is a poorly exposed green argillaceous dolomite. Toward the top, brown cherty and silty dolomite bands alternate with the green dolomite. These dolomite bands outcrop as steeply dipping and parallel sheet-like beds south of Moshaneng. The uppermost bed is marked by a cherty carbonaceous band.

Chert Breccia

The uppermost member of the Transvaal System within the map area is a brownish yellow to orange chert breccia. The breccia is a distinctive unit and consists of chert fragments up to 5 cm across. Detrital quartz grains are sometimes present. The chert breccia is infiltrated by a ferruginous, silty matrix and occasionally a black, manganiferous matrix. Cavities are commonly lined by recrystallized quartzites. The chert breccia is overlain by Waterberg strata.

Structural Features

The Transvaal rocks of the Tletletsi Area record a series of deformations. The main structural element is the arcuate swing of strike (Figure 3) from a north-south to an east-west trend, a mirror image of the Lobatse to Ramotswa swing (see Notwani River Geology, Mallick and Habgood, 1978). This change of strike is due to the emplacement of the Gaborone Granite during the early Precambrian (2300 Ma). Diabase and syenite intrusions account for the contact metamorphism of the dolomites (Moshaneng Asbestos Mine) and the locally erratic strikes of the area. Faults and fractures can be resolved into different generations starting from early Precambrian to possibly late Precambrian based on the Waterberg rocks.

A detailed stratigraphic examination of the Transvaal System within and west of the Tletletsi Area is necessary in order to define their precise relationship with similar rocks elsewhere. An original continuity with similar rocks east of the Molapo-wa-Bojang Pluton (Figure 1) prior to the intrusion of the Gaborone Granite is possible. This is particularly apparent when the similar structural features on either side of the pluton are considered (see Notwani Geology, Mallick and Habgood, 1978). It is on the basis of these structural similarities that the suggestion by Crockett (1972) of a restricted basin in the Tletletsi Area during the Transvaal times is questioned.

The Gaborone Granite

The Gaborone Granite underlies the main part of the Tletletsi Area. It comprises various distinct phases. The evolution of the granite has been explained by various concepts. The present study agrees in part with the model proposed by Key (1979).

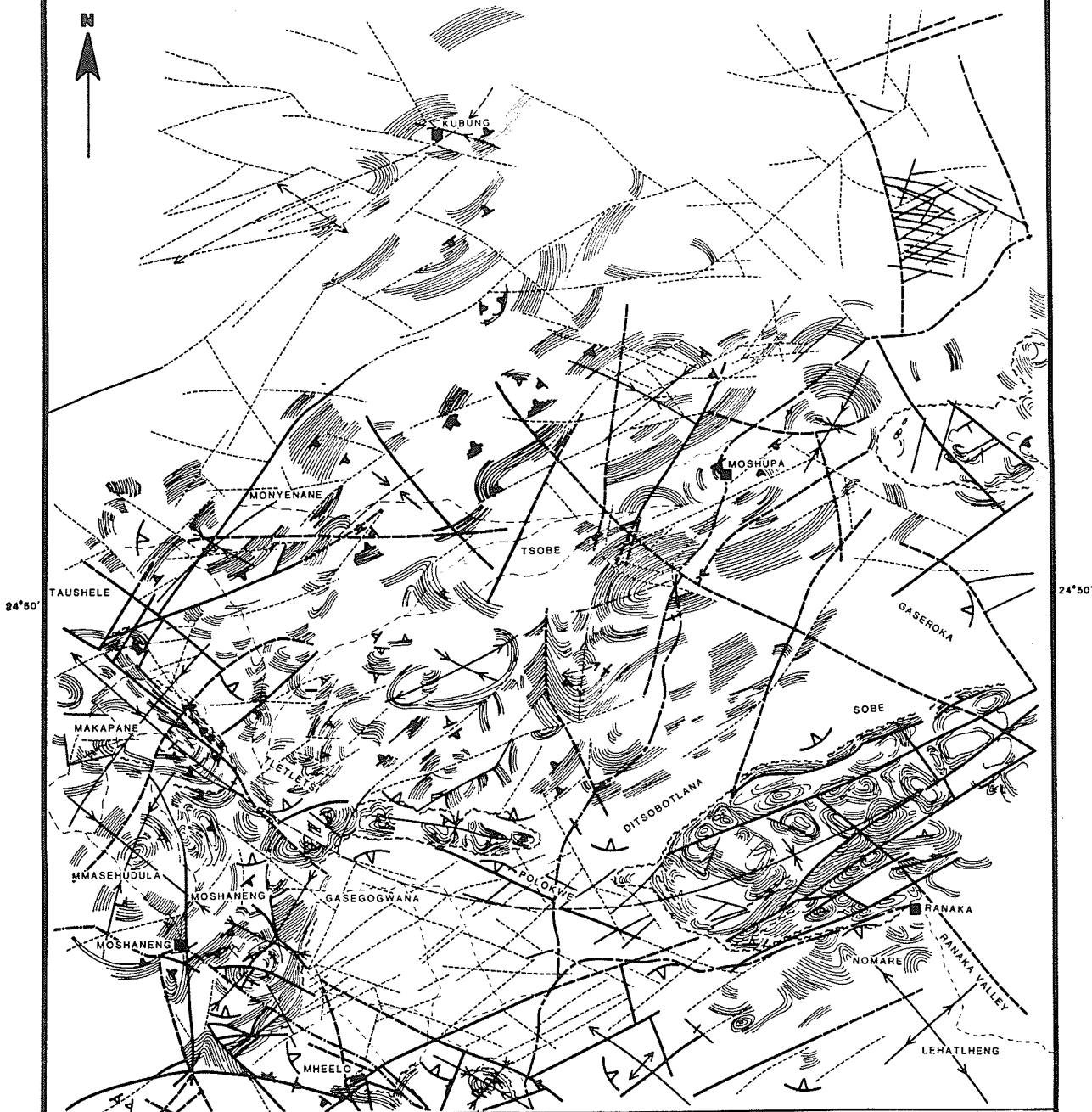
Figure 3. Structural Geology of the Tletletsi Area.

25°10'

25°20'

25°30'

STRUCTURAL GEOLOGY OF THE TLETLETSI AREA



25°10'

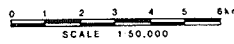
25°20'

25°30'

- STRUCTURAL TREND
- MAJOR FAULTS
- CERTAIN
- INFERRED
- SUBMAJOR LINEAMENTS
- CERTAIN
- INFERRED
- ANTICLINE & PLUNGE DIRECTION
- SYNCLINE & PLUNGE DIRECTION

- UNCONFORMITY
- MEASURED DIP & STRIKE
- VERTICAL DIP & STRIKE
- GENTLE DIP & STRIKE
- MODERATE DIP & STRIKE
- STEEP DIP & STRIKE
- SURFACE SLOPE DIRECTION
- SETTLEMENT
- MINE

- MAIN ROAD
- SECONDARY ROAD
- TRACKS



247400	247500	247600
247500	247500	247500
247600	247600	247600

The four main units as described by Key (1979) are as follows:

- a) Kanye Felsites
- b) Ntlhantlhe Granite - microgranites and granophyres
- c) Kgale Granite - medium-grained granites
- d) Thamaga Granite - coarse rapakivi granite.

The felsites are a chilled carapace of a felsic magma emplaced at a high crustal level. Marginal to the felsites are microgranites and granophyres. These pass into the medium-grained granites, and the core assemblage is represented by the coarse-grained rapakivi granites.

Kanye Felsites

The Kanye Felsites outcrop over a large area south of a line from Tletletsi to Polokwe (Figure 2). North of this line the felsites are exposed from Taushele to Tsobe.

The fresh rocks are blackish purple, very fine grained and contain 2 - 4mm long feldspar, biotite and amphibole phenocrysts. West of Mheelo, the rocks are locally rhyolitic and possess a flow banding which is accentuated by weathering grooves parallel to the flow bands. The felsites fracture along planar or conchoidal surfaces.

The petrographic and chemical properties of the felsites have been described in detail by Wright (in Key, 1979). He noted that close to the Ntlhantlhe Granite, the felsites are reddish in colour.

The upper contact of the felsites outside Tletletsi Area is with rocks of the Lobatse Volcanic Group. East of Moshaneng the felsites are overlain by a discontinuous, north-trending basal conglomerate of the Transvaal System. The lower contact with the Ntlhantlhe Granite is a rapid but sharp transition (Key, 1979) marked by the appearance of the reddish felsites.

Ntlhantlhe Granite

The Ntlhantlhe Granite outcrops over large areas that generally border the Kanye Felsites. It consists of two randomly distributed varieties; a microgranite and a granophyre (Key, 1979).

The microgranite is a brown to brownish-red, homogeneous and evenly grained rock consisting of subhedral feldspar and smoky quartz. Mafic minerals occur as fine lath-like crystals distributed randomly within the rock.

The porphyritic granophyre has a light brownish-purple to reddish-brown groundmass consisting of fine, equigranular feldspar, quartz and hornblende. The phenocrysts are commonly feldspar with grey cores and a pale brown rim which may be separated from the core by a discontinuous mafic rim. Amphibole occurs in definite clots or aggregates. Commonly, amphibole may occur totally inside the feldspar phenocrysts or straddle the phenocryst boundaries and terminate in the groundmass. The porphyritic granophyre is the dominant rock unit of the Ntlhantlhe Granite west of Tletletsi. The contact with the Kgale Granite is transitional and is taken as the point where the groundmass is increased to the phenocryst grain size.

Kgale Granite

The Kgale Granite occurs extensively within the map area (Figure 2) and occupies large areas of the Gaborone Granite Complex. It also outcrops as dikes of different sizes.

The rock is pinkish brown, medium-grained equigranular and occasionally porphyritic. Feldspars are euhedral and quartz is anhedral and variously coloured (blue, colourless and smoky). The blue quartz is the dominant variety and forms the larger grains. Mafic minerals occur interstitially and constitute less than fifteen percent of the rock.

The contact with the Thamaga Granite is variable and depends on the outcrop features of the Kgale Granite. The interface can be gradational or sharp where dike-like outcrops occur.

Thamaga Granite

The Thamaga Granite is the dominant lithology of the Gaborone Granite Complex. It is coarse to very coarse grained with ovoid feldspar phenocrysts having a white core and a grey mantle. Quartz occurs as interstitial and subhedral grains. The mafics consist of amphiboles and recrystallized biotite flakes which may be pseudomorphs of amphibole.

The Thamaga Granite hosts several other granite types which may be similar or dissimilar to the rock types described above. These occur as tongue and dike-like projections within the rapakivi granite.

Lineation within the granite varies in development from faint to very distinct due to the linear arrangement of mafic minerals, notably amphibole. Within the vicinity of Kubung and Thamaga (just outside the map area), the Thamaga Granite contains a number of peculiar enclaves some of which are schistose while others are gneissose. The latter commonly possess an overprint of coarse rapakivi feldspars.

Evolution and Age of the Gaborone Granite

Key (1979) has proposed a model on the evolution of the Gaborone Granite. He concluded that the Gaborone Granite Complex was emplaced along a north-south trending feeder zone (the Molapo-Wa-Bojang Pluton is its southernmost end, Figure 1). In the north the granite spreads laterally to form the Northern Sill, part of which is shown in Figure 1. The north and south margins are structurally controlled by the Molepolole and Moshaneng Lineaments (See Figure 12, Key 1979).

The present study does not agree with his model with regard to emplacement. The structural trends of the regional geology do not appear

to be consistent with Key's model. The Sephatlhaphatla Hills for instance do not seem to be continuous with the Molapo-Wa-Bojang Pluton. The presently accepted age of the Gaborone Granite based on Rb-Sr dating is 2300 Ma (Key, 1979).

The Waterberg System

Red clastic deposits of the Waterberg System occur within the Tletletsisi Area (Figure 2). They consist of conglomerates, sandstones, subordinate siltstones and shales. These rocks are unique and represent the last major depositional event in southeastern Botswana. Erickson and Vos (1979) quote an age of 1800 Ma for the deposition of the Waterberg. Only the lower arenaceous and conglomeratic stratigraphic units are represented in the Tletletsisi Area.

The Waterberg rocks are important in that they record some of the later events postdating and possibly coincident with the late stages of the Gaborone Granite plutonism. They characteristically possess shallow dips and overlie the different units of the Gaborone Granite, the Transvaal System and the Moshaneng Intrusion.

In Makapane (Figure 2, 3), the Waterberg System has been folded into a steep, doubly plunging syncline believed to be partly the result of the emplacement of the Moshaneng Intrusion. Parts of the Waterberg (near Mai Hills) have been metamorphosed during the emplacement of the younger intrusions.

Certain structures described by Crockett (1972) as monoclines are drag features of thrusts as in Sobe and Mheelo.

The Younger Intrusions of the Tletletsisi Area

Intrusions postdating the Gaborone Granite are widespread in the Tletletsisi Area. They exhibit wide compositional and textural differences.

In the Moshaneng Area there is an association of compositionally varied rocks referred to as the Moshaneng Intrusion.

The Younger Intrusions were emplaced as sills, dikes and stocks at shallow depths and at different times.

Moshaneng Intrusion

The Moshaneng Intrusion is described for the purpose of this study as all post-Gaborone Granite intrusions occurring within the Moshaneng-Mmasehudula Area. Crockett (1972) used the term to refer to "a number of small stocks of leucocratic granites and quartz syenites probably of post-Waterberg age".

The present usage recognizes the possible relationship between mafic and felsic rocks.

Diabases of the Moshaneng Intrusion

Diabases constitute the greater part of the Moshaneng Intrusion. They outcrop in various places within the Moshaneng Area as hillocks and flat-lying exposures. Different types have been described on the basis of distinct textural and mineralogic differences.

The oldest diabase is that which outcrops 2.5 km directly south of Mai Hills near the Moshana River. It occurs in small 1 - 3 m stocks. The rock is medium to coarse grained and has a peculiar spotty black and green colour of black subhedral amphibole in subequal amounts with green anhedral feldspar. The rock weathers to a black and white colouration; amphibole stands out in positive relief, and the feldspar forms a white powdery mass.

The diabase contains enclaves of a very fine grained porphyritic diabase, which in thin section is mineralogically similar to the host diabase. This is presumed to be its chilled phase.

The most common diabase is a greenish black variety which outcrops in several localities as hillocks and flat-lying exposures. The rock is porphyritic and consists of an uneven medium to fine-grained ground mass. Phenocrysts are mostly amphibole and the ground mass is a mixture of primary mafic minerals and feldspar. A weak lineation is defined by mafic laths in some localities. Weathering surfaces have a dark brown coating below which feldspars appear as white powdery laths. The phenocrysts impart a rough texture to the weathering surface. In the northern part of the Moshaneng Area the diabase has more mafic phenocrysts and the feldspar infrequently attains phenocryst sizes.

Syenites, Granodiorites

Leucocratic rocks form a large part of the Moshaneng Intrusion. They are exposed in various localities as ridges and stocks and occasionally as dikes.

North of Moshaneng Store is a coarse, pink syenite consisting of orthoclase, amphibole and quartz. The orthoclase is pink and Carlsbad twinned. It forms euhedral crystals up to 0.5 cm in length and sometimes encloses a whitish feldspar (presumably plagioclase) or mafic minerals. Some crystals are fractured.

The amphibole is black and occurs in three forms: as random knots, as fine disseminations forming clusters in which the feldspar content is subordinate and as an interstitial mineral between feldspars. Quartz occurs mostly as rounded grains. The quartz content is variable and can increase up to 20%, in which case the rock is a true granite.

The contact with Transvaal rocks is chilled, flow foliated and more mafic. In places the syenites have been brought into fault contact with diabases. In one locality north of Moshaneng the syenite is hosted as

xenoliths by a diabase along the contact. The relationship is taken to indicate that the syenites may be of different ages.

About 2 km south of Mokube Hills (Figure 2) a white granodiorite occurs in association with the diabases. It is medium-grained, porphyritic and weakly foliated. It consists of 3 - 5 mm green, white and pink phenocrysts and a groundmass of amphibole and feldspar. The granodiorite has inclusions of a fine grained porphyritic diabase but in some places a gradational interphase is present.

Other Intrusive Rocks

With the exception of the Mheelo Diabase, all diabase intrusions post-dating the Gaborone Granite have been emplaced as dikes of various sizes, and to a lesser degree as small stocks. They are to be found in most granite inselbergs such as the Kubung, Polokwe, Majwana, and Sephatlhaphattha Hills. Several intrusions also outcrop along the dry stream courses (for example Mheelo, Meshwana, Kubung and Mahatelo).

The main differences between the diabases are fresh and weathering colours, phenocryst contents and textures. Differences in thin section (mainly the degree of alteration and pyroxene types and amounts) were also noted. Small stocks of syenites occur west of the Kubung Dam (locally known as the Zambia Dam).

Genetic Relationships

The relationship between the different rocks of the Younger Intrusions is unclear. The contact and structural features indicate that mafic rocks comprise at least two phases. The relationship of the leucocratic rocks is not understood. However it is noted that in some of the post-Gaborone Granite intrusions different compositional phases are associated (Mallick and Habgood, 1978).

The structural relationship (Figure 3) of the Moshaneng Intrusion with other rocks imply three ages:

a) Pre-Waterberg or early post-Gaborone Granite. These are mostly granodiorites, syenites and younger granites over which the Waterberg has been deposited. Some diabases that are intruded into the Transvaal rocks may be of this age.

b) Syn-Waterberg. The large sills intruded in the Waterberg strata are an example of rocks of this age (Figure 2).

c) Post-Waterberg. Tilted blocks of Waterberg strata which overlie diabases in the north of Mmasehudula belong to this age. The Ranaka and Mheelo Diabases are post-Waterberg. Most other dikes and stocks are probably of a post-Waterberg age.

Structural Geology

The structural configuration of the Tletletsi Area, like the rest of southeastern Botswana is very complex. Several deformational features are easily recognizable and have been mapped (Figure 3). The main trend of deformation is related to the emplacement of Gaborone Granite. The Moshaneng Intrusion is associated with several structural features of the Waterberg rocks in the southwestern area of Figure 3.

In addition to controlling the surface drainage, the fractures are, in some cases, filled with minor amounts of mineralization.

The Geomorphic-Geochemical Environment

The landforms of eastern Botswana have been described by Bawden and Stobbs (1963, Sheet II). The Tletletsi Area falls within land unit b of the Metsemotlhaba Land System.

The principal geomorphic feature of the area is a gently undulating plain. Kopjes of granite outcrop in several places. The east and the

south are bound by rugged and steep-sided hills of Waterberg rocks separated by undulating plains.

The drainage pattern is intricate and consists of shallow streams with steep banks. Water flow is limited to the wet season. The entire drainage is controlled by the structural features of the underlying rock types.

The overburden is composed of a thin veneer of stony soils, brown, medium to heavy textured soils and ferruginous tropical soils. Transported and residual soils are easily recognizable. The transported soils, when not strongly weathered, consist of a fine or medium grained sand which alternates with a coarse, pebbly and stony sand. When strongly weathered, the layering is evident by the accumulation of resistate grains such as quartz at several depths in the soil profile. The residual soils consist of well-formed horizons. The soil profile grades recognizably from the A horizon to the slightly weathered bedrock.

CHAPTER III

METHODS OF STUDY

Field Methods

The field party consisted of five assistants, four of whom were engaged in digging the pits. One field assistant helped with the geological mapping. Sampling was done by digging pits approximately 1 m by 2 m with average depths of 1.5 m for the residual soils and 2 m for the transported soils. After sampling, the pits were either refilled or blocked with thorn trees to protect livestock from falling inside the pits.

Site Selection

The locations of the pits were selected on the basis of two criteria:

i) between streams with high metal content in their sediments (Marengwa, 1978)

ii) between streams with low metal contents in their sediments (Marengwa, 1978)

In some cases the pre-selected sites had to be altered slightly where the soil was too thin to give a suitable profile.

Sampling Methods

After the pits were dug, brief descriptions of the stratigraphic profile were recorded. This included horizon thickness, colour, texture, layering, etc. Samples were collected at 15 cm intervals. Each sample depth given in the downprofile trend diagrams represents the 15 cm immediately above it. This was done to ensure that each sample was as representative as possible to minimize the possibility of spurious results,

especially within the transported soils where alternations of coarse and medium or fine sand layers occur. Each sample represents an average content rather than a specific content at a given depth.

The samples were stored in plastic sample bags.

Laboratory Methods

Sample Preparation and Examination

The bulk samples were air dried to remove moisture and halved. One portion was sieved without grinding and the -80 mesh (approximately 200 μm) was retained for analysis. The bulk samples contained abundant quartz and feldspar grains of various sizes. Grinding was purposely avoided because only the fine fraction resulting from weathering was of interest to this study. Grinding of grains such as quartz would dilute the metal content of the natural fine fraction whereas magnetite (which is common in the residual pits) would give very misleading total extraction results.

The remaining portion of the bulk sample was examined with a binocular microscope in order to identify as many of the minerals as possible. In addition, other features such as smooth mineral surfaces, incipient chemical weathering of feldspar, ferric staining of fine grains and the presence or absence of windblown grains were noted. The Tletletsí Area lies adjacent to the Kalahari Desert. It was therefore necessary that the presence or absence of windblown grains be determined. However, no frosted or pitted grains were observed.

To measure the pH, 20 g of bulk sample was put in 100 ml of deionized water and stirred thoroughly. The solution was allowed to stand for two days and then the pH was determined using a pH meter (Radiometer Model pH Meter 29).

pH readings of soils are usually taken on a slurry of soil suspended in water (Garrels and Christ, 1965). In this study the pH readings were taken from the supernatant liquid in order to protect the glass electrode.

A few drops of dilute (1.2 molar) hydrochloric acid were dropped on each sample to test for carbonate. A strong hand magnet was used to determine whether the dark minerals were magnetite.

Reagents Used

The reagents used in the extractions were:

- a) Baker Analyzed 36.8% Hydrochloric Acid
- b) Baker Analyzed 70.8% Nitric Acid
- c) Baker Analyzed 49.4% Hydrofluoric Acid

Trial Extractions

Sample Dissolution

Trial extractions were carried out in order to determine the effects of digestion times, acid strength and the difference between hot and cold leaching.

A random, sieved sample was chosen from each pit and divided into four 2 g subsamples referred to as A, B, C and D. The subsamples were placed in 125 ml conical flasks and treated as shown in Table 1a. The cold leach was at room temperature and the hot leach was approximately at boiling point of the mixture.

The hot leaching in B and C was done after the subsamples had been allowed to stand initially for 60 minutes at room temperature. After heating to near dryness, the B and the C subsamples were removed from the hot plate and allowed to cool. They were then treated again with the acid strength used initially (1.2 molar HCl for B and 2.4 molar HCl for C).

Table 1(a). Trial Extraction Procedure.

Subsample	Amount and Strength of HCl	Type of Leach	Duration of Leach
A	10 ml, 1.2 molar	Cold	120 min.
B	10 ml, 1.2 molar	Hot	40 min.
C	10 ml, 2.4 molar	Hot	40 min.
D	10 ml, 1.2 molar	Cold	30 min.

All the subsamples were vigorously shaken before filtering through a Whatman 1 filter paper. A 5 ml aliquot of the filtered sample was pipetted into a 25 ml flask and diluted to volume.

A Perkin-Elmer 303 Atomic Absorption Spectrophotometer was used to measure the Fe, Mn, Zn, Ni, Cu and Cr concentrations. Lead was determined using a Model 1L 251 Laboratory Instr. Inc. Atomic Absorption Spectrophotometer.

For all elements, the B and C procedures yielded consistently higher concentrations of Fe, Mn and Zn than the A and D procedures (Figure 4a, b, c). Digestion time was less a factor than acid strength because the A and D extractions were nearly equal (Figure 4a, b, c). This was taken to indicate that the elements Fe, Mn and Zn occur as easily soluble and less soluble forms.

Hot leaching increases dissolutions of the elements very strongly (Figure 4) especially for Fe (Figure 4a). The hot leach did not yield very high results for Mn compared with the cold leach except for pits 3, 2 and 1 (Figure 4b) which occur on different rock types. This was taken to indicate that most of the Mn was more soluble than Fe.

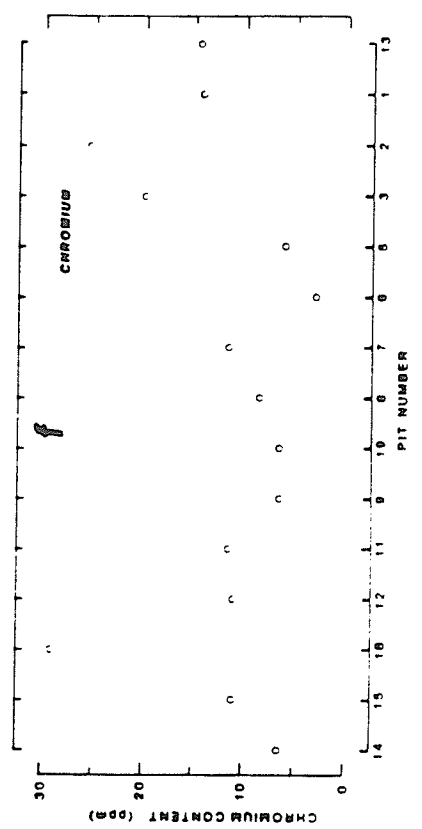
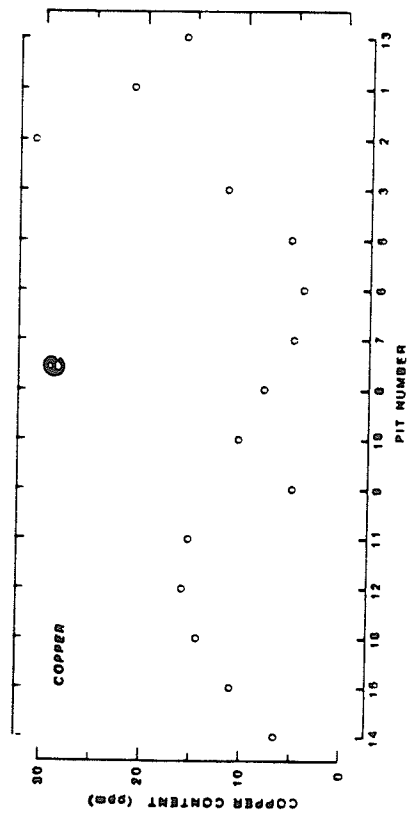
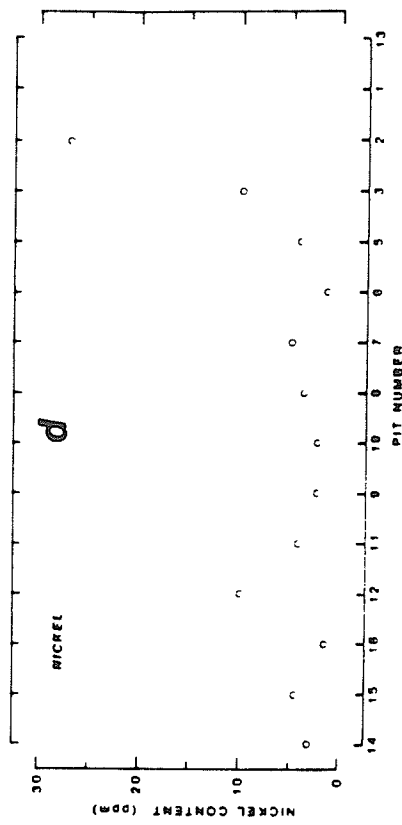
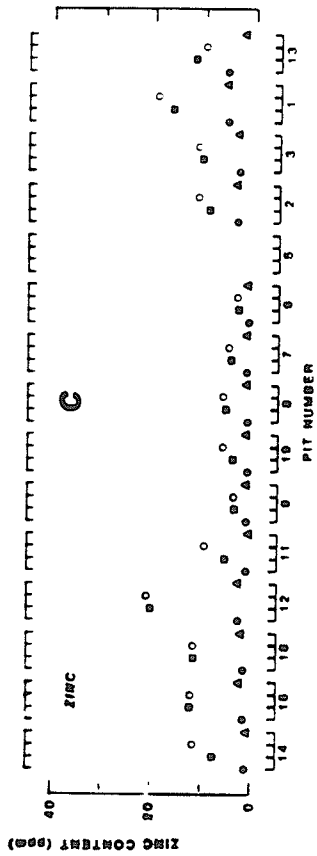
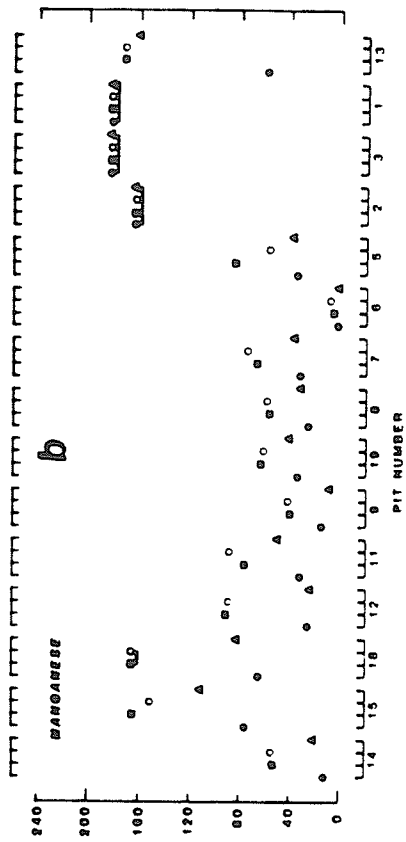
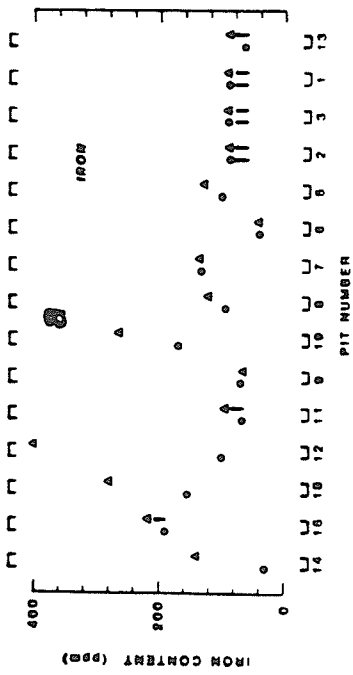
The effect of acid strength is seen in Figures 4c, d, and e. The 2.4 molar hydrochloric acid was the only procedure capable of giving detectable concentrations of Ni, Cu and Cr.

Final Extraction

Hot Partial Leach (Px)

Based on the results of the trial extractions, it was decided that the 2.4 M HCl hot leach was the most suitable extraction because it gave concentrations which were above the detection limits for the elements Fe, Mn, Zn, Ni, Cu and Cr. The time for extraction was increased to six hours (unlike the thirty minutes in the trial extractions)

Figure 4. Trial extractions for Fe, Mn, Zn, Ni, Cu and Cr
on random samples from each pit



EXTRACTION PROCEDURE:

● A ○ B ○ C ▲ D — OFF SCALE

in order to minimize the variation of results with sample type. In sampling entire soil profiles, samples vary from those rich in organic matter (as in the A horizon) to those rich in clays or Fe or Mn secondary minerals (as in the B horizon). The procedure for the hot leach is given in Table 1(b).

Total Digestion (Tx)

For total digestion the procedure followed is listed in Table 1(c).

In some cases it was necessary to dilute the partial and total extraction samples by up to 5,000 times before the trace element levels of Fe and Mn could be brought into the range of the atomic absorption determination. All analytical results are listed in Appendix.

Precision and Batch Control

Table 2(a-d) lists the repeat analysis for the elements Mn, Zn, Co and Cu. The samples were selected at random to monitor the reproducibility of analytical data.

The dilutions gave levels that were detectable by the instrument. Precision was calculated as follows:

$$P(\%) = \frac{Px_1}{Px_2} \times 100$$

where Px_1 and Px_2 are analyses of the same sample. The results were generally reproducible to better than 90% except where concentrations were low as in the Co example (Table 2(d)).

Possible differences between batches caused by inconsistent experimental conditions in one or more stages were monitored for some samples by repeating the analyses of a single chosen sample (a control sample) with every batch. In addition, blanks were also used to monitor

Table 1(b). Hot Partial Leach (Px) Procedure.

- a) Weigh 2.0 grams of sample.
 - b) Add 10 ml of 2.4 M HCl and let stand for six hours.
 - c) Add a further 10 ml HCl, shake thoroughly and heat to near dryness.
 - d) Add 20 ml using a volumetric flask of 2.4 H MCl. Let stand for 1 hour, shake vigorously and pass through a Whatman 1 filter paper into a polyethylene sample bottle.
 - e) Pipette 10 ml sample into a 100 ml volumetric flask and dilute to volume with deionized water.
 - f) Analyze by atomic absorption.
-

Table 1(c). Total Digestion (Tx) Procedure.

- a) Mix in ratio 4:1 by volume of Baker analyzed concentrated HF and HNO₃ (49, 70.8 wt. % respectively).
 - b) Weigh 2.0 grams of sample and treat with 10 ml of the acid mixture for six hours in teflon beakers.
 - c) Add a further 10 ml of the acid mixture using a volumetric flask. Shake thoroughly and fume dry.
 - d) Add 10 ml of 6.2 M HCl using a volumetric flask and fume dry.
 - e) Add 20 ml of 2.4 M HCl using a volumetric flask. Let stand for 1 hour. Shake vigorously and pass through a Whatman 1 filter paper into a polyethylene sample bottle.
 - f) Pipette 10 ml into a 100 ml volumetric flask and dilute, to volume with deionized water.
 - g) Analyze by atomic absorption.
-

Table 2(a). Reproducibility checks for Mn (ppm).*

	Px_1	Px_2	Px_1/Px_2	Tx_1	Tx_2	Tx_1/Tx_2
1	348	346	0.98	527	525	1.00
2	n.a.	n.a.	n.a.	n.a.	n.a.	
3	320	331	0.97	415	437	0.95
4	302	300	1.01	471	462	1.02
5	359	331	1.09	466	462	1.01
6	348	331	1.05	465	525	0.89
7	398	412	0.97	701	800	0.88
8	449	462	0.97	651	663	0.98

* data from Pit 13.

n.a. = no analysis

Table 2(b). Reproducibility checks for Zn (ppm).*

	Px_1	Px_2	Px_1/Px_2	Tx_1	Tx_2	Tx_1/Tx_2
1	15	18	0.83	20	19	1.05
2	14	12	1.16	16	15	1.07
3	10	10	1.00	18	15	1.06
4	15	15	1.00	18	17	1.09
5	19	17	1.09	21	21	1.00
6	20	19	1.05	22	21	1.07
7	15	14	0.94	16	18	0.91
8	11	12	0.91	17	17	1.02

* Data from Pit 11.

Table 2(c). Reproducibility checks for Cu (ppm).*

	Px ₁	Px ₂	Px ₁ /Px ₂	Tx ₁	Tx ₂	Tx ₁ /Tx ₂
1	26	29	0.90	80	74	1.08
2	46	44	1.05	115	109	1.06
3	35	31	1.13	38	37	0.97
4	45	48	0.94	44	48	0.98
5	24	27	0.92	48	52	0.92
6	43	49	0.88	60	62	0.97
7	n.a.	51		n.a.	n.a.	
8	48	49	0.98	75	62	1.21
9	47	49	0.96	69	62	0.94
10	44	51	0.86	81	83	0.98
11	44	46	0.96	82	83	0.99
12	41	46	0.89	78	82	0.95
13	50	49	1.02	63	59	1.07

* Data from Pit 1.

n.a. = no analysis

*

Table 2(d). Reproducibility checks for Co (ppm).

	Px ₁	Px ₂	Px ₁ /Px ₂	Tx ₁	Tx ₂	Tx ₁ /Tx ₂
1	6.3	6.5	0.97	8.1	5.0	0.62
2	4.0	2.0	0.50	6.9	5.1	1.35
3	7.5	7.5	1.0	8.8	7.0	1.26
4	9.5	6.0	1.46	10.6	8.5	1.25
5	9.4	6.5	1.45	10.0	6.5	1.54
6	6.9	5.0	0.73	10.0	10.0	1.00
7	13.8	12.0	1.15	19.4	24.0	0.81
8	13.8	12.0	1.15	15.0	12.0	1.25
9	14.4	12.0	1.20	20.0	15.0	1.33
10	17.5	12.0	1.46	24.4	17.0	1.44
11	10.0	10.0	1.00	16.9	16.5	1.02
12	11.0	11.0	1.00	17.5	15.0	1.67

* Data from Pit 19

batch differences and reagent contamination. The blanks were produced by following the partial leach and total digestion procedures. The background values of the blanks were used for the correction of some trace element levels (Zn, Co, Ni). The trace element levels in the blanks themselves were consistently below the detection limits of the instruments. Thus, all suspect results were not due to reagent contamination. Table 2(e) lists the pit numbers and the order in which they were taken as batches. The element concentrations of the control sample as determined during the analyses of the different batches are also shown. The precision (calculated as defined previously) of any element determination (P_x/P_x or T_x/T_x) was generally above 95%. However, the extraction ratio comparisons gave results of a lesser precision because the error in both extractions is additive when the extraction ratios are calculated.

The results in Table 2(e) indicated that the differences across batches were low compared with the total element contents of all the individual pits.

Table 2(e) . Batch control.

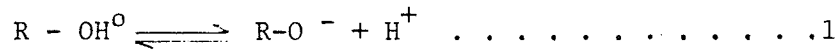
Element	Partial Extraction (Px)	Total Extraction (Tx)	Extraction Ratio Px/Tx	Batches and Pit Numbers
Fe %	1.25	1.48	0.85	11,15
	1.50	1.70	0.90	18,7
Mn (ppm)	100	140	0.71	11,15
	113	140	0.80	8,9
	110	150	0.85	18,7
Zn (ppm)	20	23	0.90	11,15
	17	21	0.83	18,7
	23	25	0.93	8,9
	25	26	0.93	12,5
Ni (ppm)	16	20	0.80	11,15
	18	23	0.78	18,7
	12	13	0.80	18,7
Pb (ppm)	11	14	0.82	6,20
	12	16	0.68	18,7
	11	14	0.79	11,15
Cu (ppm)	17	18	0.95	3,14,13
	18	20	0.95	1

CHAPTER IV

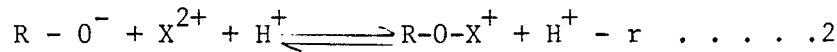
DATA TREATMENT

Colloidal Activity and Determination by Correlation Analysis

Geochemical data of any kind can be viewed from a point of sympathetic (for example in adsorption) or antipathetic (for example solid solution). In surface or near surface geochemistry, colloids (clays, humic matter and Fe-Mn secondary compounds) control the dispersion of various trace elements (Jenne, 1968). Adsorption and coprecipitation of trace elements by colloids are controlled by a simple law of mass action (Perel'man, 1967, p. 98). The basic equations are as follows:



(where R is the colloidal substance)



(where X²⁺ is a divalent cation)

The equilibrium constant, K (the selectivity constant, Farrah et al., 1980) is defined by:

$$K = \frac{a_{(R-O-X^+)} \cdot a_{(H^+)}}{a_{(R-O-H)} \cdot a_{(X^{2+})}} \dots\dots\dots .3$$

(where a is the activity of the specified species).

If the activity of the adsorbant is considered to be relatively constant, and if it is assumed that most of the metal ions are adsorbed (or attached in other forms of bonding to the adsorbing species), then equation 3 can be approximated to:

$$K = \frac{a_{(R-O-X^+)} \cdot a_{(H^+)}}{a_{(X^{2+})}} \dots\dots\dots .4$$

For single profiles, the pH usually varies slightly. Equation 4 can be further simplified to:

$$K = \frac{a_{(R-O-X^+)}}{a_{(X^{2+})}} \dots \dots \dots .5$$

Equation 5 means that the amount of ions adsorbed depends on the amount of active adsorbant present. Fe and Mn compounds adsorb most of the dispersed metal ions in soils (Jenne, 1968). $a_{(X^{2+})}$ will be small and most of the metal ions will occur in an adsorbed form (or other forms related to the chemical properties of Fe or Mn compounds).

Ions which are not immobilized by the Fe and Mn compounds can be represented by adding another term to equation 5 such that

$$a_{(X^{2+})} = K'' a_{(R-O-X^+)} + C \dots \dots \dots .6$$

If $R-O-X^+$ is analyzed (as is the case in geochemical exploration when using soils and sediments) then the amount of X recovered should vary in direct proportion with that of $R-O^-$; the adsorbant. The strength of such a variation can be expressed numerically by a Pearson correlation coefficient r. Concentration can be expressed in ppm rather than activities. r is defined as:

$$r = \frac{(\sum [R-O-X^+][X]) - \frac{(\sum [R-O-X^+]) (\sum [X])}{n}}{(\sum [R-O-X^+]^2 - \frac{(\sum [R-O-X^+])^2}{n})^{1/2} (\sum [X]^2 - \frac{(\sum [X])^2}{n})^{1/2}} \dots \dots \dots .7$$

If $[R-O-X^+]$ is plotted against $[X]$ adsorbed, it will give a straight line. The correlation coefficient is related to the slope of the line by the equation:

$$r = m \frac{d_{[R-O-X^+]}}{d_{[X] \text{ adsorbed}}} \dots \dots \dots .8$$

(where m is the slope and d are variances of the data arrays, i.e. $R-O-X$ and X adsorbed concentrations of the samples from a single profile).

The closer the correlation to unity the stronger the control of the trace element behaviour by either Fe or Mn. The slope is influenced by several factors, the most important being the extraction capacity of a particular extraction procedure. In treating the data of this study, only the correlation coefficient has been taken into account. The correlation coefficient is taken to be significant when it is greater than the critical value (CV) at a probability (f) of ten percent, i.e. $f=0.10$. The high probability value (0.10) has been chosen in view of the fact that the extractions used in this study are not 'site selective'. Metal cations can be held onto secondary Fe and/or Mn compounds in various ways (for example adsorption and occlusion). It is not possible to determine in this study which type of 'bonding' contributes the most metal ions, and which sites are resistant to the extractions. In addition, an allowance is made for ions not adsorbed by either Fe or Mn.

Stream Data

The use of factor analyses in the examination of interrelationships between trace elements is common in geochemistry. Armour-Brown and Nichol (1970), Howath et al. (1979), Closs and Nichol (1974), Nichol et al. (1969) and Tripathi (1978) give brief explanations and applications of the technique.

An R-mode principal analysis was performed on Sn, Ti, V, Cr and Mn stream sediment data taken from a regional stream sediment survey by Marengwa (1978). Two subpopulations were taken from the regional survey data. The first subpopulation, named the Tletletsi subpopulation consisted of 408 data values from streams occurring within the Tletletsi area (Figure 5(b)). The second subpopulation (492 data values), referred to as the Gaborone subpopulation, was taken from all streams occurring north of the Tletletsi Area (see Marengwa, 1978).

The latter subpopulation was used only for comparison and to increase the confidence in assessing the Tletletsi subpopulation data. The R-mode was used in preference to the Q-mode because geological and environmental associations can be more easily identified. The programs used were taken from an SPSS package (Nie et al., 1975).

The input of Pearson correlation coefficients was obtained from log-transformed variables (a variable is the element content in ppm). The transformation was required because of the strong positive skewness of raw data. Extremely high (and commonly isolated) values were omitted during correlation coefficient calculations. The high values were only used in factor score calculations. Tripathi (1978) has demonstrated how the distortions of factor analysis results can be improved by excluding high values in raw data. Howarth et al., (1979) also refer to the spurious results caused by using metal content values that are very high and isolated compared with the rest of the raw data. Terminal solutions were arrived at by varimax and quartimax rotations (Nie et al., 1975). In addition, factor-factor correlations were also investigated using an oblique solution to assess mutual factor dependence.

CHAPTER V

SOIL PROFILE DESCRIPTIONS

The nomenclature used in the description of the soil profiles of this study is illustrated in Figure 5(a) together with the generalized characteristics of a typical residual profile.

The soil profile descriptions are presented in a sequence that goes across the drainage basin (rows A-A', B-B', C-C', D-D') and from northeast to southwest (Figure 5(b)).

It can be seen from the drainage pattern that the rows go from a topographically high area in the west through the low elevations in the centre of the drainage area to higher land surface in the east. (Actual elevations in feet are found in topographic maps 2425C2, 2425D, 2425C4 and 2425D3, 1967, Geological Survey of Botswana). The arrangement of the rows (northeast to southwest is from low to high elevations).

Descriptions of all the profiles are given in the following section. Each description includes a discussion of the physical and chemical properties of the profile. The discussion of chemical properties is an element by element treatment of their downprofile trends. Correlation of Fe and Mn with other elements is presented in tables for each pit. Also included in the tables is an Fe:Mn correlation, and a critical value (CV).

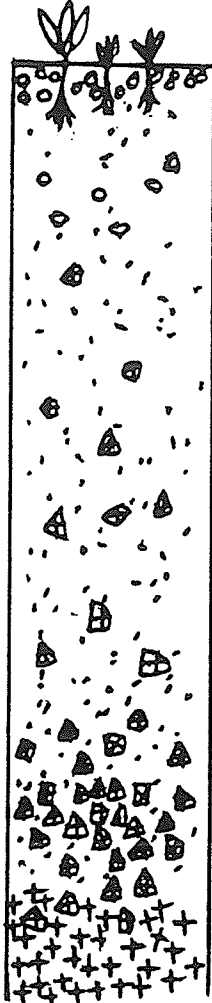
The soil distribution map (Figure 5(b)) was produced by grouping together all profiles with similar characteristics (residual or transported). This was done on the consideration of the physical properties. All the profiles are then considered collectively at the end of the individual profile discussions in a generalized presentation of their physical and chemical properties.

Figure 5(a). Generalized soil profile characteristics showing the principal subhorizons typical of residual soil profiles in the Tletletsi Area. The same scheme is used for transported soils. Profile not to scale.

Subhorizon

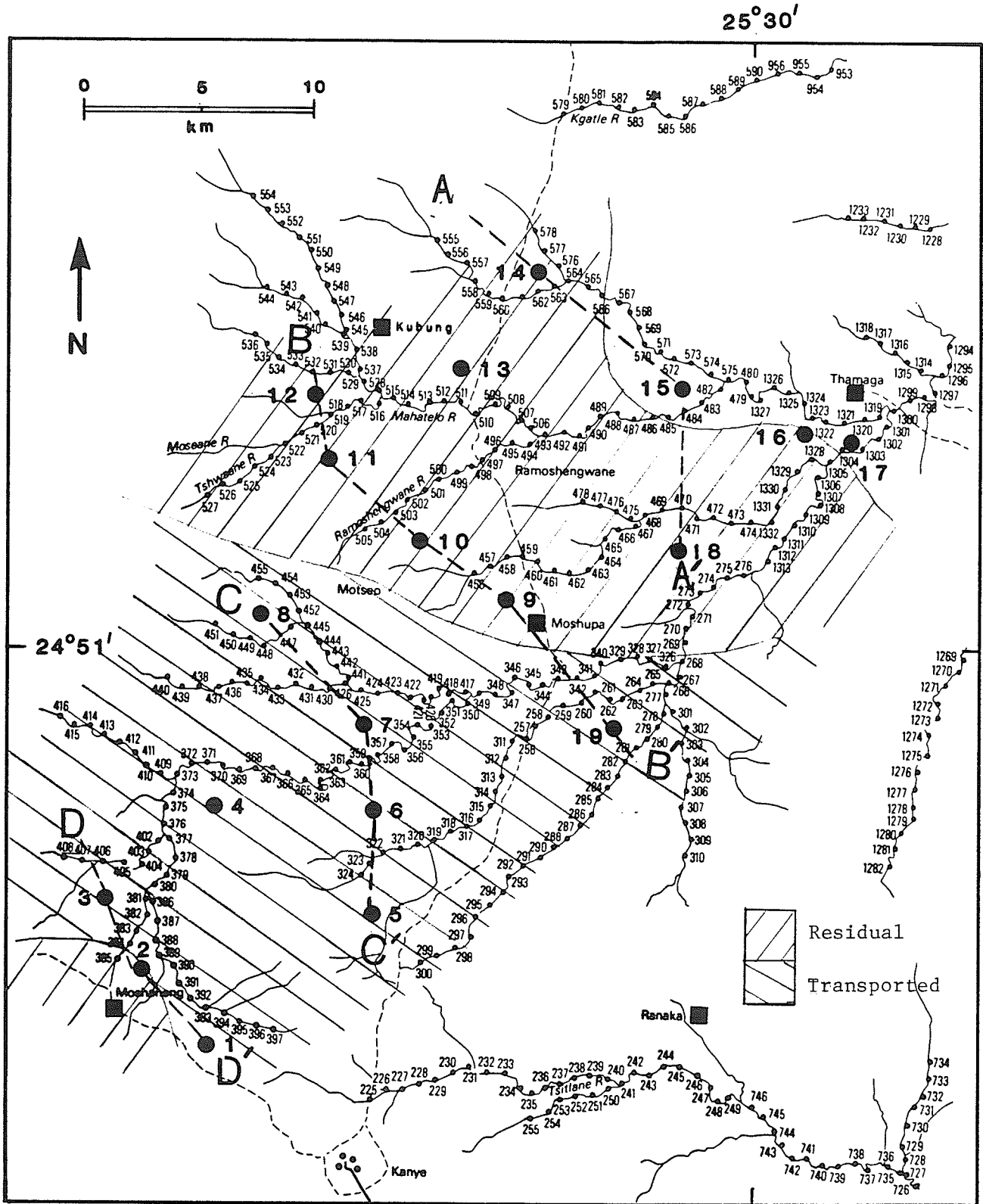
Description

A_o



- Topsoil. Brown to light reddish brown. Unweathered minerals and fresh organic (plant) matter present. Usually dominated by the coarse fraction.
- Brown, loose clayey/silty, very fine grained sand. Brown humic matter. Unweathered minerals (feldspar, dark minerals = mafics and/or magnetite) present. Dark minerals mostly in fine fraction.
- Light brownish red. Less organic matter otherwise as above. Quartz abundant.
- Reddish brown ferric hydroxide/oxide colouration. Very little organic matter. Coarse quartz grains. Unweathered and partly weathered feldspars and dark minerals present. Abundant clay and/or silt.
- Dark reddish brown. Strong ferric compound accumulation. It may be hard and compact. Commonly lateritic.
- Dark reddish brown as above with significant amount of partly weathered and coarse granite fragments.
- Abundant, loose, ferric stained friable granite fragments. Translocated B horizon material.
- Light reddish brown or mottled or chalky partly weathered granite.

Figure 5(b).The Drainage Pattern and Soil Type
Distribution in the Tletletsi Area.
Also shown are stream sampling
locations of Marengwa (1977) and
profile sampling locations of this
study.



● 320 STREAM SAMPLING SITE

● 18 SOIL PROFILE LOCATION

■ SETTLEMENTS

--- MAIN ROAD

after B.S.I. MARENGWA(1977),

with additional data from present study

Physical and Chemical Properties of Pit 14

Physical Properties

The profile has been derived from the underlying granite. Three horizons have been developed (Table 3). The A horizon is thin (14 cm), dark brownish red and consists of fresh and humic (brown) matter, fine-grained clayey/silty quartz sand, coarse quartz grains and dark minerals (mafics and magnetite).

The B horizon is mineralogically similar to the A horizon but varies by having a reddish brown colouration of ferric compounds and quartz is more abundant. The colouration increases with depth. At the bottom of the B horizon there is an increase in weathered granite fragments that make the C horizon. Below, ferric stained, friable and sometimes mottled weathered granite fragments form the middle C horizon. The transition to bedrock is a white, slightly weathered granite.

Chemical Properties

All the elements (Figure 6) have a similar tendency of maximum concentration in the lower B horizon or upper C₁ subhorizon. The strengths of similarities of the downprofile trend of the elements has been expressed in correlation coefficients (Table 4).

The variation of the iron concentration with depth is shown Figure 6a. Immediately below the transition of the A and B horizon a rapid increase occurs and the Fe content reaches a maximum accumulation in the upper C horizon. The extraction ratio (P_x/T_x) is constant except in the topsoil and the lower C horizon.

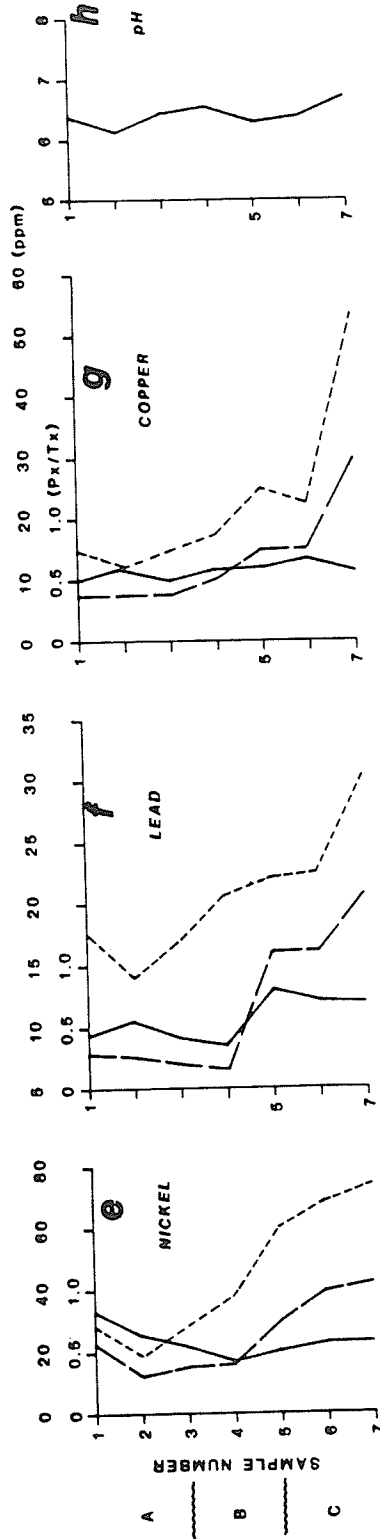
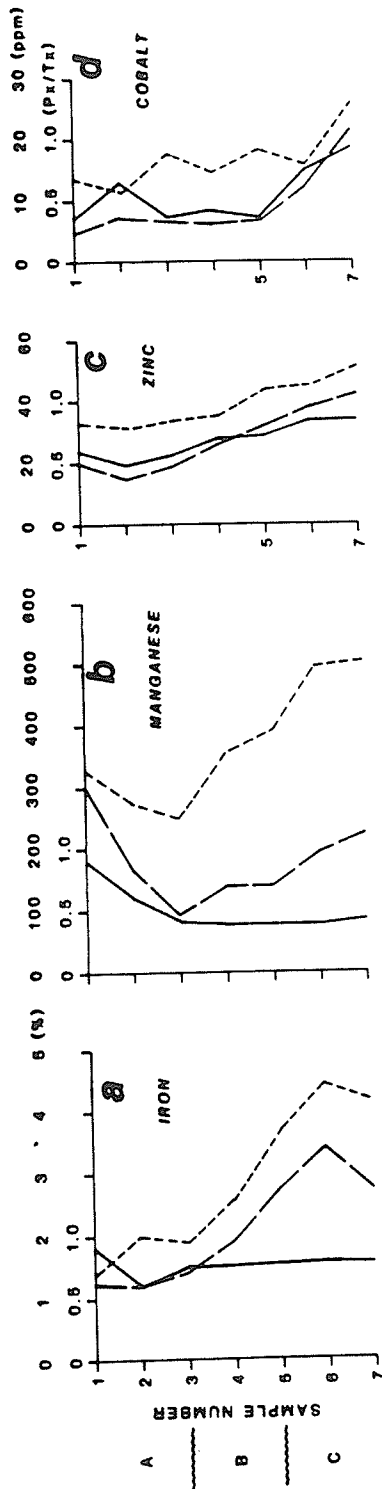
Manganese is accumulated in the A and the B horizon. The amount of Mn in the A horizon (Figure 6b) decreases from the topsoil to the lower A horizon (at a depth of 30 cm). The B horizon has a progressive accumulation

Table 3. Soil profile description of Pit 14.

Sample	Depth	Horizon	Description
1	0	A ₀	Topsoil. Light reddish brown, loose clayey/silty very fine grained quartz sand. Fresh organic matter abundant. Some coarse to very coarse quartz grains. Dark minerals (mafics and magnetite) in fine fraction.
2	0-15	A ₁ A ₂	Dark reddish brown. Loose clayey/silty sand as above. Fresh and decayed (brown) humic matter present. Grades to B horizon.
3	15-30	A ₂ B ₁	Reddish brown clayey/silty, very fine grained quartz sand. Some humic organic matter present. Top 20 cm forms transition from A to the B horizon. Partly weathered feldspars present. Dark minerals present in fine fraction.
4	30-45	B ₂	Reddish brown clayey/silty quartz sand as above. More ferric colouration and coarse quartz than above.
5	45-60	B ₂ C ₁	Reddish brown clayey/silty sand with coarse grains and weathered granite fragments.
6	60-75	C ₁	Light reddish brown clayey/silty sand with abundant granite (weathered) fragments. Mottled in upper 9 cm.
7	75-90.	C ₂	Light reddish brown staining of weathering powdery granite. White weathering granite at 90 cm.
8, 9	90-120	C ₂	White, partly weathered granite.

Figure 6. Downprofile distribution of Fe, Mn, Zn, Co,
Ni, Pb, Cu and pH. Pit 14.

PIT 14



Partial Extraction ———
 Total Extraction - - -
 Extraction Ratio . . .

Table 4. Pearson correlation coefficient (r) for (Fe,Mn):

Mn, Zn, Co, Ni, Pb, and Cu. CV = critical value.

f = confidence level. Pit 14.

Px-Px	Fe:Mn = 0.00	Px-Px	Fe:Ni = 0.88
Tx-Tx	Fe:Mn = -0.85	Tx-Tx	Fe:Ni = 0.95
Px-Px	Fe:Zn = 0.92	Px-Px	Mn:Ni = 0.38
Tx-Tx	Fe:Zn = 0.89	Tx-Tx	Mn:Ni = -0.82
Px-Px	Mn:Zn = 0.31	Px-Px	Fe:Pb = 0.85
Tx-Tx	Mn:Zn = -0.75	Tx-Tx	Fe:Pb = 0.78
Px-Px	Fe:Co = 0.57	Px-Px	Mn:Pb = 0.38
Tx-Tx	Fe:Co = 0.59	Tx-Tx	Mn:Pb = -0.62
Px-Px	Mn:Co = 0.75	Px-Px	Fe:Cu = 0.68
Tx-Tx	Mn:Co = -0.62	Tx-Tx	Fe:Cu = 0.68
CV	= 0.67	Px-Px	Mn:Cu = 0.54
f	= 0.10	Tx-Tx	Mn:Cu = -0.38

with depth down to the C subhorizon. The extraction ratio is low. It decreases with depth in the A horizon but remains constant in the B and C horizons.

Zinc increases smoothly with depth from the A, subhorizon to the C horizon. The extraction ratio behaves similarly (Figure 6c').

Cobalt Px values are constant in the A and B horizon (Figure 6d). An abrupt increase occurs in the B₂C₁ subhorizon. The variation in Tx values is less well defined. However an increase in the C horizon is present. The extraction ratio is highest in the C and A horizon (excluding A₀). It is constant in the B horizon.

Nickel (Px, Figure 6c) has an enrichment within the B and C horizons. The A and upper B horizon have similar concentrations. The Tx values increase strongly downprofile. The extraction ratio decreases into the B horizon and increases gradually in the C horizon.

The Pb Px content in the profile decreases slightly in the A horizon. A very sharp increase occurs at the beginning of the C horizon. The highest content is in the C₂ subhorizon (Figure 6f). Lead Tx values increase from the A₁ subhorizon to the C₁ subhorizon. Below, the accumulation is much more sharply pronounced. The extraction ratio in the A and B horizon is similar and much smaller than that in the C horizon.

Copper is accumulated in the C horizon. Both Tx and Px values increase with depth (Figure 6g).

The variation of the pH within the soil profile of Pit 14 is shown in figure 6h. The pH is higher in the A subhorizon, decreasing slightly in the lower B and upper C horizons. The extraction ratio is also uniform.

Physical and Chemical Properties of Pit 15

Physical Properties

The profile of pit 15 consists of transported debris derived mostly from weathered granite (Table 5).

The soil horizons are identifiable on the basis of colour. The upper 55 cm constitute an A horizon. It is a brown and humic horizon and consists of a clayey/silty and very fine-grained quartz sand. Weatherable minerals are abundant. Dark minerals (maffics and magnetite) are mostly of fine fraction size. Partly weathered feldspars are more variable in size. Coarse quartz is present.

The B horizon is mineralogically identical to the A horizon but differs in two respects - the absence of organic matter, and the strong accumulation of ferric oxides (Table 5). Consequently, the B horizon is hard, dense and lateritic.

Carbonate is present throughout the profile except in the topsoil. It occurs as solid lumps cementing the fine fraction of the soil and in fine particulate form within the clay and silt detectable only by acid treatment. The carbonate content is variable.

Chemical Properties

All the elements with the exception of Zn and Pb Tx (Figure 7) have subhorizons of higher and lower trace elements. However, the downprofile trends are not visibly similar.

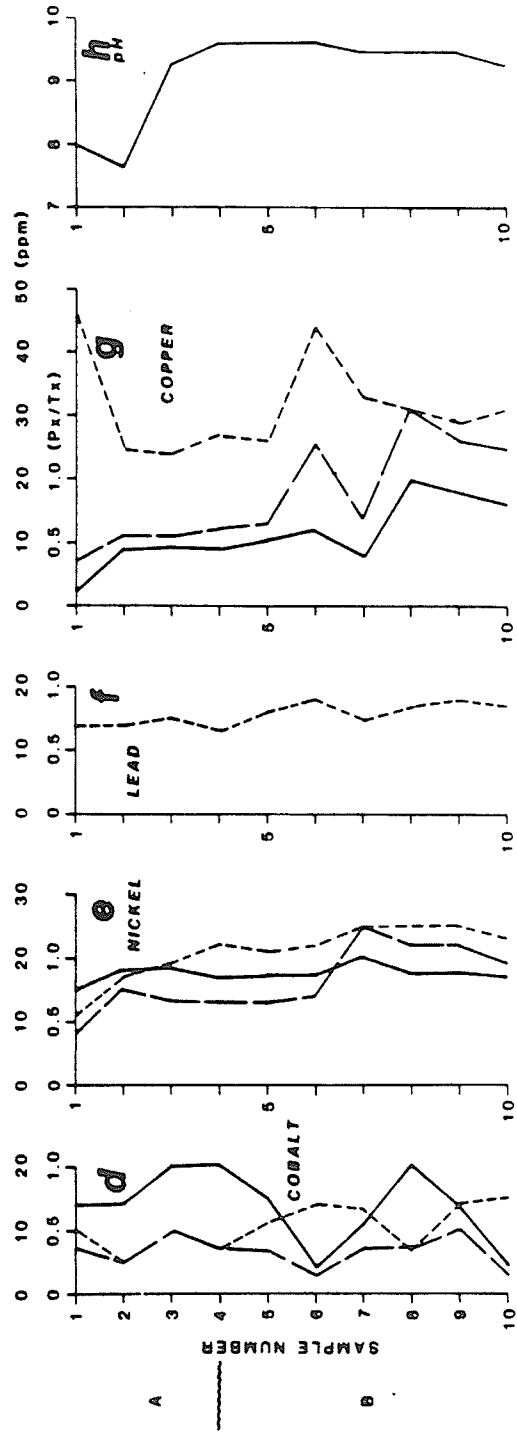
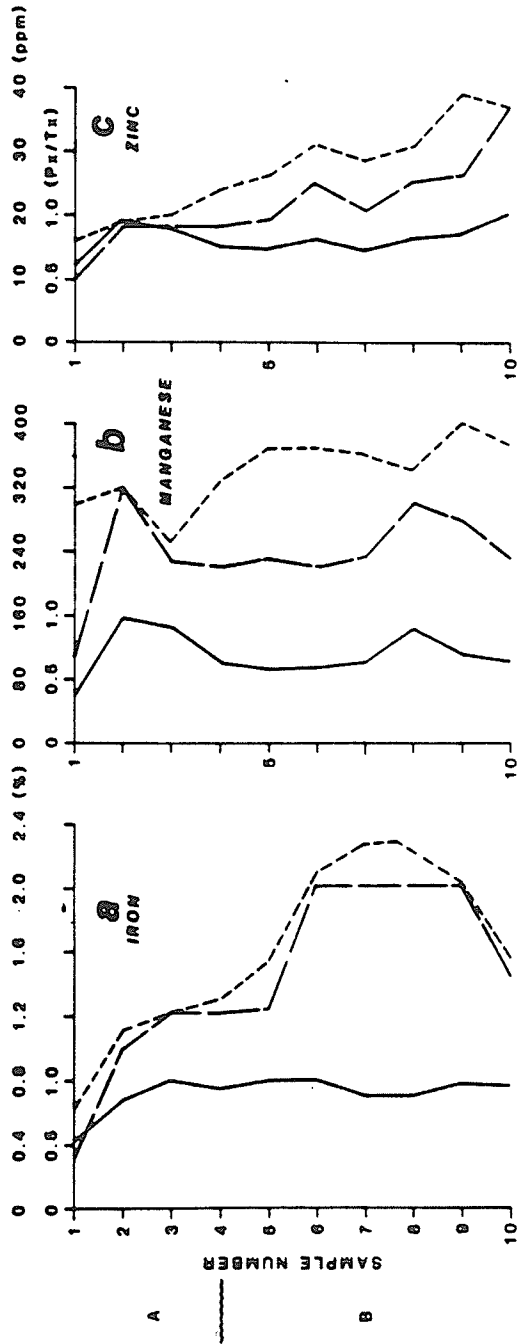
Correlation coefficients of the different trace element with the Fe and Mn contents are given in Table 6.

The iron content of the topsoil (Figure 7a) is much lower than that of the rest of the A horizon. The transition to the B horizon is very sharp

Table 5. Soil profile description of Pit 15.

Sample	Depth (cm)	Horizon	Description
1	0	A ₀	Topsoil. Brown, loose clayey/silty, very fine grained quartz sand. Fresh and humic (brown) organic matter, coarse quartz (blue, colourless), clay lumps from weathered feldspar present. Dark minerals (mafic and magnetite) in fine fraction. No acid reaction.
2	0-15	A ₁ A ₂	Brown clayey/silty soil as above. Some organic matter present. Very mild acid reaction.
3	15-30	A ₂	Brown clayey/silty soil. Slightly coherent. Contains lumps of carbonate cementing clay/silt and sand. Partly weathered, and weathered feldspar present. Dark minerals in fine fraction.
4	30-45	A ₂ B ₁	Brown clayey/silty very fine-grained sand as above. No carbonate lumps observed. Fine fraction reacts with acid. Dark mineral content much lower than above.
5	45-60	B ₂	Reddish brown soil. Hard, lateritic clayey/silty coarse sand. Strong reaction of clay/silt fraction with acid.
6	60-75	B ₂	Reddish brown soil. Hard, lateritic as above. Ferric stains on partly weathered feldspars. Acid reaction very gentle except for some rare white carbonate lumps.
7	75-90	B ₂	Reddish brown soil. Hard, lateritic as above. Strong acid reaction of lumps. Clay/silt fraction reacts mildly with acid.
8,9,10	90-150	B ₂	Reddish brown soil. Hard, lateritic and compact. Acid reaction of lumps stronger than that of clay/silt fraction.

Figure 7. Downprofile distribution of Fe, Mn, Zn, Co,
Ni, Pb, Cu and pH. Pit 15.



Partial Extraction ———
 Total Extraction - - -
 Extraction Ratio - · -

Table 6. Pearson correlation coefficients (r) for (Fe, Mn):

Mn, Zn, Co, Ni, Cu, Pb. CV = critical value,

f = confidence level. Pit 15.

Px-Px	Fe:Mn	=	0.59	Px-Px	Fe:Ni	=	0.74
Tx-Tx	Fe:Mn	=	0.72	Tx-Tx	Fe:Ni	=	0.76
Px-Px	Fe:Zn	=	0.60	Px-Px	Mn:Ni	=	0.60
Tx-Tx	Fe:Zn	=	0.55	Tx-Tx	Mn:Ni	=	0.61
Px-Px	Mn:Zn	=	0.41	Px-Px	Fe:Pb	=	n.a.
Tx-Tx	Mn:Zn	=	0.81	Tx-Tx	Fe:Pb	=	0.60
Px-Px	Fe:Co	=	0.05	Px-Px	Mn:Pb	=	n.a.
Tx-Tx	Fe:Co	=	0.42	Tx-Tx	Mn:Pb	=	0.50
Px-Px	Mn:Co	=	0.03	Px-Px	Fe:Cu	=	0.76
Tx-Tx	Mn:Co	=	-0.40	Tx-Tx	Fe:Cu	=	0.81
CV	=		0.54	Px-Px	Mn:Cu	=	0.47
f	=		0.10	Tx-Tx	Mn:Cu	=	0.12

n.a. = no analysis

due to the lateritic character of the B horizon. The maximum value is constant over a large interval (60 - 105 cm) and decreases below the 120 cm depth. The extraction ratio is high in most of the profile except in the upper A horizon and the lateritic B horizon.

Manganese Px is accumulated in two intervals, the A horizon (except the topsoil) and in the lower part of the B horizon, below 90 cm (Figure 7b). A low and constant element content separates the two intervals of accumulation. It occurs in the lower A horizon and upper B horizon (30 - 90 cm). The Tx values are markedly different. Mn contents occur between 30 and 135 cm. The extraction ratio decreases from the A₀ subhorizon to the B₂ subhorizon. Below, it is constant except at 105 cm.

Zinc (Figure 7c) is constant within the A₁ to B₂ subhorizons (15 - 60 cm). The increase with depth in the lateritic B horizon is gradual but irregular. The extraction ratio within the soil is more or less constant.

Cobalt Px values are low and show no trend with depth (Figure 7d). The lowest content is at 60-75 cm. Tx values contrast with Px values within the depth of 15 to 105 cm. The extraction ratio is erratic.

Nickel Px is constant from the A₁ subhorizon to the B₂ subhorizon at a depth of 75 cm (Figure 7e). Below B₂, there is an increase in concentration remaining more or less constant with depth. Tx values are almost uniform throughout the depth of the profile. The extraction ratio is also fairly uniform.

Lead values (Tx, Figure 7f) have no marked accumulation and remain constant with depth.

Copper (Px, Figure 7g) values are constant in the A horizon and B₂ subhorizon. There is a marked accumulation in the lateritic B horizon that is broken at 60-70 cm by a low point. The Tx values indicate an enrichment of Cu in the topsoil and a constant value with depth except at

60-70 cm where an abrupt high value is present. The extraction ratio decreases steadily with depth and is interrupted at 75-90 cm. It decreases below 105 cm.

The pH (Figure 7h) is lowest within the upper 15 cm (A₀ - A₁ sub-horizons). Below 15 cm depth, pH is uniform throughout the profile.

Physical and Chemical Properties of Pit 18

Physical Properties

The profile is made up of a residual solum formed over a granite bedrock.(Table 7).

The A horizon is marked by an accumulation of dark brown organic material within the upper part of the soil (approximately 30 cm). Minor amounts of humic and fresh organic matter also occurs in the B horizon up to a depth of 50 cm.

The B horizon is typically reddish brown and the intensity of colouration increases with depth. It consists of clayey/silty, very fine-grained quartz sand, dark minerals (mafics and magnetite) partly weathered and weathered feldspars of varying sizes. The soil is loose due to the abundance of quartz.

Chemical Properties

Strong similarities of downprofile Px /Tx element distribution patterns are exhibited by Mn, Co, Ni, Cu Px and, to a lesser extent, Cu Tx .

In general all the trace elements have distinctive intervals of accumulation or enrichment. The upper subhorizons Ao-B₂ (Figure 8), have lower contents of Fe, Mn, Zn, Ni, Co, Cu and Pb. The lower subhorizons (B₂-C₂) are characterized by an enrichment of all trace elements. The degree of similarities of the downprofile patterns between Fe, Mn and other trace elements is depicted by correlation coefficients in Table 8.

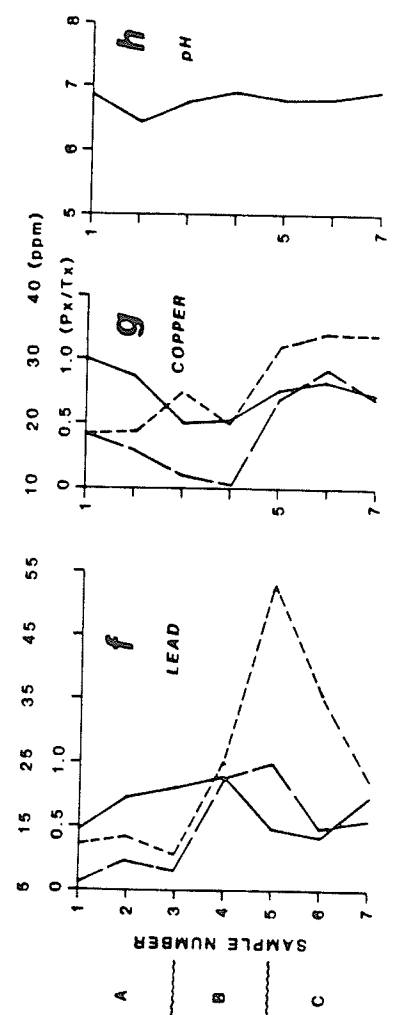
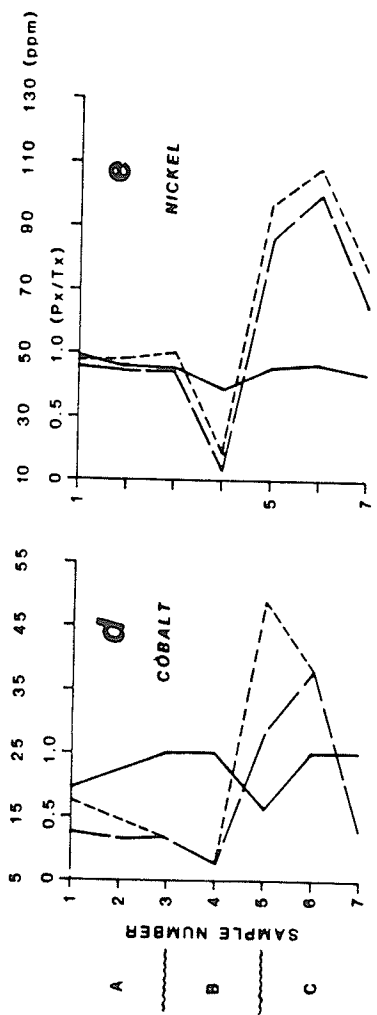
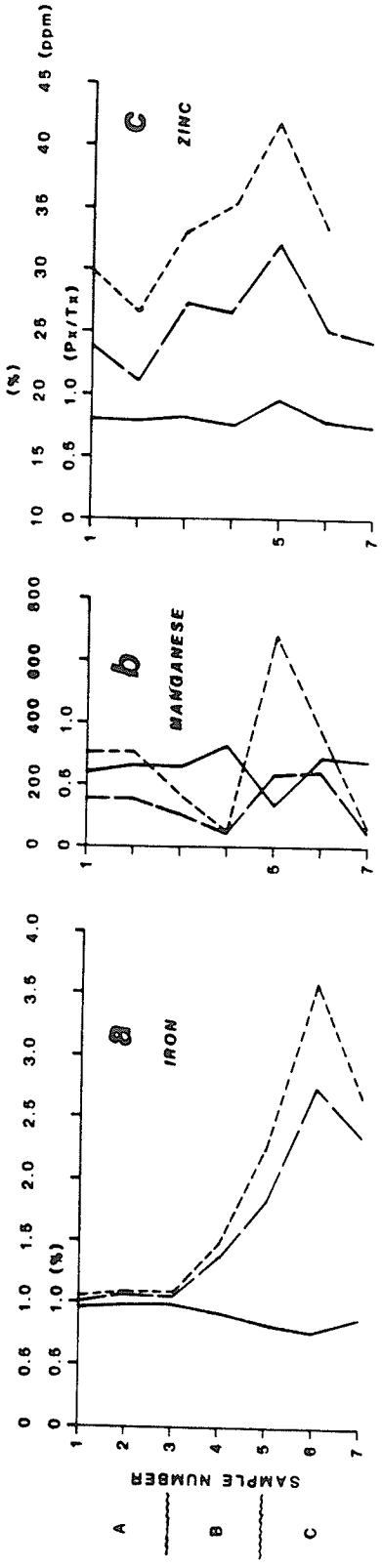
The Fe content (Figure 8a) is lowest in the A horizon. A sharp accumulation occurs in the B horizon and continues into the upper C horizon where it reaches a maximum. The extraction ratio decreases slightly with depth.

Table 7. Soil profile description of Pit 18.

Sample	Depth (cm)	Horizon	Description
1	0	A ₀	Topsoil. Brown, loose clayey/silty very fine grained quartz sand with abundant angular coarse quartz (blue colourless, white) grains, partly weathered and fresh feldspar grains of varying size. Dark minerals (maffics and magnetite) mostly in fine fraction size. Some quartz and dark minerals very well rounded. Ferric staining on quartz and some weathered feldspars.
2	0-15	A ₁	Brown clayey/silty sand as above. Abundant fresh and humic (brown) organic matter. Dark minerals more than above.
3	15-30	A ₂ B ₁	Brown loose clayey/silty quartz sand. Organic matter fresh and humic (brown). Feldspars incompletely weathered. Quartz occasionally occurs in parent rock association with some dark mineral. Lateritic at 2.3 cm depth and transitional to B horizon.
4	30-45	B ₁ B ₂	Reddish brown clayey/silty sand. Very little organic matter. Ferric staining more than above. Some weathering granite fragments present.
5	45-60	B ₂ C ₁	Reddish brown sand as above but more ferric content. Darker reddish brown than above.
6	60-75	C ₁	Reddish brown, clayey/silty, very fine grained quartz sand. Strong ferric colouration in clay/silt size fraction. Abundant fragments of partly weathered granite.
7	75-90	C ₂	Reddish brown. Weathering ferric stained granite. Dark minerals in relatively large sizes.
8	90-105	C ₂	Weathered ferric stained granite.
9	105-120	C ₂	Weathered ferric stained granite.

Figure 8. Downprofile Distribution of Fe, Mn, Zn, Co,
Ni, Pb, Cu and pH. Pit 18.

PIT 18



Partial Extraction ———
 Total Extraction - - -
 Extraction Ratio ———

Table 3. Pearson correlation coefficients (r) for (Fe:Mn):
Mn, Zn, Co, Ni, Pb, and Cu. CV = critical value.
f = confidence level. Pit 18.

Px-Px	Fe:Mn	=	0.35	Px-Px	Fe:Ni	=	0.79
Tx-Tx	Fe:Mn	=	0.14	Tx-Tx	Fe:Ni	=	0.77
Px-Px	Fe:Zn	=	0.15	Px-Px	Mn:Ni	=	0.59
Tx-Tx	Fe:Zn	=	0.46	Tx-Tx	Mn:Ni	=	0.74
Px-Px	Mn:Zn	=	0.42	Px-Px	Fe:Pb	=	0.44
Tx-Tx	Mn:Zn	=	0.10	Tx-Tx	Fe:Pb	=	0.52
Px-Px	Fe:Co	=	0.71	Px-Px	Mn:Pb	=	0.04
Tx-Tx	Fe:Co	=	0.78	Tx-Tx	Mn:Pb	=	0.13
Px-Px	Mn:Co	=	0.89	Px-Px	Fe:Cu	=	0.82
Tx-Tx	Mn:Co	=	0.76	Tx-Tx	Fe:Cu	=	0.92
CV	=	0.58		Px-Px	Mn:Cu	=	0.59
f	=	0.10		Tx-Tx	Mn:Cu	=	0.18

Manganese values (Figure 8b) decrease from an initial high value at the surface (A₀) to the upper B horizon where the profile minimum occurs. A strong enrichment occurs in the rest of the B horizon up to the middle C horizon where a sharp decrease starts. The Tx Mn content at 60 cm is much higher than the Px Mn value. The extraction ratio falls correspondingly.

Zinc accumulation (Figure 8c) starts with the A horizon and is almost restricted to the B horizon. The extraction ratio is very nearly constant throughout the profile except at 60 cm.

Cobalt, Ni and Cu Px (Figures 8d, e and g respectively) patterns have slight differences. Ni values are constant over the A horizon and the lowest value occurs in the B₁ subhorizon. Co and Cu Px contents decrease to the B₁ subhorizon. The Co, Ni and Cu are strongly accumulated in the middle C horizon with much lower amounts in the B horizon. Extraction ratios of Co increase from 0.75 (Figure 8d) to unity in the B horizon except at 60 cm. The Ni extraction ratio is constant with depth at the lowest element concentration in the pit (45 cm).

The Cu extraction ratio is affected mainly by the Tx pattern. Unlike other elements in the profile, the total extraction distribution pattern of Cu does not completely resemble that of the partial extraction. The extraction ratio is lowest at 30 cm and 45 cm depths.

Lead (Figure 8f) is enriched in the middle and lower B horizon. The extraction ratio increases from the A horizon into the B horizon and decreases in the C horizon.

The pH of the profile is slightly less than 7, with the lowest value in the A₁ subhorizon.

Physical and Chemical Properties of Pit 12

Physical Properties

The profile is made up of residual products of the weathering bedrock and distinct horizons have been developed. The A horizon is distinguished by the presence of fresh and humic (brown) organic matter occurring within the reddish brown clayey/silty quartz sand (Table 9). The B horizon is strongly coloured to a brownish red by the accumulation of ferric compounds. It is mineralogically similar to the A horizon and varies by the presence of partly weathered granite fragments. It contains abundant coarse quartz grains. It is dense and lateritic at depth towards the C₁ subhorizon. The granite fragments increase with depth. In the C₁ subhorizon the fragments are less friable and are ferric stained.

Chemical Properties

Accumulation in the B horizon (Figure 9) is the prime feature of the downprofile distribution of all elements with the exception of manganese and cobalt. Correlation of all the elements with Fe and Mn is shown in Table 10.

Iron is accumulated below a depth of 45 cm in the B horizon (Figure 9a). The B₂C₁ horizon marks a second increase of Fe values. The Fe within the B horizon does not vary significantly with depth. The A horizon has lower values. Extraction ratios are high and nearly constant throughout the profile.

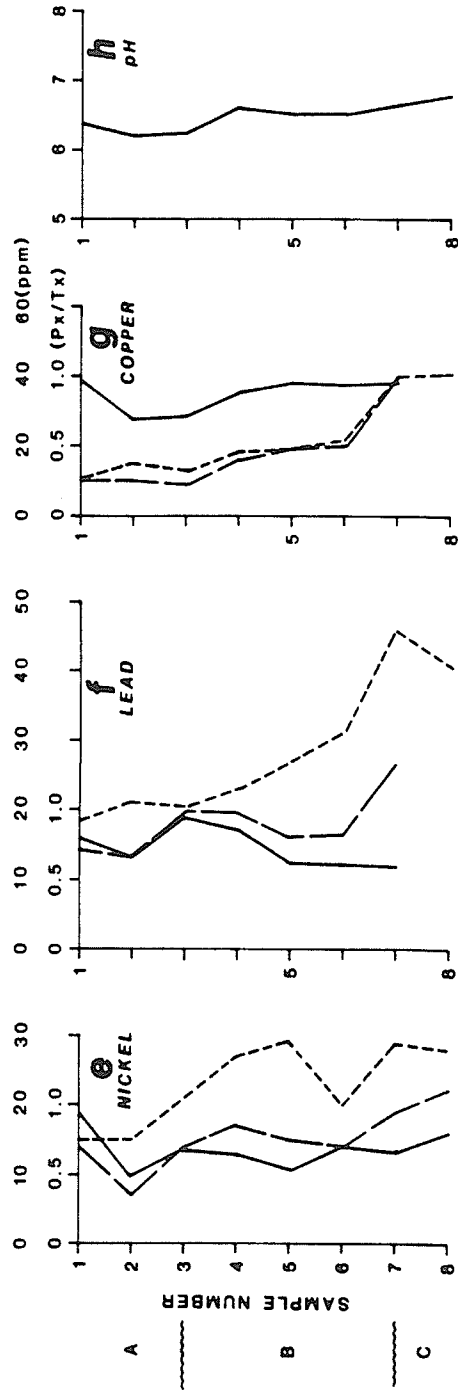
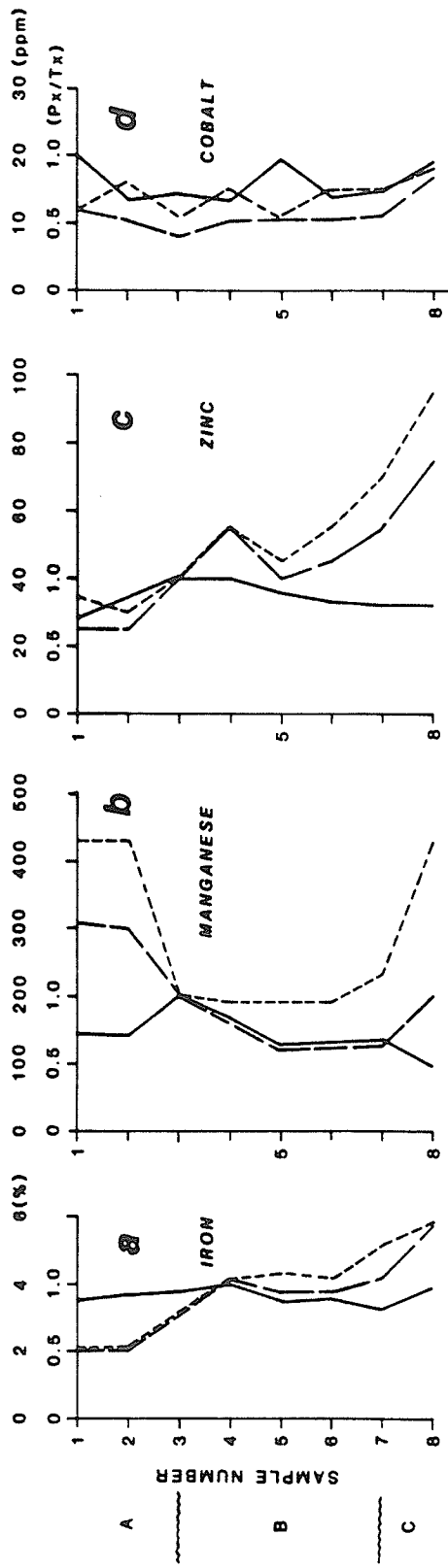
Manganese is distributed in a peculiar form. It is accumulated in the A and C horizons. Both the A and C horizons contain Mn amounts twice that of the B horizon. The extraction ratio is highest at the A₂C₁ subhorizon and decreases to a constant value in the lower B horizon.

Table 9. Soil profile description of Pit 12.

Sample	Depth (cm)	Horizon	Description
1	0	A ₀	Topsoil. Reddish brown, clayey, very fine grained quartz sand. Brown organic matter. Abundant dark minerals (mafic and magnetite) in fine fraction. Coarse quartz grains present.
2	0-15	A ₁	Reddish brown, clayey, very fine grained quartz sand. Brown, humic organic matter present. More mafic minerals than above. Weathered biotite flakes turning silver or yellow. Strong ferric colouration.
3	15-30	A ₂ B ₁	Dark reddish brown clayey/silty very fine grained quartz sand. Abundant dark minerals. Also weathering granite fragments. Ferric colouration very strong.
4	30-45	B ₂	Dark reddish brown clayey/silty very fine grained quartz sand. Dark minerals abundant. Weathering granite fragments more than above.
5, 6	45-90	B ₂	Dark reddish brown, lateritic, dense clayey/silty very fine grained quartz sand. Contains abundant dark minerals. Very strong ferric colouration. Weathering granite fragments increase with depth.
7, 8	90-120	B ₂ C ₁	Reddish brown, clayey/silty sand within weathering granite fragments.

Figure 9. Downprofile distribution of Fe, Mn, Zn, Co,
Ni, Pb, Cu and pH. Pit 12.

PIT 12



Partial Extraction ———
 Total Extraction - - -
 Extraction Ratio ———

Table 10. Pearson correlation coefficients (r) for (Fe:Mn):
Mn, Zn, Co, Ni, Pb, and Cu. CV = critical value.
f = confidence level. Pit 12.

Px-Px	Fe:Mn	=	-0.65	Px-Px	Fe:Ni	=	0.88
Tx-Tx	Fe:Mn	=	-0.29	Tx-Tx	Fe:Ni	=	0.87
Px-Px	Fe:Zn	=	0.93	Px-Px	Mn:Ni	=	-0.48
Tx-Tx	Fe:Zn	=	0.98	Tx-Tx	Mn:Ni	=	-0.48
Px-Px	Mn:Zn	=	-0.54	Px-Px	Fe:Pb	=	0.71
Tx-Tx	Mn:Zn	=	0.03	Tx-Tx	Fe:Pb	=	0.85
Px-Px	Fe:Co	=	0.59	Px-Px	Mn:Pb	=	-0.52
Tx-Tx	Fe:Co	=	0.42	Tx-Tx	Mn:Pb	=	-0.07
Px-Px	Mn:Co	=	0.41	Px-Px	Fe:Cu	=	0.67
Tx-Tx	Mn:Co	=	0.12	Tx-Tx	Fe:Cu	=	0.87
CV	=	0.62		Px-Px	Mn:Cu	=	0.54
f	=	0.10		Tx-Tx	Mn:Cu	=	0.05

Zinc (Figure 9c) has an overall increasing trend with depth. This increase in the A horizon continues into the upper B horizon (30 - 45 cm depth). Another trend of increasing Zn content begins at the low content point at 60 cm depth in the B horizon and continues smoothly into the C₁ subhorizon. Extraction ratios are lowest in the A horizon and highest in the upper B horizon. The rest of the profile has an approximately constant ratio.

Cobalt (Figure 9d) shows very little variation with depth. A slight increase is in the C₁ subhorizon. The extraction ratio is more or less constant except at 60 cm depth.

Nickel is accumulated in the A and B horizons (Figure 9e). The B₂C₁ subhorizon has a second and highest increase. The extraction ratio varies within a narrow range downprofile.

Lead Px distribution has a twofold accumulation in the A and upper B horizon and the C₁ subhorizon. The Pb Tx value increases are gradual and reach a maximum within the C₁ horizon. The change from B₂ at 90 cm depth to the C₁ subhorizon is the sharpest (Figure 9f). The extraction ratio is highest in the upper B horizon.

Copper values (Figure 9g) are constant in the A horizon and increase slightly with depth in the B horizon. The C₁ subhorizon has the maximum accumulation. Extraction ratios are lower in the A horizon, otherwise each horizon is characterized by a constant ratio.

The pH values (Figure 9h) are lowest in the A horizon and highest in the upper B horizon. At depth, the lower B horizon has slightly lower values. There is a rise in pH in the C₁ subhorizon.

Physical and Chemical Properties of Pit 11

Physical Properties

The profile is residual (Table 11) and is derived from the underlying granite. The horizons are distinguishable by their colour and textural differences. The A horizon is brown and shallow. It consists of fresh and decayed brown humic matter. The main mineral is quartz of a very fine grain size. Clay and silt are abundant. Coarse quartz and dark minerals (mafics and magnetite) are also present. Some partly weathered feldspars are ferric stained.

The upper B horizon is reddish brown and contains little organic matter. In addition to coarse quartz and dark minerals, incompletely weathered granite fragments occur within the whole horizon and increase with depth. The ferric colouration becomes more intense at depth within the B horizon.

The C horizon occurs below 75 cm. The partly weathered granite fragments are predominant and below a depth of approximately 90 cm, the weathered granite is white and friable.

Chemical Properties

In general, the lower B horizon and upper C horizon have higher element contents. The extent of similarity between Fe, Mn and the other trace elements in the patterns of downprofile distribution is indicated by correlation coefficients (Table 12).

Iron has an accumulation in the lower B horizon (Figure 10a). The A and C horizons have constant and lower contents. The accumulation within the B horizon is within a short interval (approximately 15 cm). Extraction ratios vary slightly with depth.

Table 11. Soil profile description of Pit 11.

Sample	Depth	Horizon	Description
1	0	A ₀	Topsoil. Light reddish brown clayey/silty fine grained quartz sand. Organic matter fresh. Abundant grains of coarse quartz.
2	0-15	A ₁ A ₂	Brown with greenish tint. Clayey/silty, very loose quartz sand. Organic matter fresh and humic. Coarse blue quartz grains and dark minerals (mafics and magnetite) in fine fraction. Ferric staining on partly weathered minerals.
3	15-30	A ₂ B ₁	Reddish brown clayey/silty very fine grained quartz sand. Minor organic matter. Coarse blue quartz and dark minerals present.
4	30-45	B ₁	Reddish brown clayey/silty quartz sand as above. Increase in coarse quartz grains and appearance of partly weathered granite fragments.
5	45-60	B ₂	Reddish brown, denser, clayey/silty quartz sand. Increase in coarse grains of quartz and partly weathered granite fragments.
6	60-75	B ₂ C ₁	Reddish brown clayey/silty quartz sand. Dominated by coarse quartz (blue and colourless) and by partly weathered granite fragments.
7	75-90	C ₁	Weathered granite with ferric staining of fragments and reddish brown fines. Dark minerals in larger sizes. Some feldspar completely weathered.
8, 9	90-120	C ₂	Weathered parent rock (granite). Mainly light coloured. Some friable feldspars.

Figure 10. Downprofile distribution of Fe, Mn, Zn,
Co, Ni, Pb and pH. Pit 11.

PIT 11

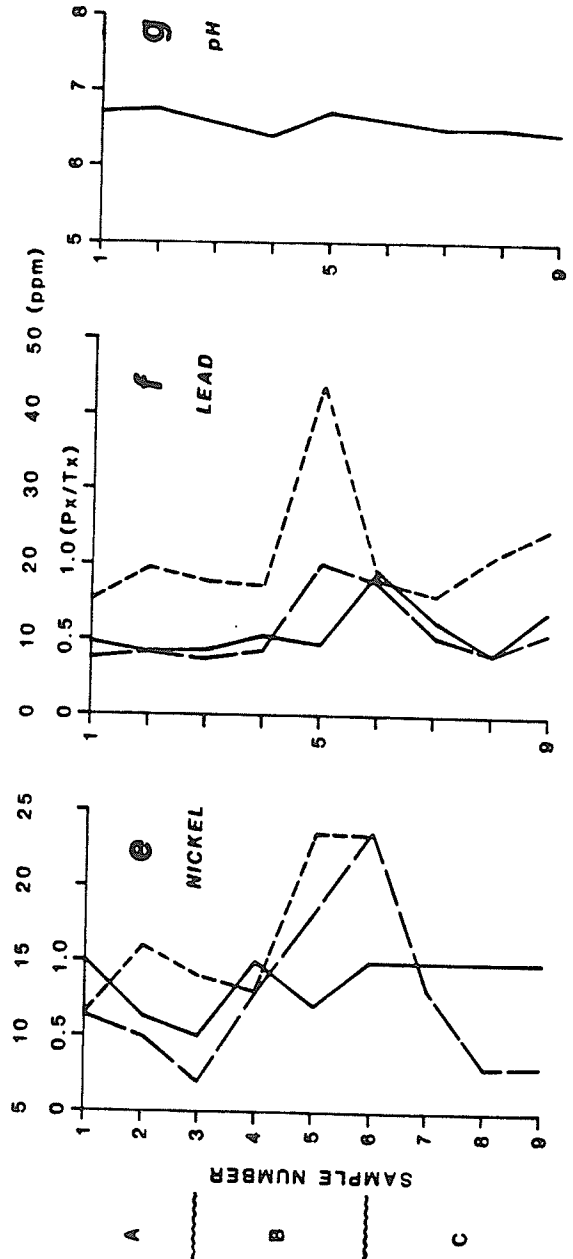
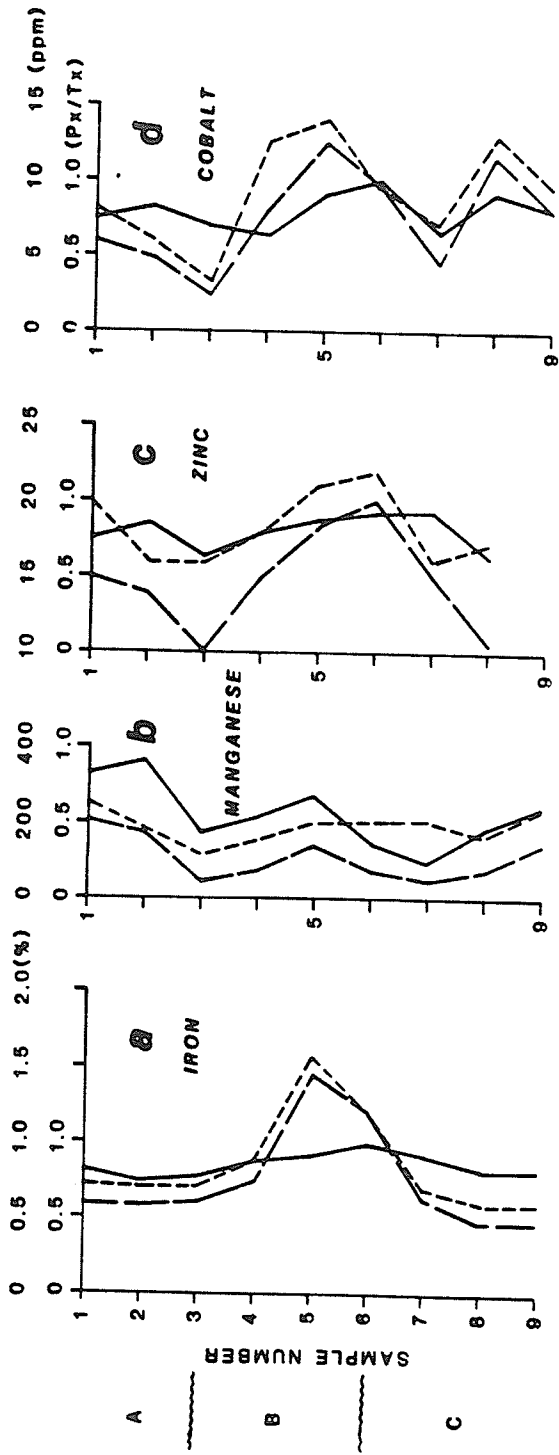


Table 12. Pearson correlation coefficients (r) for (Fe:Mn):

Mn, Zn, Co, Ni, and Pb. CV = critical value.

f = confidence level. Pit 11.*

Px-Px	Fe:Mn	=	0.28	Px-Px	Fe:Ni	=	0.86
Tx-Tx	Fe:Mn	=	0.27	Tx-Tx	Fe:Ni	=	0.94
Px-Px	Fe:Zn	=	0.82	Px-Px	Mn:Ni	=	0.03
Tx-Tx	Fe:Zn	=	0.75	Tx-Tx	Mn:Ni	=	0.30
Px-Px	Mn:Zn	=	0.39	Px-Px	Fe:Pb	=	0.85
Tx-Tx	Mn:Zn	=	0.51	Tx-Tx	Fe:Pb	=	0.71
Px-Px	Fe:Co	=	0.67	Px-Px	Mn:Pb	=	0.45
Tx-Tx	Fe:Co	=	0.41	Tx-Tx	Mn:Pb	=	0.08
Px-Px	Mn:Co	=	0.38	Px-Px	Fe:Cu	=	n.a.
Tx-Tx	Mn:Co	=	0.11	Tx-Tx	Fe:Cu	=	n.a.
CV	=	0.58		Px-Px	Mn:Cu	=	n.a.
f	=	0.10		Tx-Tx	Mn:Cu	=	n.a.

* n.a. = no analysis

Manganese Px values are highest in the A₁, lower B₂ and C₂ subhorizons. The Tx values indicate lower concentrations only in the upper B horizon. The extraction ratios vary considerably with depth.

Zinc (Figure 10c) has maximum values in the B₂C₁ subhorizon. The A and C horizons have decreasing Zn contents. The extraction ratios are more or less constant in the B and upper C horizon.

Cobalt (Figure 10d) decreases in the A horizon. It is strongly accumulated in the B horizon and high values also occur in the C horizon. The extraction ratio varies throughout the profile.

Nickel contents (Figure 10e) like Mn, Zn and Co decrease in the A horizon. The maximum value of Ni in the pit occurs in the lower B horizon (B₂C₁ subhorizon). The C₂ subhorizon contains low Ni concentrations. The extraction ratio varies in the A and B horizon but is constant, at unity, in the C horizon.

Lead is accumulated in the depths 60-75 cm. A slight increase occurs below 105 cm (Px) and 90 cm (Tx).

The profile has pH values below 7.00. The lowest pH (6.40) occurs in the upper B₂ subhorizon.

Physical and Chemical Properties of Pit 9

Physical Properties

The profile consists of residual soil formed from the weathering of the granite. Horizons are distinct. The A horizon is shallow and comprises fresh and humic (brown) organic matter. It grades into the reddish brown B horizon. The latter is developed to a depth of 73 cm. Both the A and the B horizon contain a clayey/silty very fine grained quartz sand. Coarse grains of quartz occur in abundance within the B horizon. Weathered and friable granite fragments increase with depth. The C horizon is coarse and consists of weathered granite fragments with ferric colouration of the clay/silt fraction and staining of weathered feldspars. Below the transition with the B horizon, the weathered granite is rusty brown and less disintegrated (Table 13).

Chemical Properties

The main similarity in the downprofile distribution of Fe, Zn, Co and Ni is the increase with depth through all the horizons (Figure 11). The Pb pattern is slightly different whereas that of Mn is unique. The similarities are indicated by correlation coefficients (Table 14).

Iron is accumulated in the lower B and upper C horizon (Figure 11a). The increase with depth over the upper 60 cm is slight compared with the sudden enrichment in the lower profile (below 60 cm depth). Extraction ratios are high and near constant.

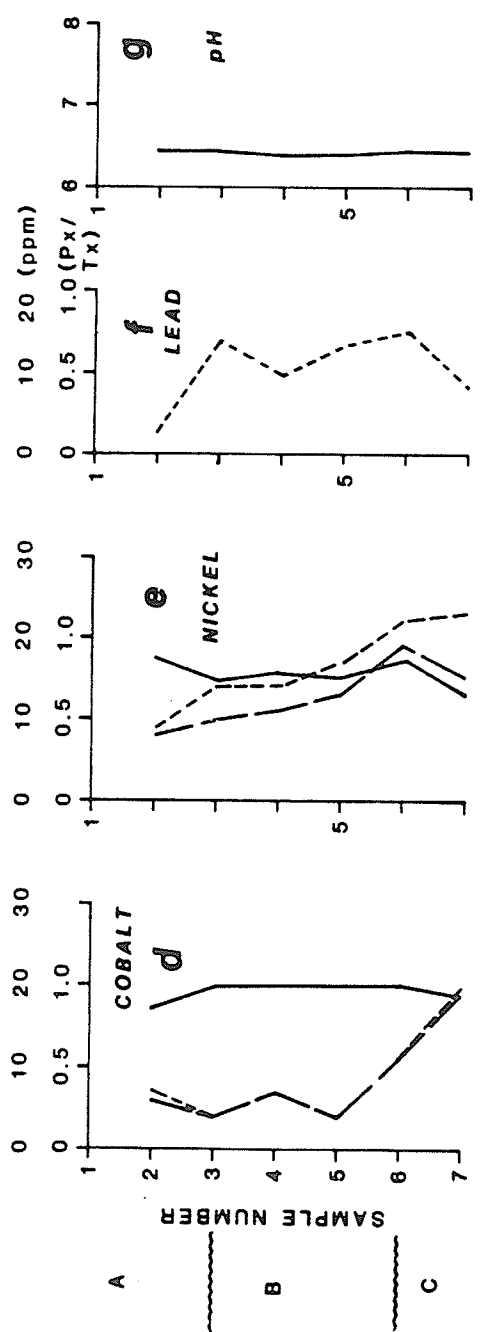
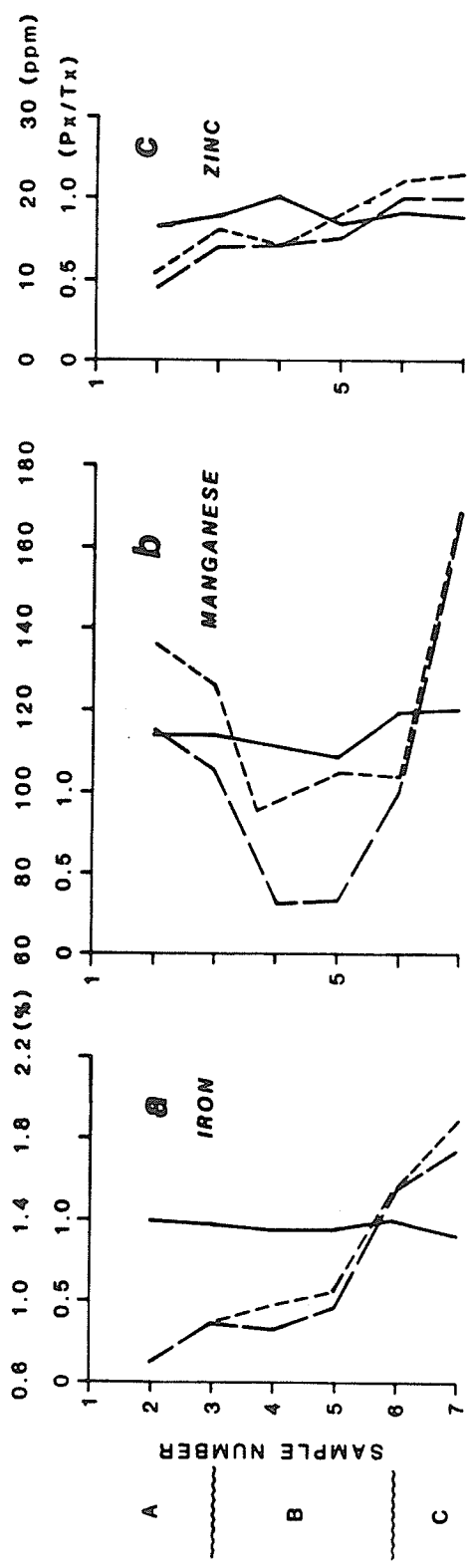
Manganese has a unique distribution, being more concentrated in the A and upper B horizon and within the C horizon (Figure 11b). Extraction ratios fall slightly with depth but increase to unity in the C horizon.

Table 13. Soil profile description of Pit 9.

Sample	Depth (cm)	Horizon	Description
1	0	A ₁	Topsoil, light reddish brown clayey/silty very fine grained quartz sand. Organic matter, coarse quartz. Some dark minerals (mafics and magnetite).
2	0-15	A ₂	Light reddish brown clayey/silty very fine grained quartz sand. Some brown humic and fresh organic matter. Dark minerals in fine fraction.
3	15-30	A ₂ B ₁	Reddish brown clayey/silty very fine grained quartz sand. Coarse (blue) quartz abundant and sometimes encloses needle-like dark minerals. Abundant small grains of weathered feldspars. Dark minerals in fine fraction.
4	30-45	B ₂	Reddish brown clayey/silty sand as above. Increase of ferric colouration and weathered granite fragments.
5	45-60	B ₂	Reddish brown clayey/silty sand. Strong ferric colouration. Increase in size and number of coarse quartz grains and rock fragments.
6	60-75	B ₂ C ₁	Reddish brown clayey/silty quartz sand. Transitional to C horizon. Weathered rock fragments dominant.
7	75-90	C ₁	Rusty brown disintegrated granite. Friable. Clay and silt from above (ferruginous) present.

Figure 11. Downprofile distribution of Fe, Mn, Zn,
Co, Ni, Pb and pH. Pit 9.

PIT 9



Partial Extraction ———
 Total Extraction - - -
 Extraction Ratio ———

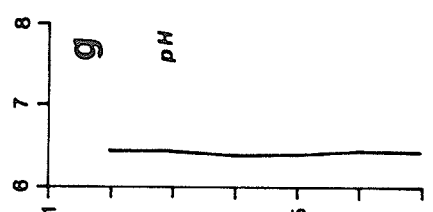


Table 14. Pearson correlation coefficients (r) for (Fe:Mn):

Mn, Zn, Co, Ni and Pb. CV = critical value.

f = confidence level. Pit 9.^{*}

Px-Px	Fe:Mn	=	0.57	Px-Px	Fe:Ni	=	0.99
Tx-Tx	Fe:Mn	=	0.24	Tx-Tx	Fe:Ni	=	0.90
Px-Px	Fe:Zn	=	0.96	Px-Px	Mn:Ni	=	0.19
Tx-Tx	Fe:Zn	=	0.97	Tx-Tx	Mn:Ni	=	0.17
Px-Px	Mn:Zn	=	0.37	Px-Px	Fe:Pb	=	n.a.
Tx-Tx	Mn:Zn	=	0.28	Tx-Tx	Fe:Pb	=	0.02
Px-Px	Fe:Co	=	0.85	Px-Px	Mn:Pb	=	n.a.
Tx-Tx	Fe:Co	=	0.77	Tx-Tx	Mn:Pb	=	0.50
Px-Px	Mn:Co	=	0.81	Px-Px	Fe:Cu	=	n.a.
Tx-Tx	Mn:Co	=	0.28	Tx-Tx	Fe:Cu	=	n.a.
CV	=	0.67	Px-Px	Mn:Cu	=	n.a.	
f	=	0.10	Tx-Tx	Mn:Cu	=	n.a.	

* n.a. = no analysis

Zinc (Figure 11c) has its lowest value in the A horizon. Both the Zn Px values in the B and C horizons have constant values with the higher contents occurring in the latter horizon. The Tx content increases smoothly with depth. The extraction ratio varies slightly within a narrow range and is constant with depth.

Cobalt (Figure 11d) is accumulated in the C horizon. The extraction ratio is unity except in the A₂ and C₁ subhorizons.

Nickel values increase smoothly with depth (Figure 11e) up to the base of the B horizon. The C₁ subhorizon has lower contents than the B₂C₁ subhorizon. The extraction ratio is nearly constant throughout the depth of the profile.

Lead has an overall higher content in the B horizon (Figure 11f).

The pH of the profile is essentially constant with depth at 6.5 (figure 11g).

Physical and Chemical Properties of Pit 19

Physical Properties

The pit consist of transported soil derived from weathering granite. Several cycles of alternating medium and coarse sand occur in the upper 60 cm of the profile. Below, the sand is dark due to organic matter and is also very coarse. The mineralogy throughout the profile is similar and consists of clay and silt size minerals (mostly quartz, clay and dark minerals) partly weathered feldspars and granite fragments and dark minerals (Table 15).

Chemical Properties

The elements Zn, Co, Ni, Pb and Cu have greater abundances within the C horizon and below 60 cm depth.

Zinc (Figure 12a) is low in the A horizon but is high within the C horizon below 60 cm. Extraction ratios are erratic in the upper 60 cm but are uniform below 60 cm.

Cobalt (Figure 12b) contents vary slightly with depth. The lower C horizon (below 60 cm) contains slightly higher contents but there is no significant change with depth. The extraction ratio is fairly uniform throughout the profile.

Nickel (Figure 12c) has a near uniform and low Px values downprofile. The Tx contents differ by reflecting higher contents in the lower parts of the profile. Extraction ratios are low and show slight variation with depth.

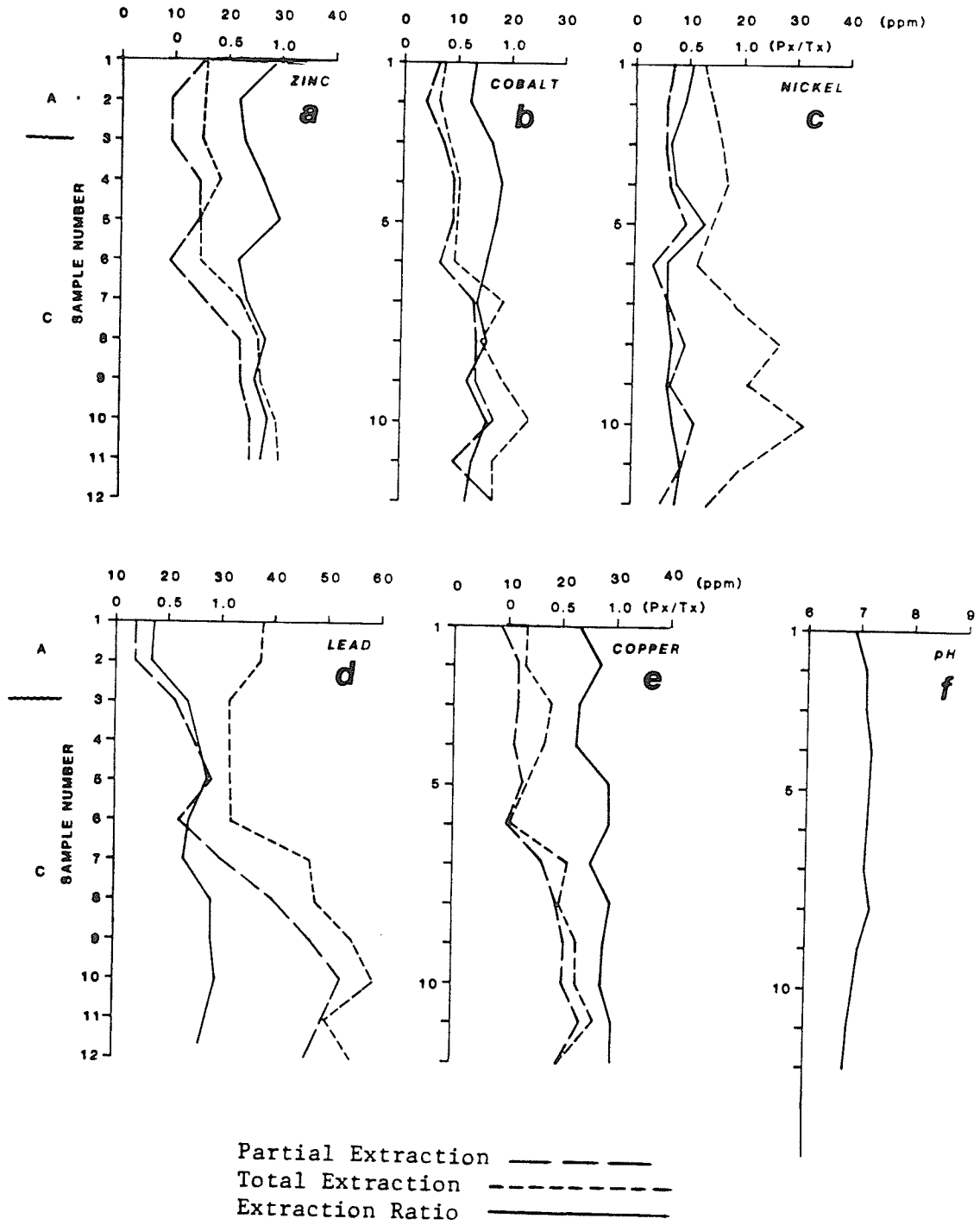
Lead (Figure 12d) is distinctly accumulated below 60 cm depth. The Pb contents increase with depth and reach a maximum value at 150 cm. The extraction ratios vary significantly and are slightly higher at depth.

Table 15. Soil profile description of Pit 19

Sample	Depth (cm)	Horizon	Description
1	0	Ao	Topsoil. Brownish red, clayey/silty sand. Fresh and humic (brown) organic matter. Partly weathered feldspars and biotite. Magnetite grains with brownish black coating. Some weathering feldspars and clay lumps are ferric stained.
2,3	0-30	A ₁ C	Light brownish red clayey/silty sand. Less and smaller dark minerals (mafics and magnetite). Some magnetite enclosed by quartz. Granite fragments abundant. Weathered and partly weathered feldspars present.
4	30-45	C	Light brownish red. Weathered feldspar as above. Dark minerals occur in fine fraction. Clay and silty about 30-45%. Fine grains cemented by clay.
5	45-60	C	Light brownish red, clayey/silty coarse sand. Feldspars partly weathered. Dark minerals in fine fraction. Black needle-like minerals in quartz weather with a ferric stain.
6,7,8	60-105	C	Dark brown clayey/silty coarse sand. Black humic organic matter abundant. Partly weathered feldspars. Dark minerals comparatively low.
9	105-120	C	Dark brown coarse sand as above. Abundant coarse quartz grains, partly weathered feldspars, clay lumps (from weathered feldspars). Low content of dark minerals. Organic matter (black).
10,11,12	120-165	C	Very coarse granite fragments, rounded grains of cemented quartz and dark minerals. Weathered silvery biotite and partly weathered feldspars. Organic matter present.

Figure 12. Downprofile distribution of Zn, Co, Ni,
Pb, Cu and pH. Pit 19.

PIT 19



Copper contents below 60 cm depth are higher than above (Figure 12e). The extraction ratio is erratic in the upper profile and more uniform below.

The soil has a slightly acidic pH. The pH increases slightly with depth.

Physical and Chemical Properties of Pit 8

Physical Properties

The profile consists of transported soil derived from a weathered granite. Only the A and B horizons have been developed. The A horizon differs from the B by the presence of dark to dark brown humic matter and has a finer texture than the B horizon. In the latter horizon, coarse quartz grains are abundant. Granite rock fragments are weathered and are rare at depth. The soil is moist below 80 cm. (Table 16).

Chemical Properties

All elements with the exception of iron (Px) and manganese are generally featureless with respect to distribution downprofile. The extent of similarities is represented by correlation coefficients in Table 17.

Iron (Figure 13a) has Px values that indicate an accumulation. Below 80 cm, there is a constant and higher Fe content. Mottling has resulted in the lowering of the Fe content below 150 cm. The Tx values are less affected by depth. Extraction ratios are constant above and below 80 cm. In the latter interval they are higher.

Manganese (Figure 13b) has a higher content in the upper A horizon. The middle B horizon (45-150 cm) has constant values. In the mottled zone (below 150 cm), the Mn content decreases sharply with depth. Extraction ratios are constant.

Zinc (Figure 13c) downprofile distribution is featureless and shows slight decreases below 150 cm. Extraction ratios are constant.

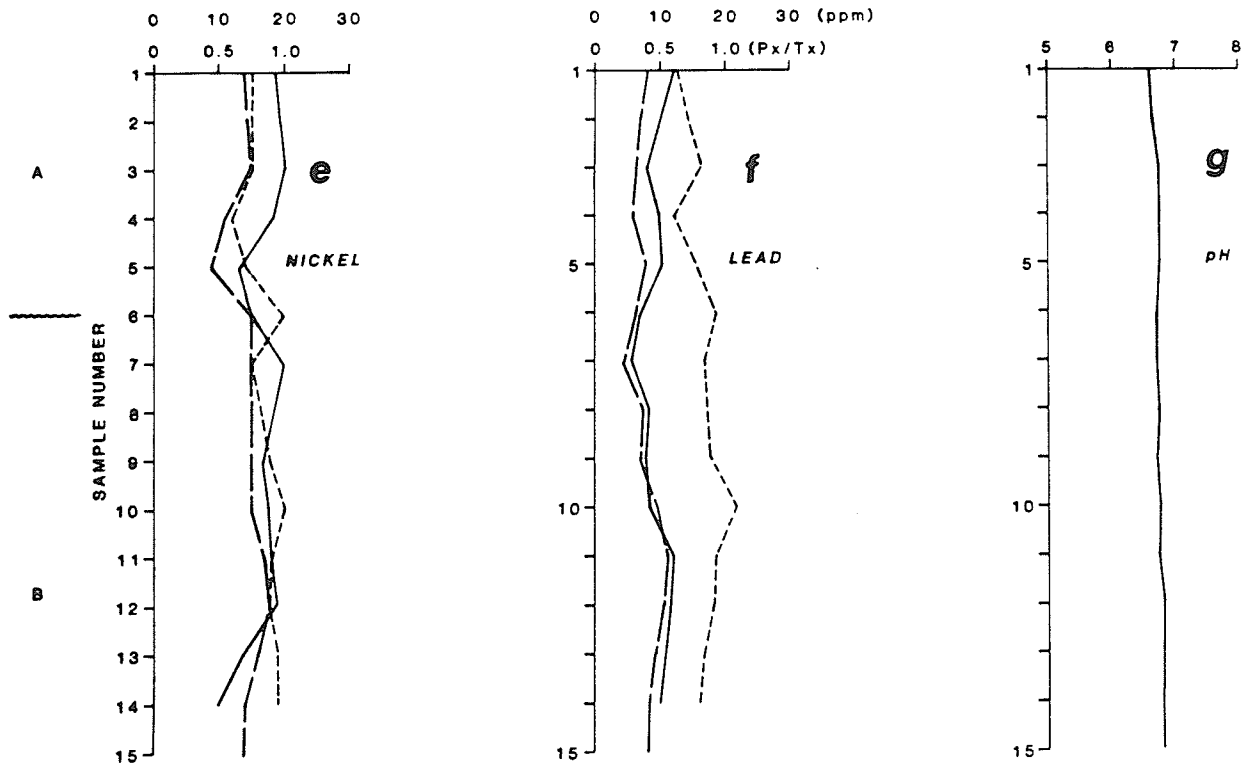
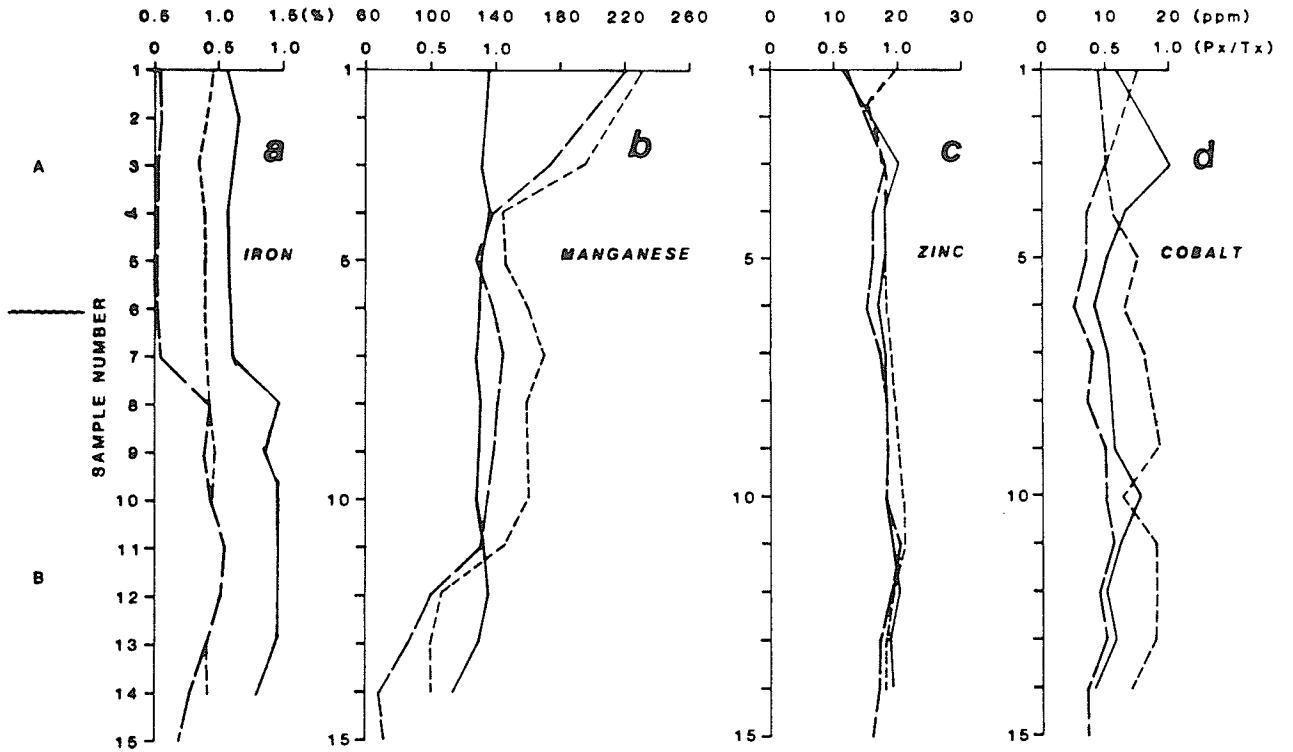
Cobalt (Figure 13d) values are nearly constant downprofile. The extraction ratio is highest at 30 cm depth, otherwise, it remains uniform throughout the profile.

Table 16. Soil profile description of Pit 8.

Sample	Depth (cm)	Horizon	Description
1	0	A ₀	Topsoil. Dark brown clayey/silty medium grained quartz sand. Organic matter mostly fresh. Dark minerals (mafics and magnetite) rare.
2	0-15	A ₁	Dark brown clayey/silty medium grained quartz sand. Fresh and decayed (brown, humic) organic matter. Some weathering feldspars (medium-grained).
3,4,5, 6	15-60	A ₂ A ₂ B ₁	Dark brown clayey/silty medium grained sand. Brown, humic organic matter decreases with depth. Coarser fragments (quartz and some dark minerals). Few granite fragments.
7,8,9,10		B ₂	Light brownish red. Moist clayey/silty quartz sand. Increase in coarse quartz grains with depth. Some granite fragments (rare). Some dark minerals also rare.
11,12, 13,14 15	135-240		Yellowish brown, mottled (at 150 cm), clayey/silty quartz sand. Coarse grains of blue quartz abundant. Lumps of completely weathered feldspars present. Granite rock fragments almost completely absent below 150 cm depth. Dark minerals equally rare.

Figure 13. Downprofile distribution of Fe, Mn, Zn,
Co, Ni, Pb and pH in Pit 8.

PIT 8



Partial Extraction — — — — —
 Total Extraction - - - - -
 Extraction Ratio —————

Table 17. Pearson correlation coefficients (r) for

(Fe, Mn): Mn, Zn, Co, Ni, and Pb.

CV = critical value. f = confidence level.

Pit 8.

Px-Px	Fe:Mn	=	0.10	Px-Px	Fe:Ni	=	0.66
Tx-Tx	Fe:Mn	=	0.11	Tx-Tx	Fe:Ni	=	0.46
Px-Px	Fe:Zn	=	0.75	Px-Px	Mn:Ni	=	0.49
Tx-Tx	Fe:Zn	=	0.79	Tx-Tx	Mn:Ni	=	-0.26
Px-Px	Mn:Zn	=	0.40	Px-Px	Fe:Pb	=	0.71
Tx-Tx	Mn:Zn	=	0.32	Tx-Tx	Fe:Pb	=	0.49
Px-Px	Fe:Co	=	0.65	Px-Px	Mn:Pb	=	-0.28
Tx-Tx	Fe:Co	=	0.65	Tx-Tx	Mn:Pb	=	-0.29
Px-Px	Mn:Co	=	0.19	CV	=	0.46	
Tx-Tx	Mn:Co	=	0.46	f	=	0.10	

Nickel decreases slightly in the A horizon and below 165 cm depth (Figure 13e). Extraction ratio values are high and variable.

Lead values (Figure 13f) are low and do not vary with depth. The Tx and Px patterns are different. Extraction ratios vary within a narrow range.

The profile has a slightly acidic and uniform pH.

Physical and Chemical Properties of Pit 7

Physical Properties

The profile consists of transported material derived from a weathered granite. Layers of gravelly and medium grained sand are recognizable.

The A horizon is 15 cm thick and is marked by the dark colouration of organic matter. The humic matter is present to a depth of 90 cm (Table 18) within the C horizon. Coarse grains of feldspar, quartz and granite are abundant throughout the profile. Clay and silt occur in all parts of the soil.

Chemical Properties

The distribution of Fe, Mn, and Zn within the profile show similarities of trends. Cu and Ni also have similar patterns (Figure 14). Correlation of the different element patterns with Fe and Mn is listed in Table 19.

Iron (Figure 14a) has maximum contents in the depth interval of 135 to 150 cm, in the very coarse pebbly sand. Above and below these depths the Fe content is constant. Extraction ratios decrease slightly with depth.

Manganese (Figure 14b), like Fe, attains maximum contents of the 135-150 cm depth. Extraction ratios also fall with depth.

Zinc (Figure 14c), like Fe and Mn, has maximum contents in the coarse and pebbly sand at 135-150 cm depth. The extraction ratios have an overall decrease with depth.

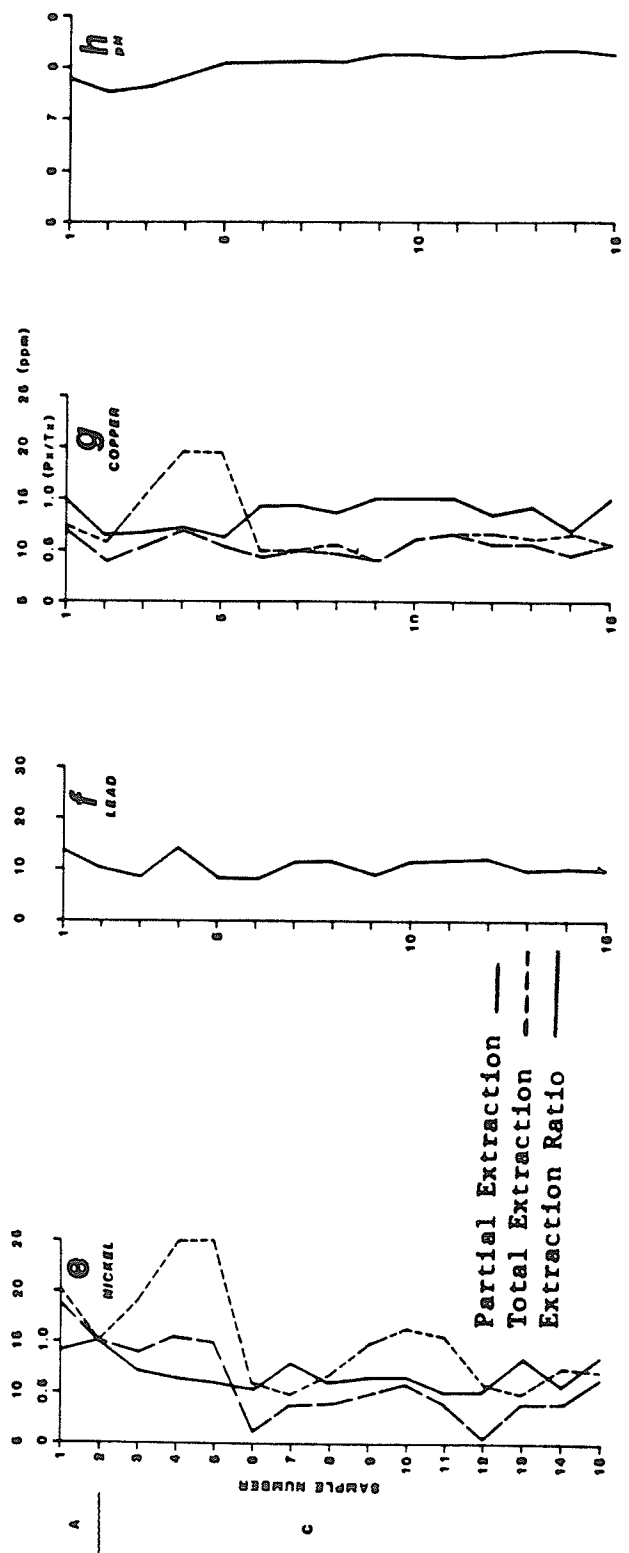
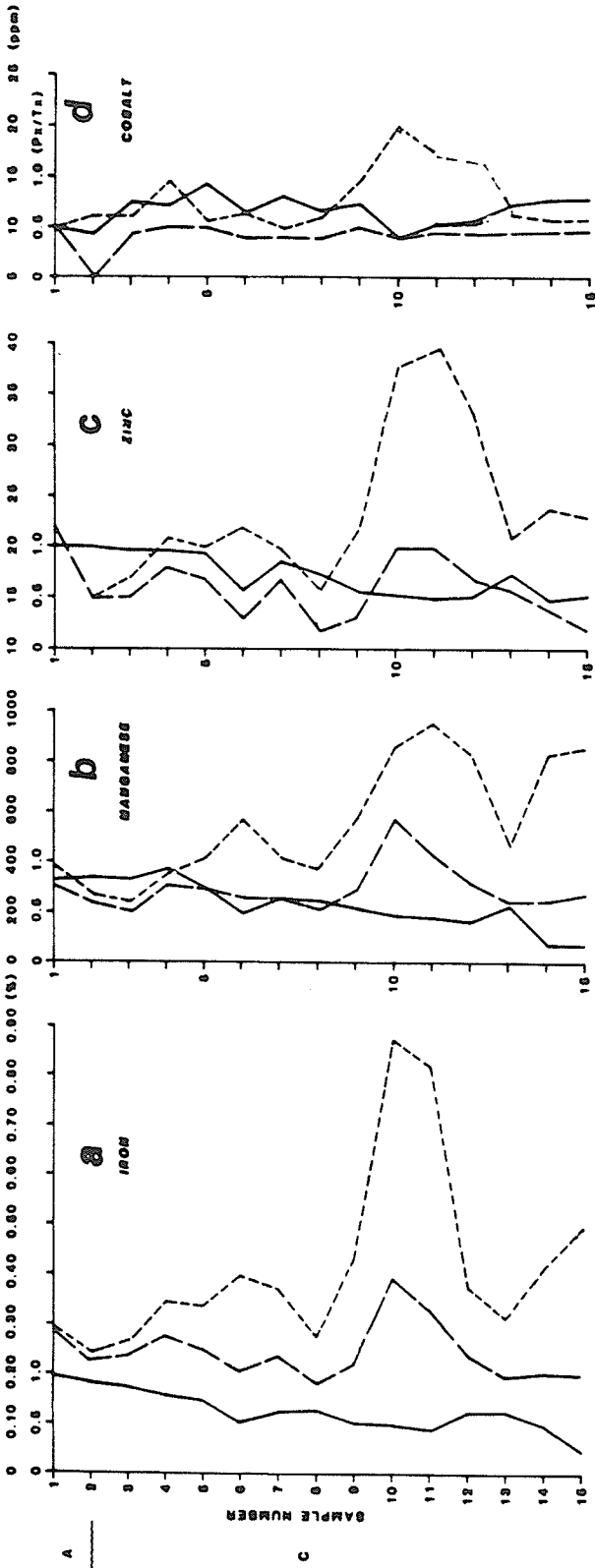
Cobalt values (except for Tx at 135-145 cm) are fairly uniform throughout the profile. The extraction ratio varies but the overall pattern is a uniform one (Figure 14d).

Table 18. Soil profile description of Pit 7.

Sample	Depth (cm)	Horizon	Description
1	0	Ao	Topsoil. Dark brown. Loose clayey/silty very fine grained quartz sand. Fresh and humic (brown) organic matter. Weathered biotite. Other dark minerals (mafics and magnetite) in fine fraction. Ferric staining on some quartz grains.
2	0-15	A ₁ C	Dark reddish brown. Loose clayey/silty quartz sand as above. Brown organic matter. Dark minerals abundant. Slight reaction with acid. Abundant rock fragments.
3,4	15-45	C	Dark brownish red, loose, clayey/silty quartz sand as above. Dark minerals in fine and coarse fractions. Some weathering with accompanying ferric stain. Some magnetite still attached to feldspar. Granite fragments present. Some humic organic matter.
5,6,7	45-90	C	Reddish brown, clayey/silty quartz sand. Coarse angular quartz dominant. More dark minerals with depth, both angular and rounded. Organic matter up to 60 cm. Abundant rock fragments, weathered feldspars. Mild reaction with acid.
8	90-105		Reddish brown coarse clayey/silty sand. Weathering silvery biotite and other dark minerals. Dark minerals occur in all grain sizes except as coarse grains. The dark minerals (except magnetite) are more than above.
9	105-120		Reddish brown with lesser ferric staining than above. Abrupt change from above to coarse pebbly gravel. Weathering feldspars and rock fragments.
10,11, 12,13, 14,15			Reddish brown clayey/silty very coarse pebbly sand with a high content of dark minerals in fine and coarse fraction. Coarse, angular, partly weathered granite fragments. Other rock fragments present.

Figure 14. Downprofile distribution of Fe, Mn, Zn, Co,
Ni, Pb, Cu and pH. Pit 7.

PIT 7



Partial Extraction —
Total Extraction - - -
Extraction Ratio —

Table 19. Pearson correlation coefficients (r) for

(Fe, Mn): Mn, Zn, Co, Ni, Pb and Cu.

CV = critical value. f = confidence level. Pit 7.*

Px-Px	Fe:Mn	=	0.55	Px-Px	Fe:Ni	=	0.26
Tx-Tx	Fe:Mn	=	0.76	Tx-Tx	Fe:Ni	=	0.04
Px-Px	Fe:Zn	=	0.77	Px-Px	Mn:Ni	=	0.01
Tx-Tx	Fe:Zn	=	0.87	Tx-Tx	Mn:Ni	=	0.13
Px-Px	Mn:Zn	=	0.60	Px-Px	Fe:Pb	=	n.a.
Tx-Tx	Mn:Zn	=	0.86	Tx-Tx	Fe:Pb	=	0.42
Px-Px	Fe:Co	=	-0.10	Px-Px	Mn:Pb	=	n.a.
Tx-Tx	Fe:Co	=	0.81	Tx-Tx	Mn:Pb	=	-0.22
Px-Px	Mn:Co	=	0.25	Px-Px	Fe:Cu	=	0.56
Tx-Tx	Mn:Co	=	0.70	Tx-Tx	Fe:Cu	=	0.20
CV	=	0.44	Px-Px	Mn:Cu	=	0.55	
f	=	0.10	Tx-Tx	Mn:Cu	=	-0.22	

* n.a. = no analysis

Nickel (Figure 14e) is abundant in the organic matter-rich part of the profile (above 75 cm). Extraction ratios are variable, but have no depth related pattern.

Lead contents (Figure 14f) do not vary with depth within the profile.

Copper is accumulated in the upper part of the profile where organic matter is present (Figure 14g).

The profile is slightly alkaline, with the lowest pH value of 7.5 occurring in the upper A horizon. There pH increases slightly and gradually with depth to a maximum of about 8.3

Physical and Chemical Properties of Pit 6

Physical Properties

The profile consists of transported material. The A horizon is made of 60 cm of sand with dark brown humic matter. The humus content decreases with depth, and at 60 cm, a white uniform B horizon begins. The A and the B horizon are mineralogically similar and contain clay, silt and very fine quartz. Coarse quartz grains increase with depth. Partly weathered feldspars or granite fragments are very rare (Table 20).

Chemical Properties

The distribution of Fe, Mn, Co, Ni, Pb and Cu down profile is relatively featureless (Figure 15). Fe, Mn and Ni have slightly higher abundances in the upper A horizon. Correlation coefficients of the relationship between Fe, Mn and other elements is given in Table 21.

Iron (Figure 15a) has slightly higher values in the upper A horizon. The rest of the pit has a fairly uniform Fe content and extraction ratio.

Manganese (Figure 15b) is enriched in the A horizon. The increase with depth is very slight for both Px and Tx values. Extraction ratios increase slightly with depth.

Cobalt variations (Figure 15c) are erratic due to very low concentrations which approach the detection limit of the instrument.

Nickel is accumulated in the upper A horizon (Figure 15d). The rest of the profile (below 90 cm) has more or less uniform contents of Ni. The Tx content has a more gradual decrease of Ni from the A to B horizon. The extraction ratios are variable in the upper 90 cm but become more uniform below this depth.

Table 20. Soil profile description of Pit 6.

Sample	Depth (cm)	Horizon	Description
1	0	Ao	Topsoil. Brown clayey/silty loose very fine grained quartz sand. Appears sorted. Feldspar grains rare. Dark minerals (maffics and magnetite) in fine fraction. Abundant organic matter (fresh and decayed).
2	0-15	A ₁	Brown clayey/silty quartz sand. Humic, brown organic matter and coarse quartz grains. Low content of dark minerals.
3,4,5	15-60	A ₂ A ₂ B ₁	Light brownish colouration decreases with depth as organic matter decreases. Dark minerals very scarce. No granite fragments or partly weathered feldspars.
6,7,8, 9,10 11,12	60-165	B ₂	White, clayey, very fine grained quartz sand. No granite fragments or partly weathered feldspars. Dark minerals very scarce. More coarse quartz toward bottom.

Figure 15. Downprofile distribution of Fe, Mn,
Co, Ni, Pb, Cu and pH. Pit 6.

PIT 6

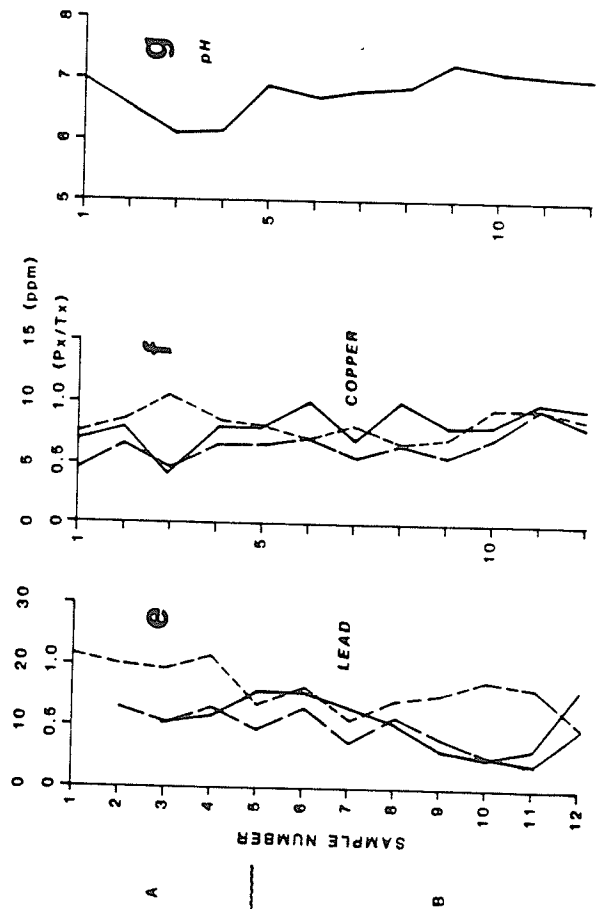
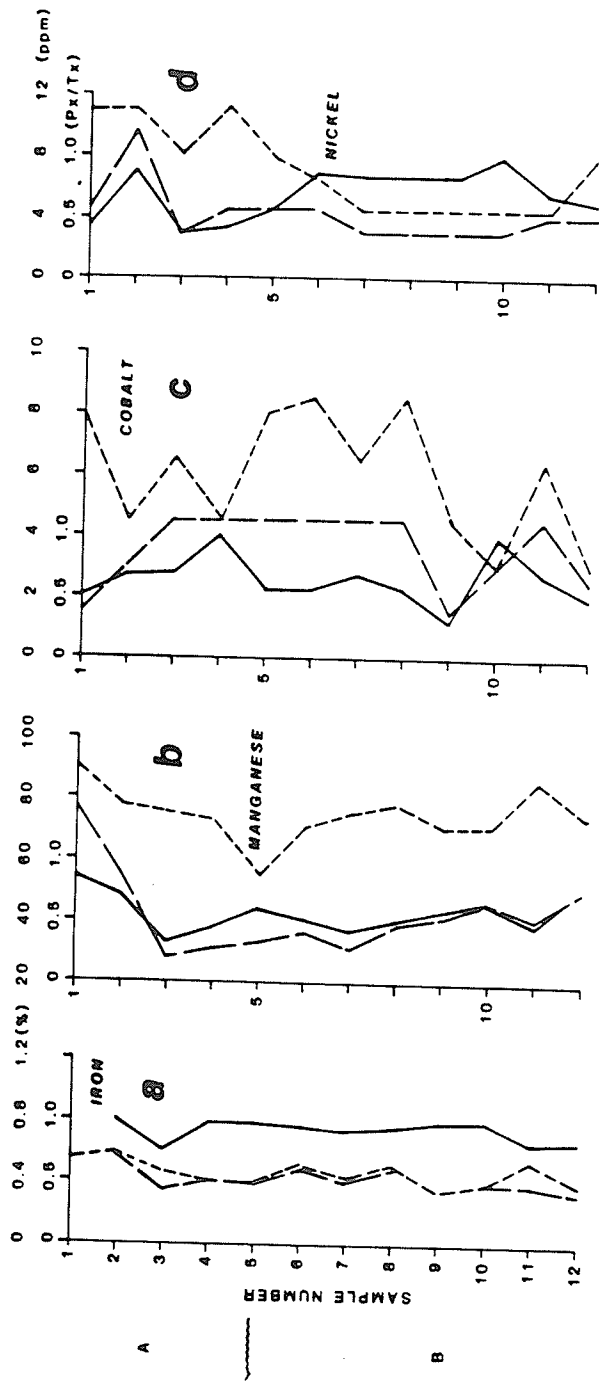


Table 21. Pearson correlation coefficients (r) for
(Fe:Mn): Mn, Co, Ni, Pb and Cu.

CV = critical value. f = confidence level.

Pit 6.*

Px-Px	Fe:Mn	=	0.39	Px-Px	Fe:Ni	=	0.62
Tx-Tx	Fe:Mn	=	0.53	Tx-Tx	Fe:Ni	=	0.44
Px-Px	Fe:Zn	=	n.a.	Px-Px	Mn:Ni	=	0.39
Tx-Tx	Fe:Zn	=	n.a.	Tx-Tx	Mn:Ni	=	0.15
Px-Px	Mn:Zn	=	n.a.	Px-Px	Fe:Pb	=	0.62
Tx-Tx	Mn:Zn	=	n.a.	Tx-Tx	Fe:Pb	=	0.05
Px-Px	Fe:Co	=	0.62	Px-Px	Mn:Pb	=	0.26
Tx-Tx	Fe:Co	=	0.44	Tx-Tx	Mn:Pb	=	0.27
Px-Px	Mn:Co	=	0.73	Px-Px	Fe:Cu	=	0.05
Tx-Tx	Mn:Co	=	0.37	Tx-Tx	Fe:Cu	=	0.01
Cv	=	0.50		Px-Px	Mn:Cu	=	-0.04
f	=	0.10		Tx-Tx	Mn:Cu	=	0.24

* n.a. = no analysis

Lead values (Figure 15e) decrease gradually with depth. Tx values have a slight increase at depth below 120 cm. The extraction ratio decreases downprofile.

Copper (Figure 15f) values are very low and nearly uniform with depth. Extraction ratios are correspondingly uniform.

The pH is lowest in the upper (30 cm) of the A horizon (Figure 15g) and generally increases with depth.

Physical and Chemical Properties of Pit 5

Physical Properties

The soil is very thin and fine grained and with some coarse quartz grains. It has a deep reddish brown colouration and consists of B horizon-type material.

Chemical Properties

The distribution of Fe, Mn, Zn, Co, Ni, Pb and copper is shown in Figure 16.

Iron (Figure 16a) shows very little variation with depth. Manganese (Figure 16b) like Fe, has a variation with depth. Zinc (Figure 16c) contents are uniform. Cobalt values (Figure 16d) are also uniform. Nickel Px (Figure 16e) is uniform but the Tx content at 30 cm depth is higher than the content in upper part of the profile. Lead (Figure 16f) increases with depth. Copper values (Figure 16g) also increase with depth. The extraction ratios of all elements vary slightly except for Ni.

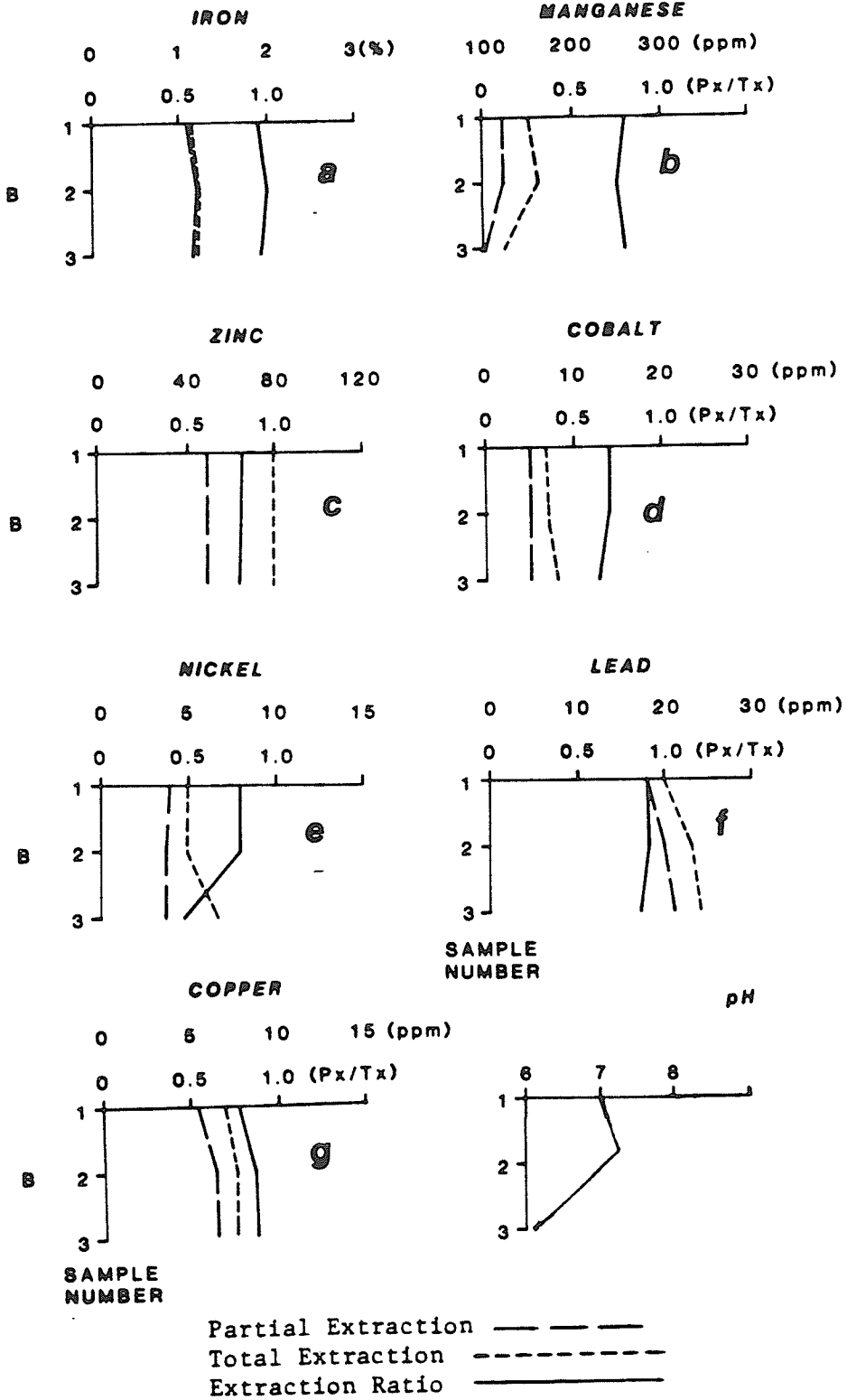
The pH of the profile is below 7.0 except at the 15 cm depth.

Table 22. Soil profile description of Pit 5.

Sample	Depth (cm)	Horizon	Description
1	0	A	Topsoil. Reddish brown, clayey silty quartz sand with abundant coarse quartz grains. Dark minerals in fine fraction. No granite fragments. Organic matter mostly fresh plant material.
2,3	0-30	B	Reddish brown, clayey/silty very fine grained quartz sand as above.

Figure 16. Downprofile distribution of Fe, Mn, Zn,
Co, Ni, Pb, Cu and pH. Pit 5.

PIT 5



Physical and Chemical Properties of Pit 3

Physical Properties

The soil is lateritic and contains some organic plant matter (in the upper 30 cm). Quartz, weathering feldspars and magnetite occur in coarse and fine fractions throughout the profile. It is well cemented and hardened below 50 cm.(Table 23).

Chemical Properties

All the elements show a general increase in concentration with depth.

Zinc (Px, Figure 17a) values are uniform within the upper 45 cm. Below 45 cm, the Zn contents increase abruptly. The topsoil Tx value has the lowest content. There is no significant increase of Tx values of Zn with depth. The extraction ratio is not uniform but it does not show any trend with depth.

Cobalt Px (Figure 17b) values increase gradually with depth up to the 45 cm depth. Below 45 cm, the increase is sharper than above. Tx values increase from top down to 30 cm depth and decrease within the rest of the profile. The extraction ratio is variable.

The lowest Ni values (Figure 17c) occur within the topsoil. Both Px and Tx contents of Ni are uniform throughout except at 60 cm depth where slight increases of contents occur. The extraction ratios are nearly uniform throughout the profile except at 60 cm depth.

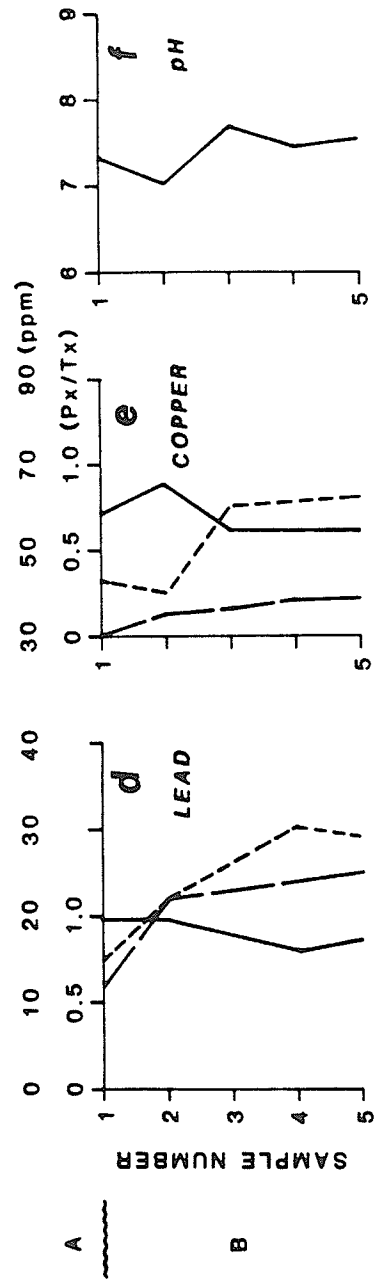
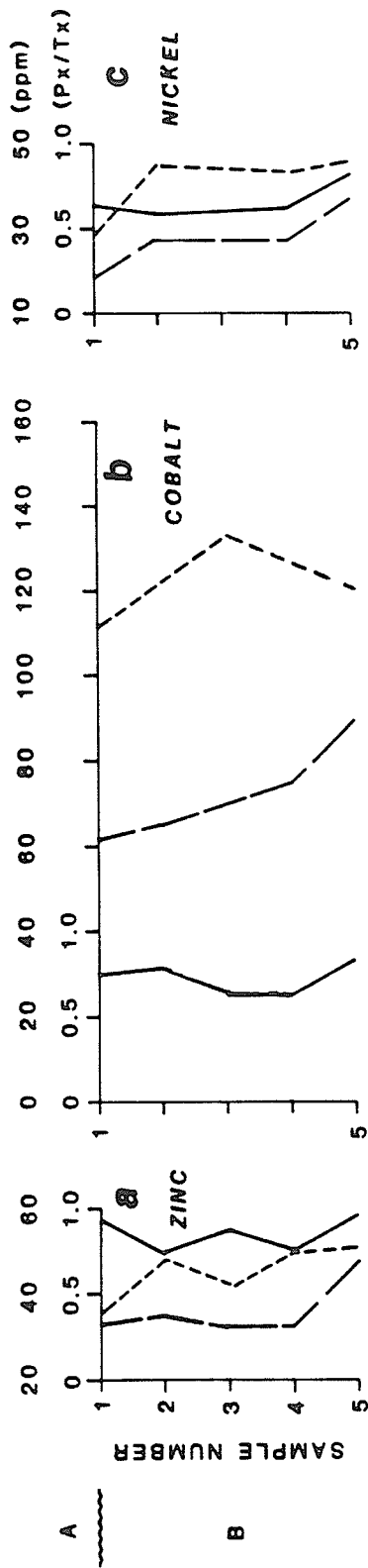
Lead increases gradually with depth (Figure 17d) below 15 cm. The lowest Pb content occurs in the topsoil. The extraction ratios decrease gradually with depth except at 45 cm where a small increase occurs.

Table 23. Soil profile description. Pit 3.

Sample	Depth (cm)	Horizon	Description
1	0	AoB	Topsoil. Brownish red clayey/silty very fine grained sand. Fresh and decayed brown organic matter. Coarse grains of quartz, weathered biotite. Abundant magnetite in coarse and very fine grained fraction. Some magnetite with ferric coating.
2	0-15	B	Dark brownish red, lateritic dense clayey/silty sand. Abundant magnetite in coarse and fine fraction. Organic (Humic) matter present.
3	15-30	B	Lateritic. Partially weathered feldspars, higher magnetite content than above. Decayed organic matter present.
4	30-45	B	Lateritic. Very high magnetite content, coarse, angular, occasionally associated with quartz. Chloritized mafics. Partially weathered feldspars. Hard and compacted.
5	45-60	B	Lateritic. Magnetite content high. Weathered biotite and feldspars present. Hard compact.

Figure 17. Downprofile distribution of Zn, Co, Ni, Pb,
Cu and pH. Pit 3.

PIT 3



Partial Extraction ———
 Total Extraction - - -
 Extraction Ratio ———

Copper Px contents increase with depth (Figure 17e). The Tx value decrease within the upper 15 cm but increase sharply below 15 cm depth. The extraction ratio is uniform below 15 cm.

The profile is slightly more alkaline at depth than at the surface (Figure 17f).

Physical and Chemical Properties of Pit 2

Physical Properties

The pit consist of residual overburden formed from a weathering diabase.

The B and C horizons are well formed. The A horizon is marked by the very strong ferric (deep brownish red) colouration. The B horizon is lateritic and coherent and consists of resistate minerals (coarse magnetite and to a lesser amount, quartz). Lumps of completely weathered feldspar are intact and increase in size with depth and abundance as does magnetite.

The transition to the C horizon is rather sharp and is marked by the significant decrease in ferric colouration, the appearance of mottling and the saprolitic character of the profile. Weathered biotite is the remnant mafic mineral. The saprolite is thick compared to the B horizon.

Chemical Properties

All the elements (with the exception of Cu) have an increasing content downprofile (Figure 18). The relationship of Fe, Mn to other elements is expressed as correlation coefficients in Table 25.

Iron (Figure 18a) contents decrease from the top to the bottom. The highest Fe contents correspond to the lateritic part of the profile. The saprolitic or C horizon has the lower contents. Extraction ratios decrease very slightly with depth.

Manganese (Figure 18b) is considerably enriched in the saprolite zone as is reflected by the Tx extraction values. The extraction ratios decrease with depth.

Zinc (Figure 18c) has a Px value which shows very little variation with depth. The Tx values are more variable and have the lowest values in the depth interval of 60-90 cm in the upper C. horizon. The extraction

Table 24. Soil profile description. Pit 2.

Sample	Depth (cm)	Horizon	Description
1	0	Ao B ₂	Topsoil. Brownish red clayey/silty coarse sand, abundant magnetite (up to 2%) of sample in all grain sizes. Fresh organic matter and weathering feldspars present. Quartz in very fine fraction.
2	0-15	B ₂	Deep brownish red clayey/silty sand. Magnetite coarse and abundant. Also fine-grained quartz. Lumps of weathered feldspars present. Coherent.
3,4,5	15-60	B ₂	Strongly lateritic, deep reddish brown, hard. Magnetite increases with depth. Also size of magnetite more coarse. Higher content of clay lumps from completely weathered feldspar. No mafic minerals. At 60 cm beginning of transition to C horizon. Slight reaction with acid.
6	60-75	B ₂ C ₁	Reddish brown stained saprolite. Large almost completely weathered feldspars. Friable. Reacts with acid more strongly than above.
7	75-90	C ₂	Reddish brown saprolite with greenish tints on partly weathered feldspar (mottling). Reaction with acid strong.
8,9,10	90-135	C ₂	Light reddish brown saprolite and yellowish mottling stains on partly weathered feldspars. Coarse mafics (mainly biotite) present. Abundant coarse (primary association with feldspar). Strong reaction with acid.

Figure 18. Downprofile distribution of Fe, Mn, Zn,
Co, Ni, Cu, Cr and pH. Pit 2.

PIT 2

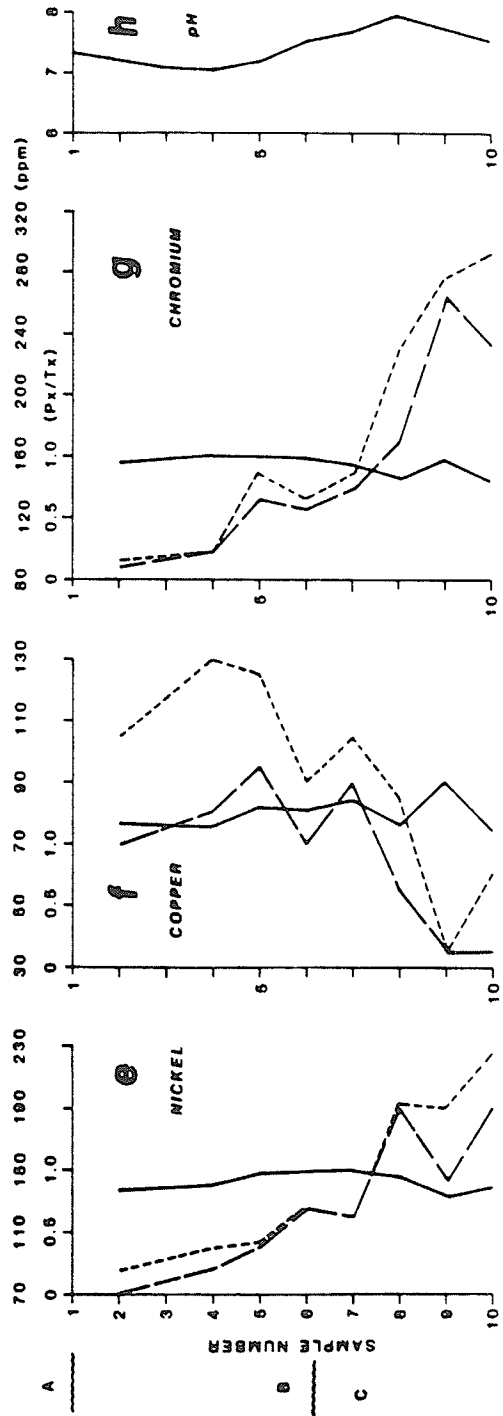
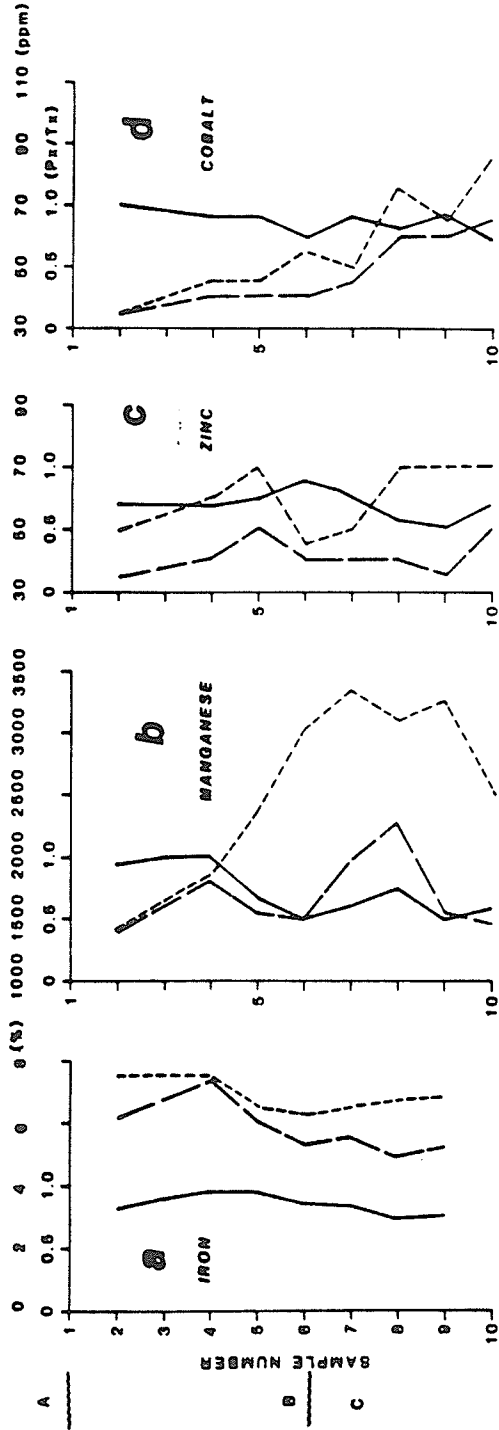


Table 25. Pearson correlation coefficients (r) for
 (Fe, Mn): Mn, Co, Ni, Cu. CV = critical
 value. f = confidence level. Pit 2.*

Px-Px	Fe:Mn	=	-0.26	Px-Px	Fe:Ni	=	-0.81
Tx-Tx	Fe:Mn	=	-0.78	Tx-Tx	Fe:Ni	=	-0.32
Px-Px	Fe:Zn	=	-0.05	Px-Px	Mn:Ni	=	0.34
Tx-Tx	Fe:Zn	=	-0.06	Tx-Tx	Mn:Ni	=	0.54
Px-Px	Mn:Zn	=	n.a.	Px-Px	Fe:Cu	=	0.53
Tx-Tx	Mn:Zn	=	n.a.	Tx-Tx	Fe:Cu	=	0.28
Px-Px	Fe:Co	=	-0.68	Px-Px	Mn:Cu	=	0.16
Tx-Tx	Fe:Co	=	-0.51	Tx-Tx	Mn:Cu	=	0.54
Px-Px	Mn:Co	=	0.24	CV	=	0.54	
Tx-Tx	Mn:Co	=	0.54	f	=	0.10	

* n.a. = no analysis

ratio decreases slightly with depth. Higher values at 60-90 cm depth interrupt the trend in the C horizon.

Cobalt (Figure 18d) is accumulated at depth in the C horizon. The increase from the top to the bottom is strongest below 105 cm. Extraction ratios decrease slightly with depth.

Nickel (Figure 18e) is accumulated very strongly in the lower C horizon. Above 75 cm the increase is smooth and gradual. The extraction ratios are high and nearly uniform throughout the profile.

Copper (Figure 18f) accumulation occurs in the upper lateritic B horizon. The decrease with depth is rapid and very irregular. Extraction ratios are variable but have a very slight overall increase with depth.

Chromium (Figure 18g) is very strongly accumulated at depth in the lower C horizon. Extraction ratios decrease with depth.

The profile has an overall alkaline pH (Figure 18h). The pH values increase gradually with depth up to 105 cm depth. Below 105 cm the pH decrease slightly.

Physical and Chemical Properties of Pit 1

Physical Properties

The profile consists of transported debris from various sources. The soil is darkish brown and is essentially a B horizon for most of its depth. It consists of abundant clay/silt size material. Coarser grains include blue quartz, incompletely weathered feldspars, granite and other rock fragments. In addition, carbonate lumps are present in most of the profile (Table 26).

A 15 cm thick carbonate band occurs at 47 cm depth. Carbonate is also present in the profile in fine particulate form as is indicated by the acid reaction of the fine fraction.

Chemical Properties

The downprofile distribution of the different elements is varied. Some show enrichment in specific zones, while others do not (Figure 19). The similarities of profile trend with comparison to Fe and Mn is indicated by the correlation coefficients, (Table 27).

Iron contents (Figure 19a) in the A horizon are the lowest. The B horizon is relatively enriched in Fe. Minimum Px values occur between 120 and 150 cm depth. The Tx extraction has nearly uniform values throughout the profile except for the upper 30 cm. Extraction ratios are variable.

Manganese (Figure 19b) is accumulated at depth below 120 cm. The A horizon has decreasing values within the upper 30 cm. Below 30 cm, the Mn contents increase gradually up to the enrichment depth. The extraction ratio is nearly constant except at 30 cm depth.

Zinc contents (Figure 19c) are lowest in the topsoil and at the 135 cm and 180 cm depths. The rest of the profile has near equal contents

Table 26. Soil profile description. Pit 1.

Sample	Depth (cm)	Horizon	Description
1	0	A ₀	Topsoil. Greenish brown, clayey/silty very fine grained quartz sand. Fresh and black humic organic matter. Coarse red, blue and colourless quartz. Some rock fragments. Few dark minerals (mafics and magnetite).
2	0-15	A ₂ B	Blackish brown clayey/silty fine grained sand. Black to brown decayed organic matter. Some dark minerals. Coherent. No acid reaction.
3	15-30	A ₂ B	Blackish brown sand as above. Abundant organic matter. Partly weathered feldspars. Fine to medium grained dark minerals. Coarse blue quartz present. Very slight reaction with acid.
4	30-45	A ₂ B	Blackish brown clayey/silty sand. Dark minerals and organic matter abundant. Coarse quartz generally larger than above. Mild acid reaction.
5	45-60	B	Brown, hard sand. White, carbonate band at 47 cm.
6	60-75	B	Very coarse sand. Strong acid reaction.
7,8	75-105	B	Brownish black, clayey/silty, very fine grained sand. Acid reaction of carbonate lumps and fines. Some rock fragments weathered granite fragments and feldspars present.
9	105-120	B	Blackish brown sand. Some organic matter. Dark minerals in fine fraction. Different rock fragments present. Mild acid reaction of fine fraction.
10,11 12,13	120-180	B	Brown clayey/silty gravel. Granite fragments weathered but intact. Nodules of carbonate. Different rock fragments (slate, chert, felsite), gravelly. Abundant carbonate below 165 cm as lumps, cement and coating on some grains. Some humic organic matter. Some partly weathered feldspars. Strong acid reaction.

Figure 19. Downprofile distribution of Fe, Mn, Zn,
Co, Ni, Pb, Cu, Cr and pH. Pit 1.

PIT 1

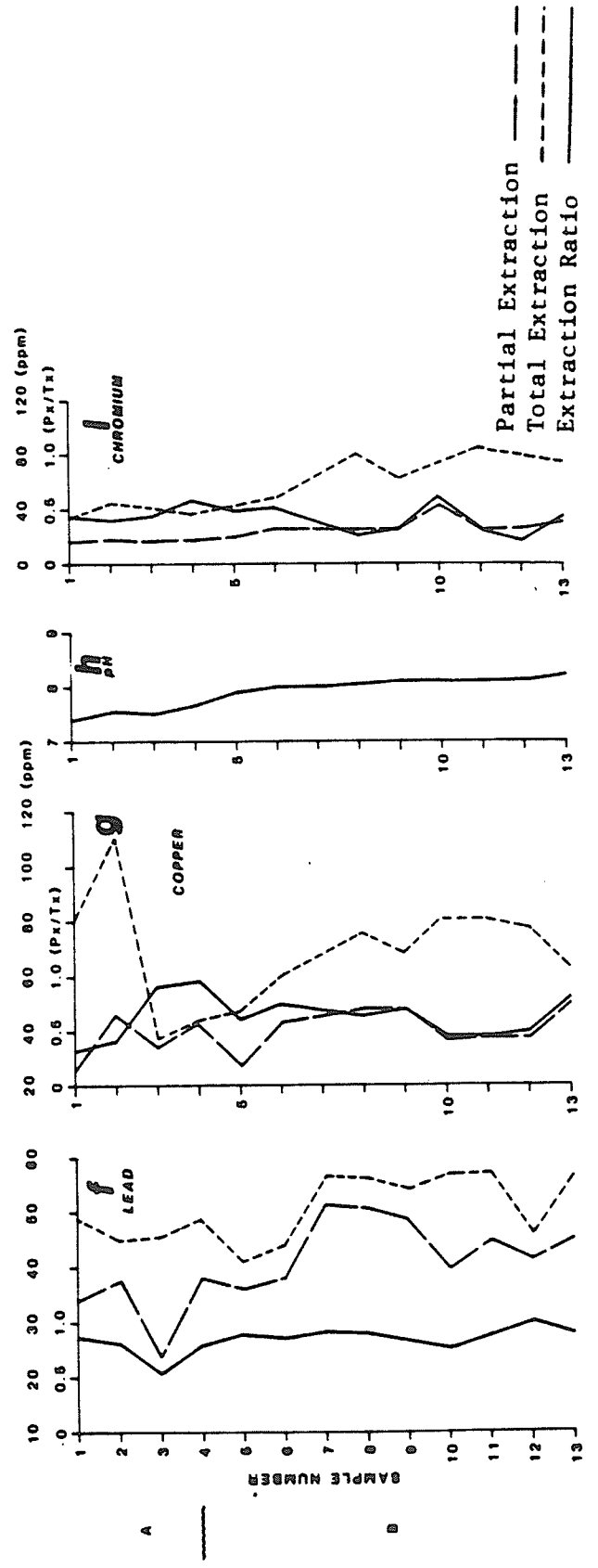
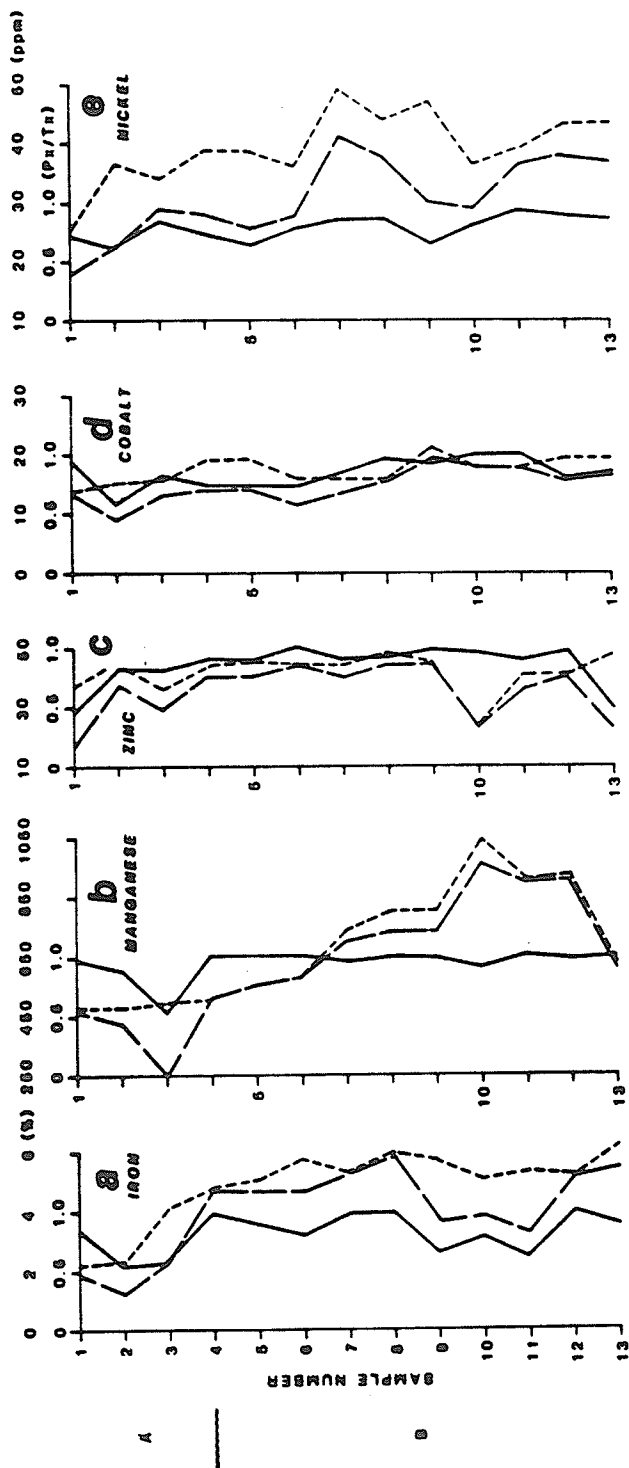


Table 27. Pearson correlation coefficients (r) for
(Fe:Mn): Mn, Zn, Co, Ni, Pb, and Cu.

CV = critical value. f = confidence level.

Pit 1.

Px-Px	Fe:Mn	=	0.28	Px-Px	Fe:Ni	=	0.79
Tx-Tx	Fe:Mn	=	0.55	Tx-Tx	Fe:Ni	=	0.67
Px-Px	Fe:Zn	=	0.41	Px-Px	Mn:Ni	=	0.56
Tx-Tx	Fe:Zn	=	0.29	Tx-Tx	Mn:Ni	=	0.46
Px-Px	Mn:Zn	=	0.19	Px-Px	Fe:Pb	=	0.35
Tx-Tx	Mn:Zn	=	0.35	Tx-Tx	Fe:Pb	=	0.56
Px-Px	Fe:Co	=	0.26	Px-Px	Mn:Pb	=	0.69
Tx-Tx	Fe:Co	=	0.63	Tx-Tx	Mn:Pb	=	0.49
Px-Px	Mn:Co	=	0.72	Px-Px	Fe:Cu	=	0.02
Tx-Tx	Mn:Co	=	0.22	Tx-Tx	Fe:Cu	=	0.54
CV	=	0.44	Px-Px	Mn:Cu	=	0.19	
f	=	0.10	Tx-Tx	Mn:Cu	=	0.22	

of Zn. The extraction ratio is lowest in the topsoil and at the bottom of the profile (180 cm depth).

Cobalt (Figure 19d) has a very slight increase with depth. The extraction ratio is more or less uniform with depth.

Nickel contents (Figure 19e) are nearly uniform except for the enrichment at 75 to 120 cm depth and below 135 cm. Extraction ratios vary randomly but show a slight increase with depth.

Lead (Figure 19f) is accumulated below 90 cm depth. The extraction ratio is nearly uniform throughout the profile except at 30 cm depth due to the low P_x value.

Copper (Figure 19g) is accumulated at the surface subhorizons within the upper 30 cm. The T_x values show a gradual increase with depth up to 150 cm depth. The extraction ratio varies significantly throughout the profile.

The extraction ratios are variable, particularly in the upper 60 cm of the profile. Below 60 cm the extraction ratios do not vary strongly and they show a very slight overall decrease.

Chromium (Figure 19h) values do not reflect any significant enrichment in the profile. Both P_x and T_x values increase slightly with depth. The extraction ratio varies significantly at depth below 120 cm but the overall pattern is a slight decrease from the upper to the lower part of the profile.

The profile has alkaline pH values. The lowest occurs at the surface (7.4). The pH increases gradually with depth (Figure 19i).

Physical and Chemical Properties of Pit 13

Physical Properties

The profile consists of residual material derived from the underlying granite rock. The A horizon is represented by an approximately 8 cm thick dark, humus-laden brown soil, below which the humus content decrease within the next 16 cm.

The B horizon consists of clayey/silty quartz sand with abundant coarse fragments of quartz and partly weathered feldspars. Concretion-like ferruginous lumps occur below 45 cm. The lumps show some mottling in their outer parts.

Chemical Properties

All the elements show significant enrichment at depth (Figure 20).

The strength of the similarity of their trends is indicated by their correlation coefficients in Table 29.

Iron Px values (Figure 20a) increase strongly with depth. The increase is smooth unlike the Tx extraction which shows the strong enrichment below 75 cm more distinctly. The extraction ratio is uniform except at 90 cm depth where a decrease occurs due to the abrupt increase of the Tx values.

Manganese (Figure 20b) is accumulated below 75 cm. The Px values increase less sharply compared to the Tx values. Extraction ratios have an overall decrease with depth.

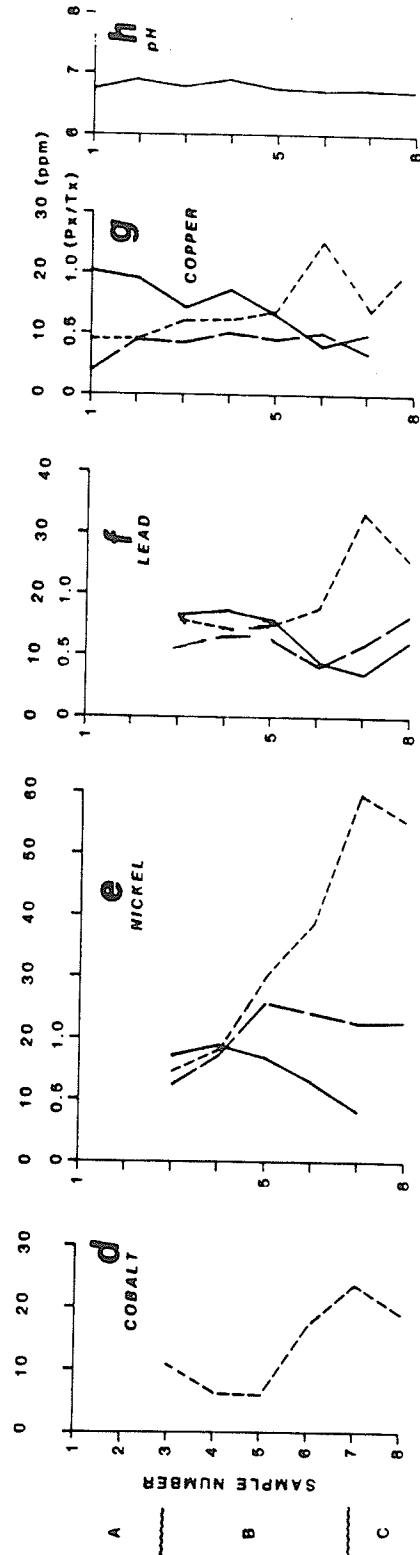
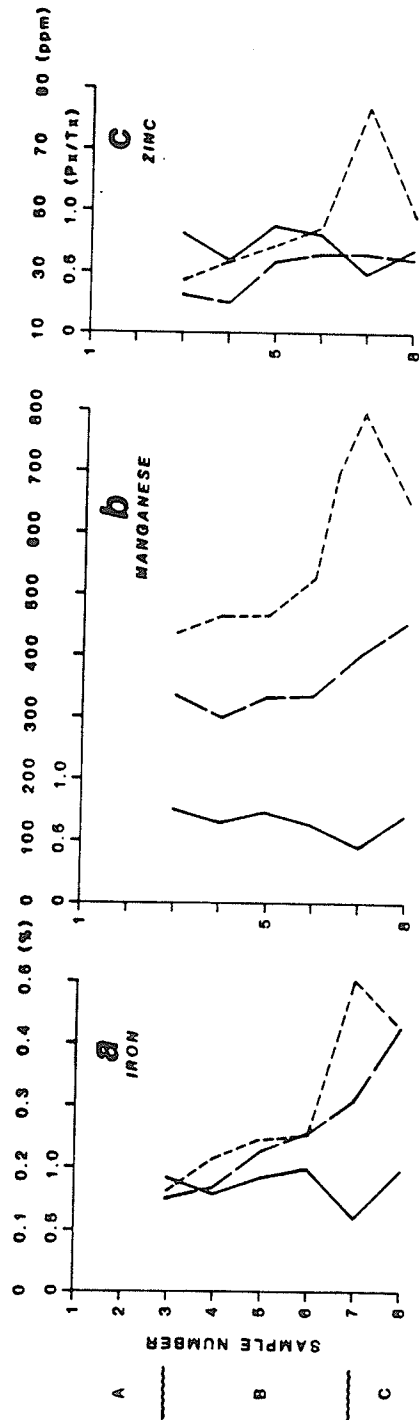
Zinc (Figure 20c) generally increases with depth. The Px values are nearly uniform below 60 cm whereas the Tx values increase gradually up to 75 cm depth. An abrupt increase occurs at 90 cm depth. The extraction ratios are variable.

Table 28. Soil profile description. Pit 13.

Sample	Depth (cm)	Horizon	Description
1	0	A ₀	Topsoil. Light reddish brown clayey/silty fine grained quartz sand. Coarse angular quartz grains present. Partly weathered feldspars, granite fragments weathering biotite present. Abundant fresh organic matter. Also rounded quartz. Dark minerals (mafics and magnetite) in fine fraction.
2	0-15	A ₁	Dark brown clayey/silty fine grained quartz sand. Dark brown humic matter in upper 8 cm. Coarse quartz grains present. Also partly weathered feldspars and granite fragments.
3	15-30	A ₂ B ₁	Dark reddish brown sand as above. Less humic material. Dark minerals in fine fraction, smooth rounding in some quartz grains.
4	30-45	B ₂	Dark reddish brown clayey/silty fine grained quartz sand. Granite fragments with feldspars weathered to different extents. Mafic minerals absent in granite fragments.
5	45-60	B ₂	Dark brownish red clayey/silty sand as above.
6	60-75	B ₂	Dark brownish red clayey/silty sand. Coarse blue quartz present. Some rounded ferruginous lumps with pale reddish outside colouration. They consist of cemented fine grained quartz and clay. Different extents of weathering of feldspars prominent.
7	75-90	B ₂ C ₁	
8	90-105	C ₁	Reddish brown clayey/silty sand. Partly weathered granite fragments dominant. Ferruginous lumps present.
9	105-120	C ₂	Partly weathered ferric stained granite.

Figure 20. Downprofile distribution of Fe, Mn, Zn,
Co, Ni, Pb, Cu and pH. Pit 13.

PIT 13



Partial Extraction ———
 Total Extraction - - - -
 Extraction Ratio ———

Table 29. Pearson correlation coefficients (r) for

(Fe, Mn): Mn, Zn, Co, Ni, Pb and Cu.

CV = critical value. f = confidence level.

Pit 13.

Px-Px	Fe:Mn	=	0.75	Px-Px	Fe:Ni	=	0.66
Tx-Tx	Fe:Mn	=	0.79	Tx-Tx	Fe:Ni	=	0.73
Px-Px	Fe:Zn	=	0.80	Px-Px	Mn:Ni	=	0.76
Tx-Tx	Fe:Zn	=	0.48	Tx-Tx	Mn:Ni	=	0.28
Px-Px	Mn:Zn	=	0.56	Px-Px	Fe:Pb	=	0.50
Tx-Tx	Mn:Zn	=	0.92	Tx-Tx	Fe:Pb	=	0.60
Px-Px	Fe:Co	=	n.a.	Px-Px	Mn:Pb	=	0.55
Tx-Tx	Fe:Co	=	0.57	Tx-Tx	Mn:Pb	=	0.93
Px-Px	Mn:Co	=	n.a.	Px-Px	Fe:Cu	=	0.25
Tx-Tx	Mn:Co	=	0.83	Tx-Tx	Fe:Cu	=	0.33
CV	=	0.58	Px-Px	Mn:Cu	=	-0.18	
f	=	0.10	Tx-Tx	Mn:Cu	=	0.94	

Cobalt (Figure 20d) is strongly accumulated below 60 cm depth.

Nickel Px values (Figure 20e) increase up to a depth of 60 cm below which they fall gradually. In contrast, the Tx contents increase sharply below 60 cm to a maximum value at 105 cm. The extraction ratio decreases regularly below 45 cm.

Lead (Figure 20f) Px values do not indicate any enrichment in the profile. The Tx extraction shows an abrupt accumulation at 90 cm depth. The extraction ratios have an overall decrease with depth.

Copper contents (Figure 20g) are uniform throughout the profiles except at 75 cm depth where the Tx values have an abrupt increase. The extraction ratio decreases with depth. The pH is nearly uniform with depth.

CHAPTER VI

RESULTS AND DISCUSSION

Development of Soil Profiles

The Tletletsi Area is a geochemical environment of active physical and chemical weathering. The overall morphological, textural, mineralogical and chemical properties reflect a continuing process of soil formation.

Two principal soil groups have been recognized; residually accumulated soils and transported soils.

Residual Soils

Generalized features and the nomenclature used to describe the various horizons have been depicted in Table 3a.

The residual profiles samples are typically shallow and average about 120 cm in depth. Soil horizons are rather well developed and the boundaries between the horizons are sharp to transitional.

The A horizons are thin and contain fresh and humic plant matter. The latter imparts a brown colouration (Pits 18, 11, 13) to the near-surface subhorizons. In Pits 14, 12, 9 and 2, the brown colouration is masked by the ferric pigment.

The mineralogy of the A horizon is quite diverse. Quartz, by virtue of its abundance in the parent rock and its resistant nature, is the major constituent. Dark minerals (mafics and magnetite) occur in quantities that vary from profile to profile depending on the specific granite phase the soil overlies. Partly weathered and unweathered feldspars and, occasionally, granite fragments are present.

The A horizon is usually loose, clayey/silty and tends to be gravelly where coarse quartz is in abundance, as in all topsoils. Most of the minerals are of a very fine size fraction presumably resulting from more intense chemical and physical weathering in the upper parts of the profile. Binocular examination revealed smooth surfaces on many grains of the primary quartz and this is taken to indicate dissolution. The transition to the underlying B horizon is marked by a significant decrease in organic matter and an increase of ferric colouration. The B horizon is usually well developed irrespective of its thicknesses. It is reddish brown and its colouration visibly intensifies with depth in Pits 12 and 18.

The mineralogy comprises quartz, dark minerals, partly weathered and fresh feldspars and various clay and/or silty size mineral grains. The quartz, mafics and magnetite tend to be coarser and more angular than those in the A horizon. At depth in the horizon, friable fragments of parent rock become more abundant. The soil is a fine-grained quartz sand and contains much clay and/or silt. It is moderately dense and coherent to hard where ferric compounds have caused cementation. The transition to the C horizon occurs where friable parent rock fragments dominate. The typical C horizon is white and may be infiltrated by lower B horizon clay/silt material (Pit 12) or have some ferric staining.

The maturity of any soil profile is important for geochemical exploration because the product formed early in the stages of soil development will be different from those formed at more advanced stages. Maturity can be determined from the extent of horizon development, the mineralogical content and the nature of trace element dispersion.

Harriss and Adams (1966) conducted studies on the chemical and mineralogical changes that accompanied the weathering of granites in Oklahoma and Georgia. They noted that the early, intermediate and final stages of weathering were characterized by the release of specific elements. The trace elements resident in mafic minerals were released and mobilized in the early stages of the weathering.

The relative instabilities of the minerals in the three granites they studied followed the sequence plagioclase > biotite > K-feldspar > quartz. This sequence, they concluded, was consistently observed irrespective of the climatic or physiochemical variations.

From the mineralogy of the residual soils in the Tletletsi Area, the following conclusions have been reached:

a) Quartz is slightly soluble and grains with very smooth and rounded surfaces are taken to indicate a slight solubility of quartz. A significant amount of dissolution is not favoured because of the low pH values. pH values lower than 9.0 tend to suppress the solubility of quartz (Krauskopf, 1979, p. 133).

b) The feldspars are weathered differently. Weathered and unweathered feldspars are found side by side in all the horizons. The rapakivi feldspar which comprises most of the Thamaga Granite is susceptible to this form of weathering. It is also noted that the abundance of the clay-size fraction in the profile indicates significant weathering. The plagioclase feldspars appear to be the most weathered.

c) Most mafic minerals have been weathered due to their greater susceptibility to chemical weathering. The presence of magnetite reflects a slower rate of weathering in comparison with other mafic minerals.

d) The profiles are in the intermediate stage of weathering, using the criterion of Hariss and Adams (1966).

e) Under the conditions of the Tletletsi area where the fresh feldspars are probably K-feldspars (hence low $[K^+]$) and where the low pH of the soils i.e. low $[H^+]$ leads to low solubility of quartz (Krauskopf, 1979, p. 133) and low $[H_4SiO_4]$, the clay mineral that is mostly likely to be dominant is montmorillonite (Young, 1976, p. 429).

Transported Soils

Unlike the residual soils, the transported overburden is more variable texturally, and comprises soils weathered to different degrees.

The main distinguishing feature between residual and transported soils is the structure of the soils. In contrast to the residual soils which show a continuous transition of horizons from the bedrock to the surface subhorizons, the transported soils have alternations of fine or medium sand layers and gravelly layers where weathering has not been intense. The layering is the result of the differential transportation of the different grain sizes by water during rainstorms and subsequent surface runoff of loose debris.

The least weathered transported soil is exemplified by Pit 7. It consists of small amounts of clay and silt compared to the coarse fraction. The coarse and angular grains usually consist of granite fragments, feldspar, quartz and less commonly, dark minerals. The coarse fraction constitutes the bulk of the soil and grains are only slightly weathered. Layers of the coarse sand and gravelly material are clearly distinguishable from the finer-grained fraction. The gravel represents physically dislocated and partly weathered parent rock (granite) and is comparable to a C horizon.

The coarse and the fine grained layers occur in several repetitive layers which are believed to represent periods of intense rainfall in the past. Black humic plant matter is present to a depth of 90 cm within the finer sediment. Ferric colouration is not related to depth in any manner, unlike in the residual soils. The pH values are mildly alkaline.

Pit 8 is more weathered and slightly acid (Table 16). Pit 3, although laterized due to development from a different rock type, is placed in this category.

Rock fragments (Pit 8) are much less (than in Pit 7) to nearly absent at some depths (Table 16). Quartz constitutes the coarse fraction. Dark minerals are rare, and where present, are confined to the fine fraction. Ferric pigmentation is uniform except where mottling occurs. The upper subhorizons of the soil are dark brown due to humic organic matter. The presence of coarse grained, friable clay lumps formed from the complete weathering of feldspars indicate that most of the weathering occurred after the soil was transported. Layering is almost obliterated and is faintly represented by coarse quartz at some depths.

The high degree of weathering in this environment is perhaps typified by Pit 6 (Table 20). The soil is extremely leached, to the extent that the clays do not have any ferric colouration. Transportational features are completely absent, except for the occurrence of coarse quartz at depth. Dark minerals, feldspars and granite fragments are absent. The profile is slightly alkaline at depth.

In Pit 15 (Table 5), the weathering is comparable to that of the residual soils. The main difference is the development of a hard lateritic subhorizon at depth and (Table 6) the alkaline nature of the profile. It may be that the leaching in this case has been prevented by the alkaline conditions. Alkaline conditions in this environment would lessen weathering

because high pH is, as a general rule, less effective than low pH in the weathering environment.

In general, the transported soils are deeper than the residual ones and they are more alkaline. The alkalinity is probably associated with transported carbonate from the south, where Transvaal rocks occur.

The approximate distribution of the residual and transported soils as determined by this study is shown in Figure 4. The transported soils occur mostly in the southern part of the Tletletsi Area adjacent to the higher relief.

Chemical Results of Soil Sample Analysis

Due to the large amount of data (over 2,000 elemental analyses), it was not possible to do large numbers of replicate analyses. Therefore, except for the replicates shown in Table 2(a-d), the results are based on single analyses.

Significance of the Extraction Ratio

The results of a statistical analysis of the extraction ratios (defined as the partial extraction value, P_x , divided by the total extraction value, T_x) for the individual elements are shown in Table 30.

The data indicate that the amount of specific trace element extracted by either or both P_x and T_x is variable. The total extraction procedure using HF mixed with an oxidizing agent such as $HClO_4$ is known to dissolve almost 100% of all the constituents of soil samples (Gedeon et al, 1977). In this study, HNO_3 was used as the oxidizing agent (Table 1(c)). Since HF is the reagent that actually dissolves samples it is believed that the amount of sample dissolved is also approximately 100%. The variation of the extraction ratios is attributed to a varying effectiveness of the partial extractions on the samples. The inconsistencies in the P_x extraction could be due to:

Table 30: Statistical parameters of the extraction ratios*.

Element	Mean	Mean Class	Median	Median Class
Fe	0.83	0.86 - 0.81	0.88	0.86 - 0.81
Mn	0.71	0.76 - 0.71	0.71	0.76 - 0.71
Zn	0.80	0.86 - 0.81	0.82	0.76 - 0.71
Co	0.75	0.76 - 0.71	0.73	0.76 - 0.71
Ni	0.76	0.80 - 0.77	0.78	0.80 - 0.77
Pb	0.65	0.66 - 0.61	0.62	0.66 - 0.61
Cu	0.74	0.76 - 0.71	0.76	0.76 - 0.71

*The extraction ratio for an element is defined as the partial extraction value divided by the total extraction value.

a) presence of primary minerals such as silicates which are not completely dissolved by the Px extraction.

b) the presence of secondary compounds such as clays and humic matter which are not completely soluble in the Px extraction reagents

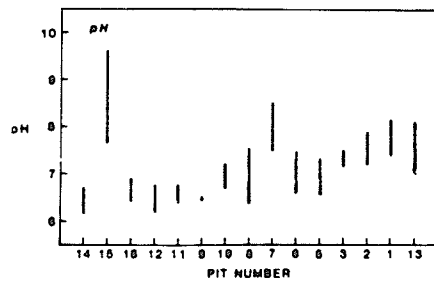
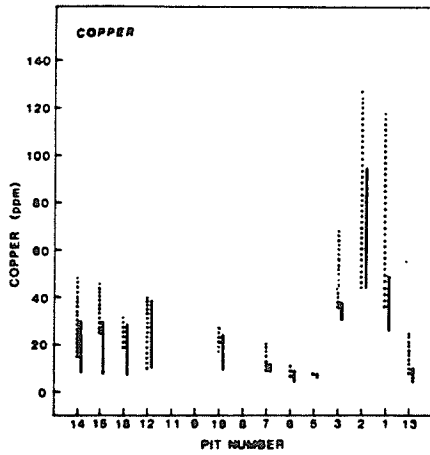
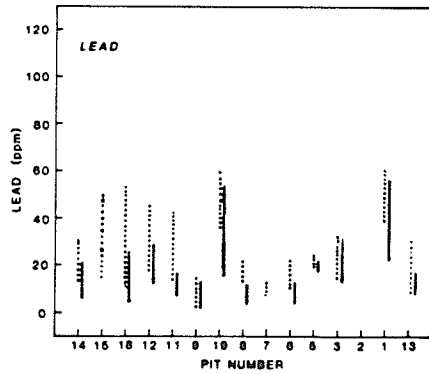
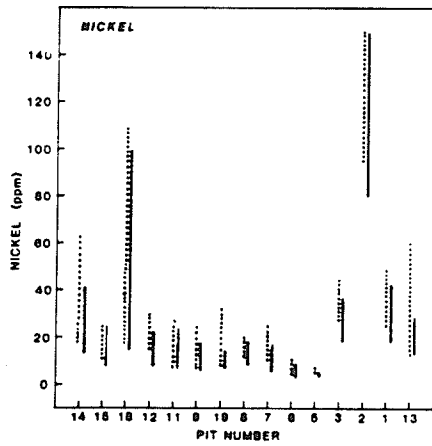
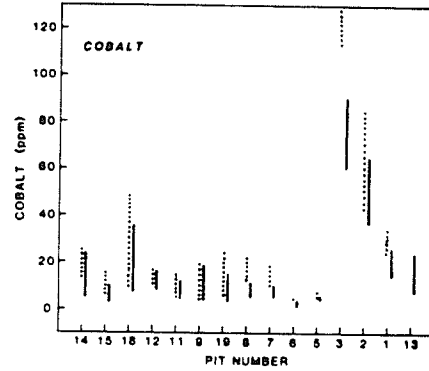
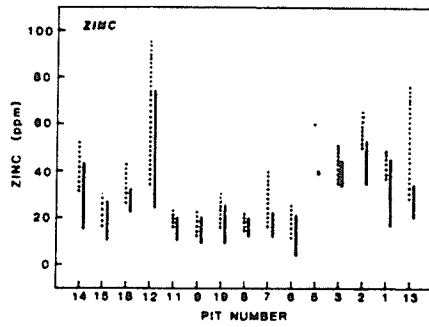
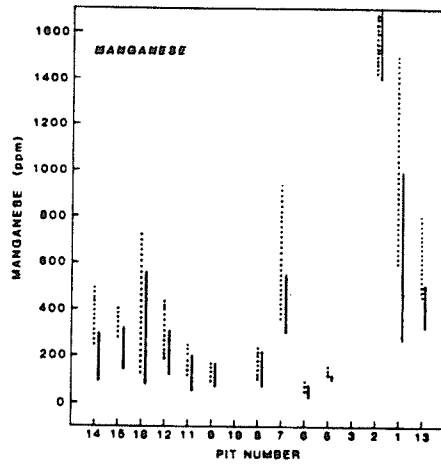
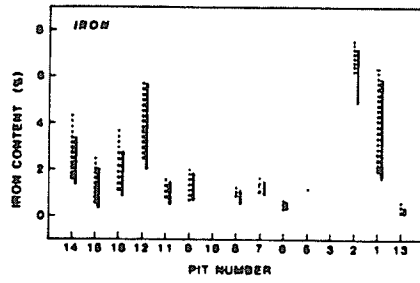
c) partial dissolution of Fe and Mn compounds leading to an incomplete release of elements associated with them.

The extraction ratio means and mean classes, median and median classes indicate that Fe and Zn are the most easily extracted elements in these soils because their extraction ratios are the highest, and also that the Px procedure has an over 80% effectiveness in extracting these elements. The effectiveness decreases in the order Ni, Cu, Co, Mn, Pb.

Geochemical Dispersion Within the Soil Profiles

The ranges of the different elements within the profiles are illustrated in Figure 21. The widest ranges and the highest contents for all elements generally occur in the residual profiles (Pits 14, 18, 12, 11, 9, 2, 13). This is a result of enrichment or accumulation of the elements in specific horizons or subhorizons. The influence of the rock type on the geochemical response of all elements is indicated by both ranges and contents of the elements. Pit 2 is a residual lateritic profile developed on a diabase. Pits 3 and 1 consist of transported overburden. The former is mainly derived from a granodiorite parent rock (Table 16) and the latter from Transvaal rocks (Table 18). The contents of Fe, Mn, Co, Ni, Pb and Cu of Pits 3, 2, and 1 are well in excess of those obtained from granites. Pit 18 occurs over a granite and contains anomalous contents and ranges of Mn, Co, Ni and Pb (Figure 21).

Figure 21. Element content ranges in soil profiles of the Tletletsi Area. Missing ranges indicate no analysis.



... Total Extraction Range (Tx) | Partial Extraction Range (Px)

Iron Dispersion

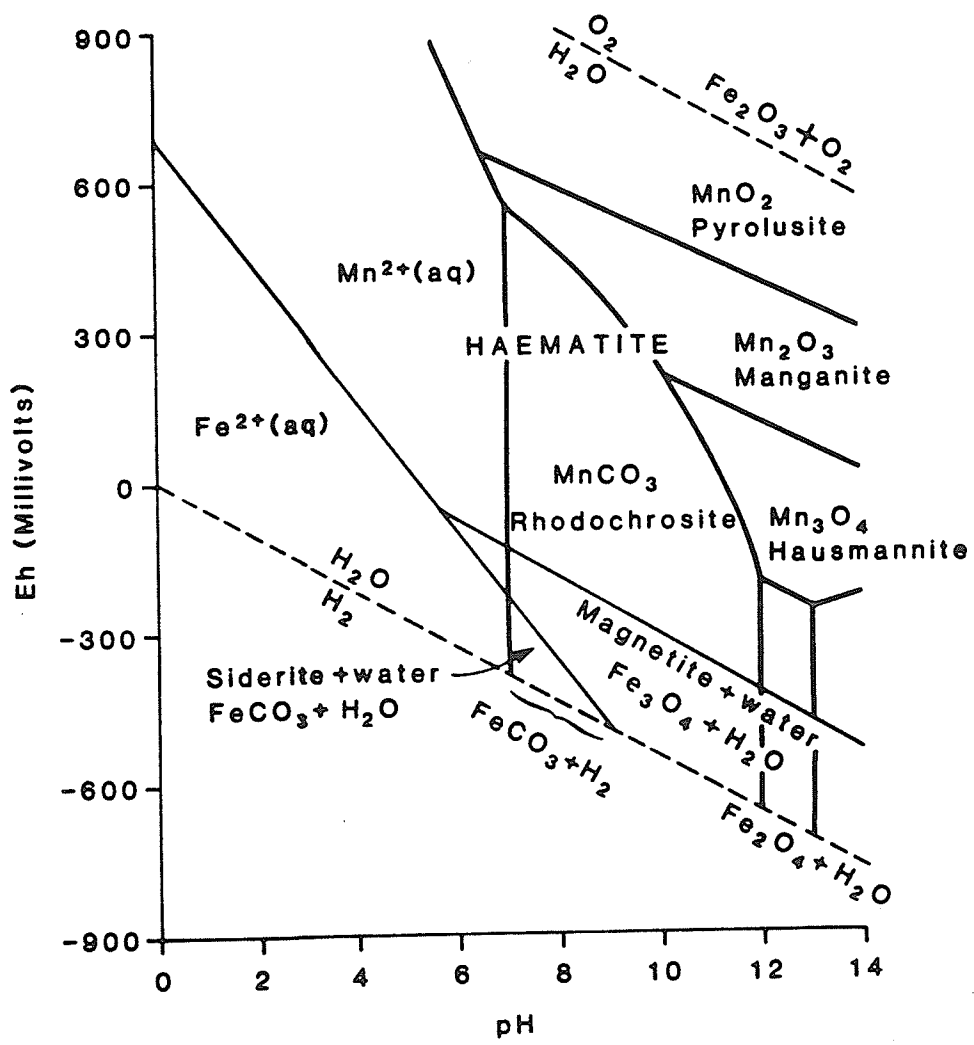
The ranges of the Fe contents of the different profiles in Figure 21 indicate that the residual profiles generally have higher contents and broader ranges than transported for the soils developed on granites. In the transported soils, the lower ranges and contents are due to incomplete weathering and also leaching as in Pit 6. Pit 7 for example, contains abundant magnetite (of a coarse and fine fraction) and also has a low Fe Tx and Px ranges of the fraction analyzed. The Tx range is much larger than that for Px. The small Px range reflects the incomplete weathering of Fe minerals. Losses of Fe during the transportation of debris by water can also result in low contents. The amount of pre-transportation weathering can therefore be a crucial factor.

The Fe contents are also dependent on the rock types and the source of detritus. Pit 2 and 1 contain soil derived from diabase and Transvaal rocks respectively and have higher contents than those from granites.

Figure 22 gives the stability fields of Fe and Mn compounds in the weathering environment. It can be seen that magnetite is an unstable mineral in this soil environment because the Eh values are oxidizing and the pH values of the soils are too low for magnetite stability. The presence of magnetite can be accounted for by its slower rate of weathering relative to the other primary minerals of the parent rocks.

Low and constant Fe values in the A horizons of Pits 14, 18, 11 and 8 indicate the effect organic matter has on Fe. Organic matter is known to promote the mobility of Fe by the formation of soluble organometallic complexes. Rose et al (1979, p. 208) state that the movement of Fe and Al out of surface horizons probably involves chelation by organic acids. Baas-Becking et al (1960) state that the reduction of Fe may take place even in topsoils in the presence of organic matter. According to Cloke (1966),

Figure 22. Stability relationships of Fe (light lines) and Mn (heavy lines) compounds at 25° and 1 atmosphere pressure. For Mn compounds: total dissolved carbonate species = $10^{-1.4}$ m (Garrels and Christ, p. 242). For Fe compounds: total dissolved carbonate = 10^{-2} m, log (dissolved iron) = -4.0.



the upper A horizon is an environment of Fe leaching in many soil profiles. Decaying organic matter keeps pH low and the Eh weakly reducing. Low values of Fe in A horizons do not occur in all of the profiles.

In the residual soils and some of the transported soil profiles (Pits 14, 18, 11, 9, 8, 13, 15) the Fe is distinctly accumulated in specific subhorizons. The increase of Fe content with depth is accompanied by a noticeable deepening of the reddish brown colouration with depth. The enrichment is strongest in the B_2C_1 subhorizons (Pits 18, 11, 9, 13). Below this the Fe content may drop sharply and mottling may be present (Pits 14, 15, 8, 13).

This upper zone indicates the upper level of groundwater fluctuation. If Fe is carried down in solution during the wet season, it is possible that it could be oxidized during the dry season. The B_2C_1 subhorizon in the residual soils is about 30 cm thick and the enrichment of Fe is so strong that the gradual increase of Fe with depth is abruptly broken by the intense accumulation.

Pits 15, 3 and 2 are lateritic and have been cemented into hard subhorizons. Seasonal variations in groundwater are a cause of laterization and hardening of soils.

Manganese Dispersion

The Mn ranges of the profiles are shown in Figure 21. As with Fe, the more pronounced variations are due to rock type differences. Pit 2 and 1 show very wide ranges and very high contents. Pit 18 is anomalous in that it has a high Mn range and contents despite being developed from a granite.

In the transported soils, the Tx and Px ranges are very similar. Pit 7 has an extremely high Tx range and a small Px range. This indicates

that much of the Mn could still be in finely comminuted primary minerals or removed in solution during the erosion of the debris or in a relatively insoluble form of a secondary Mn mineral. The high correlation of Mn with Fe, Zn and Co favours the latter explanation because the association of Mn with these elements is possibly due to adsorption and/or coprecipitation.

The downprofile distributions of Mn are divisible into three categories:

a) accumulation in the A (Figure 6) or B horizon (Figure 19) or C horizon (Figure 14, 18).

b) accumulation in two separate non-adjacent subhorizons or intervals (Figure 9,11).

c) no significant accumulation (Figure 13, 15).

The accumulation of Mn in the A horizon is due to uptake by plants and fixation into organic (humic) matter (Horsnail and Elliot, 1971; Boyle and Dass, 1967).

A number of factors suggest that Mn may be mobile in the soils of the Tletletsi Area:

a) accumulation in A horizon - plants can only take up 'available' Mn, that is, Mn in solution.

b) accumulation in the A and C horizons and lack of enrichment in the B horizon in some profiles.

c) low correlation with some elements known to have strong affinity for Mn compounds. Mobile ionic Mn does not adsorb or coprecipitate other ions in solutions.

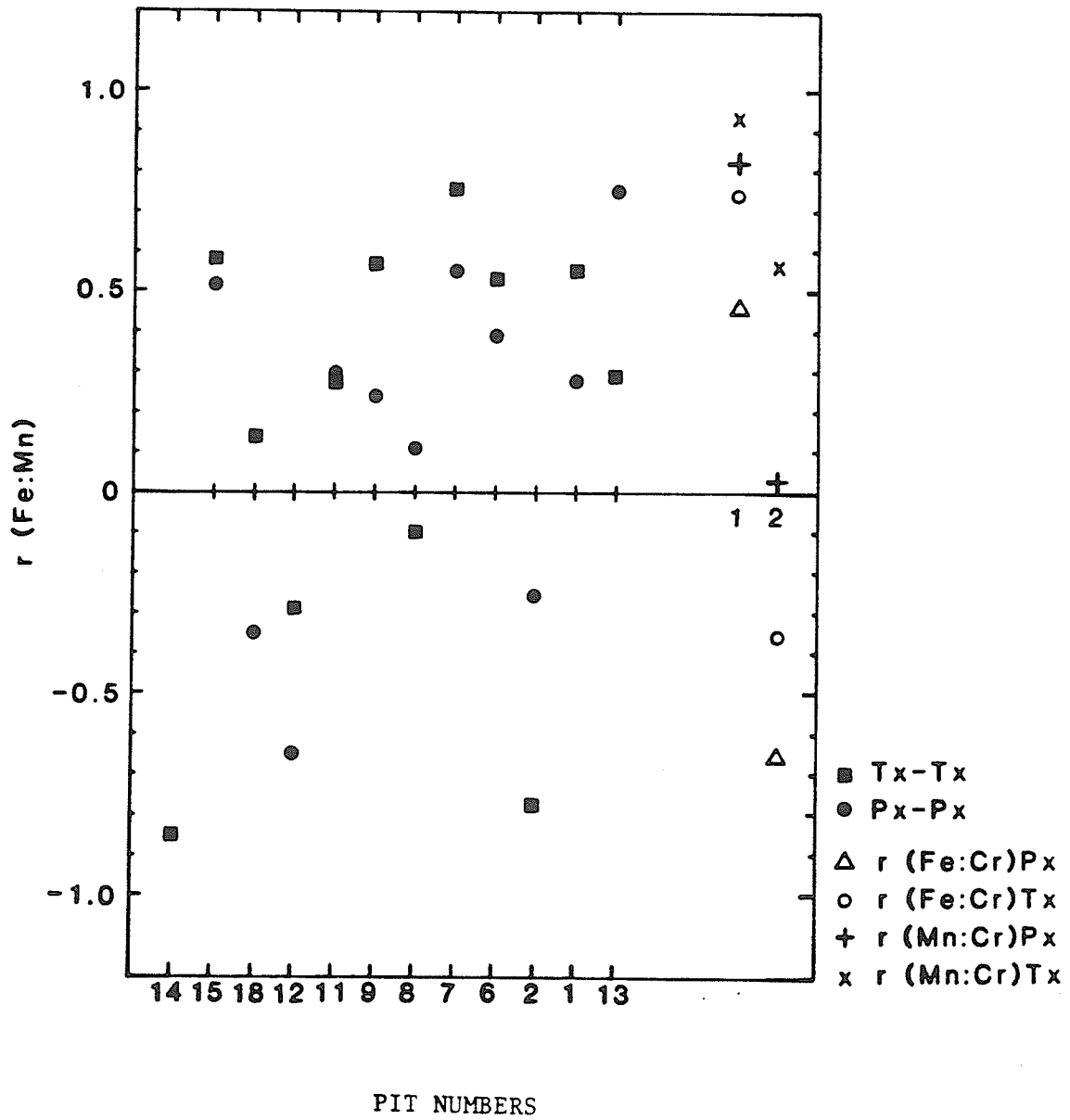
d) no correlation with Fe in most profiles.

The acid pH values of the Tletletsi Area soils are favourable to mobility of Mn.

A comparison between the trends of Mn and Fe is depicted in Figure 23 by the correlation coefficients from each of the profiles where both Mn and Fe data were obtained. The statistically significant correlations are those of Pit 15 (CV = 0.54), Pit 13 (CV = 0.62), Pit 7 (CV = 0.44) and Pit 1 (CV = 0.44). The Pit 6 correlation is doubtful because extreme leaching and depletion can lead to apparent similarities of downprofile trends. In Pit 9, the high correlation is only apparent because it is less than the critical value (0.67).

For most of the pits, the Mn, Fe contents vary in an antipathetic or weakly sympathetic manner. The cycles of Fe and Mn in the secondary environment are usually the same in essential features, and where differences occur, they can be explained by the lower affinity of Mn for oxygen (Rankama and Sahama, 1950, p. 649). Ionic Mn (divalent) can remain in solution until the bulk of Fe is precipitated. Krauskopf (1979, p. 218) attributes the difference of Mn and Fe behaviour to the differences of their colloidal oxides or relative stability of organic complexes (p. 219). Garrels and Christ (1965, p. 387) utilized thermochemical data to show that Fe compounds to be expected in nature are less uniformly soluble than Mn compounds and that the ferrous ion is more readily oxidized than the manganous ion under any naturally occurring pH conditions. Inorganic processes should always lead to the precipitation of Fe before Mn from solutions containing both elements, unless the Mn/Fe ratio is very high. Jenne (1968) notes that more Mn is 'available' (in solution for plant uptake) from more acid soils. In alkaline soils precipitation tends to be favoured. The alkaline pits in this study (Pit 15, 2, 1, 13) have weak Fe:Mn associations like some profiles with non-alkaline pH values. The pH therefore does not contribute significantly to the dissimilar behaviour or lack of sympathetic association of Mn and Fe in the soils of the Tletletsi Area.

Figure 23. Pearson correlation coefficients of Fe:Mn for
all Pits and (Fe, Mn):Cr for Pit 1 and 2 only.



Other Trace Element Correlations

An examination of the trace element distribution graphs (Figure 6 to 20) indicates that there is a strong and recurring similarity of downprofile trends of the elements in various pits. These similarities can be correlated with either Fe and/or Mn. Figure 24 a to j is a graphical representation of the strengths of similarities by correlation coefficients. Negative correlations have not been plotted to simplify the presentation.

Zinc Correlations

Figure 24 a and b shows the correlations of Zn with Fe and Mn respectively. The residual profiles (Pits 14, 12, 11, 9, 13) have significant Fe:Zn correlations and only Pits 8 and 7 of the transported soils show a significant Fe:Zn correlation. The Pit 8 correlation is probably more apparent than real because of leaching.

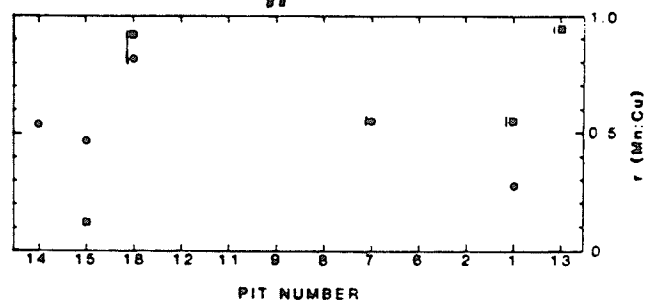
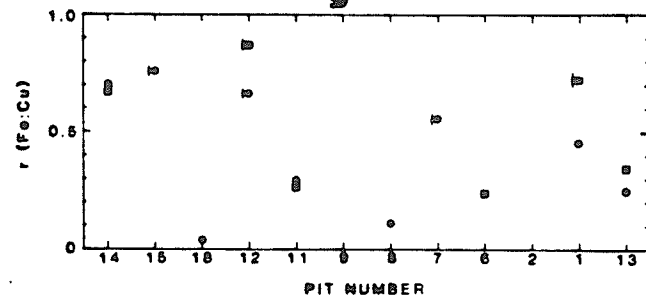
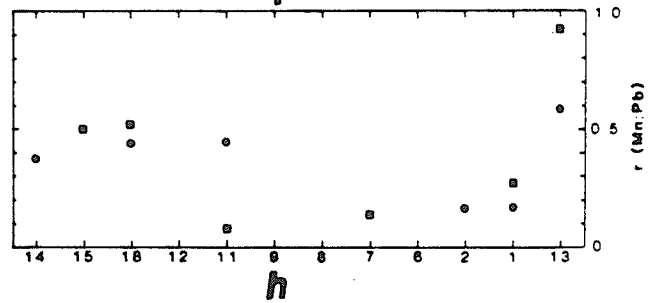
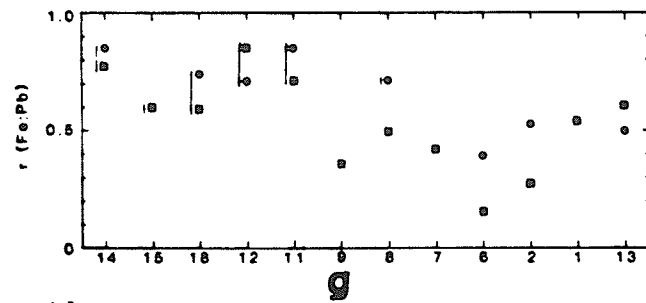
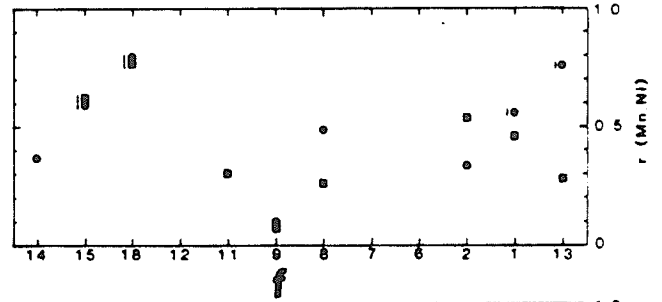
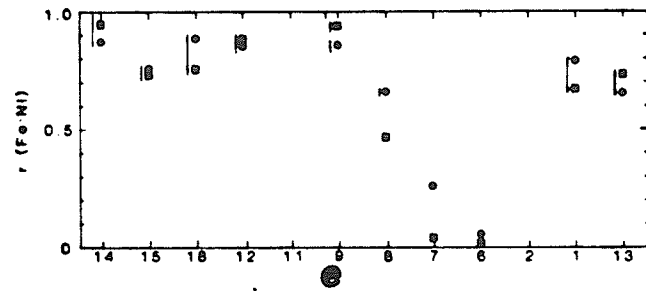
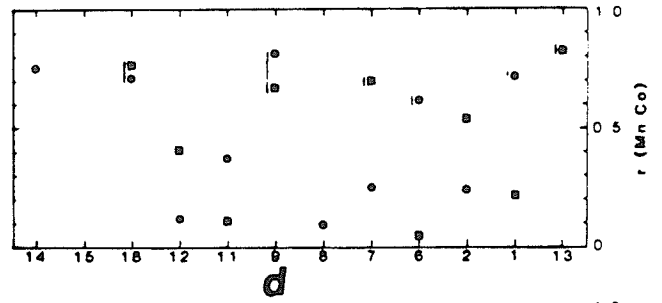
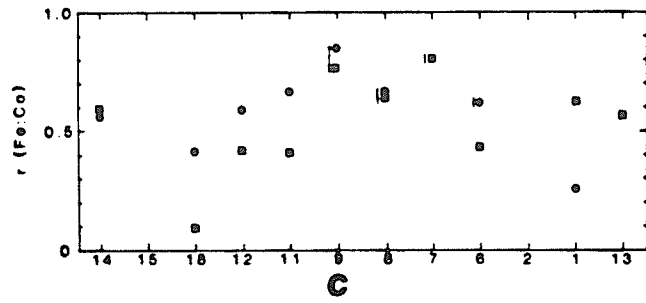
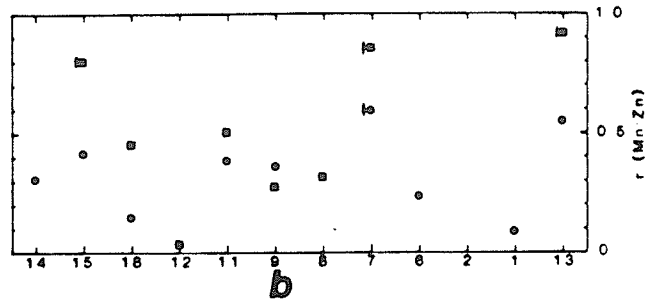
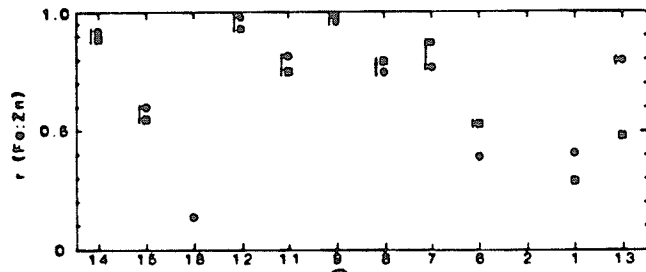
Significant Mn:Zn correlations are restricted to the alkaline profiles (Pits 15, 7, 13). Zinc correlates more strongly with Fe than Mn in this environment.

Cobalt Correlations

Figure 24 c and d show correlations of Fe and Mn with Co. Significant Fe:Co correlations are those of Pits 11, 9, 8, 7 and 6. Pits 8 and 6 correlations may be more apparent than real because their soils are strongly leached.

Manganese correlates with higher values of r than Fe. The significant correlations are in Pits 14, 18, 9, 7, 6, 1 and 13. Pit 6 correlation may also be a result of leaching. Mn has a stronger covariance with Co in this environment.

Figure 24: Pearson correlation coefficients
for (Fe, Mn):Zn, Co, Ni, Pb and Cu.
Vertical lines indicate significant
correlations.



PIT NUMBER

PIT NUMBER

○ Tx-Tx ■ Px-Px

Nickel Correlations

Figure 24 e and f show correlations of Fe and Mn with Ni, respectively. Significant Fe:Ni correlations are those of Pits 14, 15, 18, 12, 9, 8, 1 and 13. Pit 8 is more apparent than real because of intense leaching in the profile.

Mn has lower values of correlation and the significant correlations are for Pits 15, 18, 1 and 3. Ni has a stronger covariance with Fe than Mn in these soils.

Lead Correlations

Correlations of Pb with Fe and Mn are shown in Figure 24 g and h respectively. Significant Fe:Pb correlations are those of Pits 14, 15, 18, 12, 11 and 8 which are all residual profiles except Pits 15 and 8. The significant correlations in Pit 8 could be caused by leaching in the profile. The significant correlation of Mn and Pb is that of Pit 13 only. Lead has a stronger covariance with Fe than Mn in this environment.

Copper Correlations

Figures 24 i and j show the covariance of Cu with Fe and Mn. Significant Fe:Cu correlation is in Pits 15, 12, 7 and 1. Mn:Cu correlation is significant for Pits 18, 7, 1 and 13 only. Except for Pit 18, Cu correlates more strongly with Fe than with Mn in the soils of the Tletletsi Area.

Chromium Correlations

Cr correlations for two pits (Pit 2 and 1) gave very significant correlations, suggesting that some Cr is released during weathering in the soils (Figure 23).

The Effects of Carbonate in the Soils

The reaction with dilute acid of samples from Pits 15, 7 and 1 indicates that alkaline carbonate conditions of weathering in these profiles

have to be considered. The presence of carbonate in soils affects the migration of several trace elements. Bradshaw and Thompson (1979) note that in soils of transported origin, trace element distribution patterns will be determined by the composition of the parent material and modified by the presence of carbonate material by the formation of insoluble or soluble complexes or by precipitation of simple carbonates.

The effect of carbonate in the soils can be estimated by using the following equations from Mann and Deutsher (1980):

$$\text{Log } a_{(\text{CO}_3^{--})} = \text{Log } f_{(\text{CO}_2)} - 18.17 + 2 \text{ pH} \dots\dots\dots 1$$

(where a = activity and f = fugacity)

In Pit 15, where the average pH = 9.5,

$$\text{Log } a_{(\text{CO}_3^{--})} = -3.50 - 18.17 + 19.00 \dots\dots\dots 2$$

(f at atmospheric CO₂ equilibration with water is -3.50)

$$\text{Log } a_{(\text{CO}_3^{--})} = -2.67 \dots\dots\dots 3$$

$$\text{thus } \text{CO}_3^{--} = 10^{-2.67} \dots\dots\dots 4$$

(where CO₃⁻⁻ is the molar concentration). In very dilute solutions the activities of the ionic species are practically equal to concentrations.

The solubility product of a simple carbonate compound is defined as:

$$K_{\text{XCO}_3} = [\text{CO}_3^{--}] [\text{X}^{++}] \dots\dots\dots 5$$

(where X is a trace element cation).

Table 31 lists the solubility products of simple Fe⁺⁺, Mn⁺⁺, Zn⁺⁺, Co⁺⁺, Ni⁺⁺, Pb⁺⁺ and Cu⁺⁺ carbonates. It can be seen from Table 31 (concentrations at equilibrium) and the individual analytical pit data that the precipitation of carbonates is likely to have taken place within the soils. The concentrations of Fe, Mn, Zn, Co and Pb as determined by atomic absorption is much higher than the equilibrium carbonate concentrations.

Table 31. Carbonate solubility products, atomic weights and concentration of the trace elements (ppm) at equilibrium. Solubility products from Krauskopf (1979, p. 553)*.

Element	Solubility product (k) of carbonate	Atomic Weight of element	Element Concentration at Equilibrium ($\times 10^{-7.3}$)
Fe ⁺⁺	$10^{-10.7}$	56	56
Mn ⁺⁺	$10^{-9.3}$	55	55
Zn ⁺⁺	$10^{-10.0}$	65	65
Co ⁺⁺	$10^{-10.0}$	59	59
Ni ⁺⁺	$10^{-6.9}$	59	59
Pb ⁺⁺	$10^{-13.1}$	207	207
Cu ⁺⁺	$10^{-6.8}$	64	64

*Equilibrium at pH = 9.5

In addition, figures 22 and 25 indicate that the Eh and pH conditions of the soils are suitable for the precipitation of carbonates of the trace elements Mn, Co, Ni and Pb.

The correlations in the neutral to alkaline profiles could, therefore, be apparent (for example, MnCO_3 and ZnCO_3 could be accumulated together due to pH conditions rather than adsorption). Carbonate complexes (charged and non-charged), can also be present and cause unpredictable trace element variations with adsorbents.

Control of the trace element dispersion by Fe and Mn compounds

The control of trace elements by Fe and Mn compounds and by other phases in the secondary environment is an observation that is well documented in surface and near-surface geochemistry. Jenne (1968) has cited a substantial amount of literature that deals with the effects of hydrous oxides of Fe and Mn on trace elements in the secondary environment. Among the various forms of direct and indirect evidence, the parallel increase or decrease of trace elements with Fe and/or Mn content in soils was found to be consistent in several investigations.

Jenne (1968) proposed that the hydrous Fe and Mn oxides furnish the principal controls on the fixation of Co, Ni, Cu and Zn in soils and fresh water sediments, and that they exert chemical activity far in excess of their total concentration. Thus, the use of correlation analysis is a suitable method in the determination of such chemical activity.

The similar behaviour of Mn, Co and Ni to Fe during laterite formation was interpreted by Norton (1973) as suggesting the effect of the same controlling mechanism. He attributed it to similar relationships among solubility, Eh and pH during weathering.

Tessier et al (1982) found, in a study of stream sediments, that for a given sample, the variation of trace metal levels specifically adsorbed

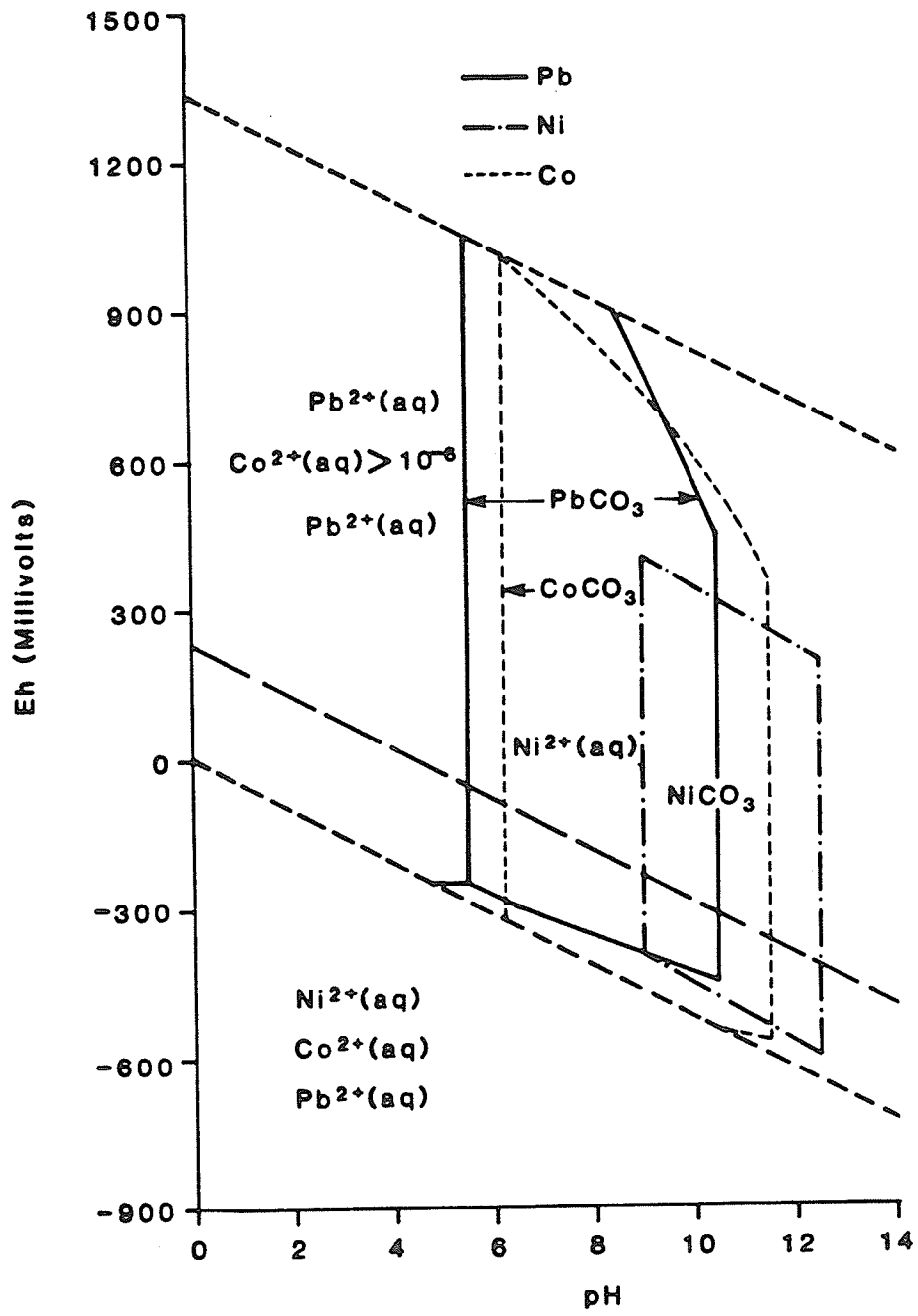
Figure 25. Stability relationships of Co, Ni and Pb carbonates at 25°C and 1 atmosphere pressure.

For Co: total dissolved carbonate species = $10^{-1.5}$ m

For Ni: $P_{\text{CO}_2} = 10^{-0.8}$ atm.

For Pb: total dissolved carbonate species = $10^{-1.5}$ m

(after Garrels and Christ 1965, p. 249, 246, 235).



or bound to carbonates and to Fe-Mn oxides reflected changes in available quantities of the inorganic scavenging phase (Fe oxide/Mn oxide). Whitney (1980) found that Zn, Cd, Co, Ni, Pb and Cu showed strong positive correlation with Mn, reflecting the well known tendency to adsorb and incorporate trace metals.

Murray (1975) proposed a model for adsorption. He suggested that the interaction of metals with hydrous MnO_2 involves the separation of a proton from the covalent bond at the surface, and the association of a solute cation with this site. The sequence of affinity for adsorption is $Co \geq Mn > Zn > Ni$.

Wagner et al (1979) proposed that the isomorphous substitution of Al^{3+} for Mn^{4+} results in a negative charge of Mn adsorbant phases and that charge neutralization by divalent base metal ions (Co, Cu, Ni, Zn, V) leads to adsorption.

The exact metal content associated with either Fe or Mn can be determined by sequential analysis using various extractants (Mitchel, 1972; Tessier et. al., 1982; Chao, 1972; Gatehouse et. al, 1977), and the contribution of adsorbed metal can be appraised in a direct manner. Such an approach would be more effective in isolating the adsorptive contribution of Fe and Mn to the total metal content of the soils. The correlation analysis in such procedures is more appropriate than the approach adopted in this study.

Farrah et. al. (1980), approached the study of metal adsorption by clays using the Langmuir isotherm equation. The equation minimized the scatter in the data obtained using the equations of the type applied in this study. Furthermore, the equation was adjusted to a "competitive" form in which the relative affinities of different metal ions for adsorptive sites were taken into account.

The underlying principles of the treatise can be extended to Fe and Mn hydrous oxide adsorption.

It has been shown by Taylor and McKenzie (1965) that adsorption also depends on the particular secondary mineral present or dominant. Lithiophorite, for example, adsorbed Co more strongly than birnessite in the soils they studied.

The correlation coefficients of Px-Px and Tx-Tx pairs differ significantly for the same element (figure 23 and 24). These differences are believed to be due to the following factors:

a) incomplete weathering. Elements that are still held in primary minerals will not correlate with Fe and Mn secondary compounds because the latter compounds have no control over them. The Tx-Tx correlation will be more strongly affected by incomplete weathering because the Tx procedure dissolves both primary and secondary minerals.

b) presence of different secondary Fe and Mn compounds in the soils. Taylor and McKenzie (1965) found that lithiophorite adsorbed more Co than birnessite in the soils they studied. Partial leaching could decompose the compounds differently.

Stream Sediment Data Examination

Stream sediment data from a previous study by Marengwa (1978) were examined and it was found that the sediments contain very high Ti, Sn and V concentrations. An R-mode principal component analysis was used. The initial assumption in the treatment of the stream data in this study was that clastic and very fine-grained Ti, Sn, and V bearing primary and resistant minerals account for the high abundances. It was also assumed that if Ti and V were associated in the fine-grained magnetite, occurring in the stream sediments, as was suggested by Key (1979), a high positive

correlation would be found between the Ti and V from the stream sediment data. Magnetite was separated from several composite samples of some pits from the present study and analyzed for V, Cr and Ti in order to determine the amounts of V, Cr and Ti that occur in the magnetites. The results of the analysis are shown in Table 32. The magnetites have high abundances of V, Cr and Ti. Thus magnetite would probably be one of the sources of high V, Cr and Ti in the soils. No soil samples were analyzed for V and Ti. Only Pits 2 and 1 soil samples were analyzed for Cr content.

Factor Analysis Results

The five factor models of quartimax and varimax rotations using the data of Marengwa (1978), gave a data variance of 100%. The first three factors accounted for more than 85% of the variance in both rotations. Tin did not load within the first three varimax factors of the Tletletsi Subpopulation (Table 33). The quartimax rotation gave a high Sn loading within the first three factors (Table 33). Tin loaded very significantly within the first three factors of both quartimax and varimax rotations for the Gaborone Subpopulation (Table 34). Comparisons of the first three factors from both rotations indicated similarities between the factors 2V and 2Q. Factor 3V resembled factor 1Q. The higher loading of the V and Cr is likely due to the rotational method and characteristic high loadings on the first factor of any solution. Factor 3Q is the Sn factor.

The significance of an element to an association is defined in various ways. In this study it was taken as any loading that is over one third the variance of the minimum eigenvalue of the first three factors. The loading for both rotations are shown in Figure 26 and the dominant metals of the first three factors of each solution are listed in Table 33. In addition, the statistical parameters of their factor scores are also listed in Table 33. All factor scores with values above the standard deviation

Table 32. V, Cr and Ti contents of some magnetites
from Pits 15, 18, 12, 7, 13 and 2*.

Pit	V (ppm)	Cr (ppm)	Ti (ppm)
15	> 20000	1830	6790
18	> 20000	1900	3430
12	> 20000	n.a.	2800
7	15620	610	n.a.
13	> 20000	1060	4500
2	12370	1160	5300

* n.a. no analysis

According to the 1L 251 manufacturer,

"Al, Ti and Fe have been reported to enhance V absorption. This absorption is most probably a consequence of the metals competing with V for available oxygen in the flame and thus minimizing the formation of refractory V oxide."

Table 33. Factor Analysis Results:

Tletletsi Area Subpopulation.*

FACTOR	EIGENVALUE	% VARIANCE	CUM %
1	2.316	46.3	46.3
2	1.268	25.4	71.7
3	0.839	16.8	88.5

FACTOR MATRIX

VARIMAX ROTATION

	FACTOR 1	FACTOR 2	FACTOR 3
Sn	0.152	-0.067	0.005
V	0.376	-0.043	0.382
Ti	0.005	0.985	0.159
Cr	0.908	0.010	0.210
Mn	0.216	0.221	0.896

FACTOR MATRIX

QUARTIMAX ROTATION

	FACTOR 1	FACTOR 2	FACTOR 3
Sn	0.055	-0.069	0.990
V	0.943	-0.082	0.020
Ti	0.092	0.993	-0.068
Cr	0.567	-0.007	0.226
Mn	0.867	0.276	0.004

FACTOR CORRELATIONS

OBLIQUE ROTATION

	FACTOR 1	FACTOR 2	FACTOR 3
FACTOR 1	1.000	0.000	0.096
FACTOR 2	0.000	1.000	-0.131
FACTOR 3	0.098	-0.131	1.000

*CUM% = Cumulative Percentage

Data from Marengwa (1978).

Table 34. Factor Analysis Results:
Gaborone Area Subpopulation*

FACTOR	EIGENVALUE	% VARIANCE	CUM %
1	2.499	50.0	50.0
2	0.982	19.6	69.6
3	0.870	17.4	87.0

FACTOR MATRIX

VARIMAX ROTATION

	FACTOR 1	FACTOR 2	FACTOR 3
Sn	0.015	0.996	0.058
V	0.116	0.067	0.370
Ti	0.981	0.015	0.056
Cr	0.064	0.077	0.886
Mn	0.207	0.042	0.273

FACTOR MATRIX

QUARTIMAX ROTATION

	FACTOR 1	FACTOR 2	FACTOR 3
Sn	0.099	0.013	0.995
V	0.905	0.107	0.052
Ti	0.155	0.982	0.013
Cr	0.936	0.037	0.063
Mn	0.566	0.218	0.034

FACTOR CORRELATIONS

OBLIQUE ROTATION

	FACTOR 1	FACTOR 2	FACTOR 3
FACTOR 1	1.000	0.144	0.259
FACTOR 2	0.144	1.000	0.043
FACTOR 3	0.259	0.043	1.000

* CUM % = Cumulative Percentage

Data from Marengwa (1978).

Table 35. Element associations and statistical
Parameters of Factor Scores for the
Tletletsi Subpopulation.*

Factor	Element Association	σ	Mode	Median	Samples > σ	Samples > 2σ
1V	Cr-V	1.327	3.494	0.045	42	23
2V	Ti-Mn	1.065	0.612	0.419	12	0
3V	Mn-V	1.308	2.610	-0.317	46	18
1Q	V-Mn-Cr	1.989	5.265	-0.455	50	25
2Q	Ti-Mn	1.085	0.488	0.418	12	0
3Q	Sn	1.050	-0.080	-0.212	40	10

* σ = standard deviation
V = varimax factor
Q = quartimax factor

Data from Marengwa (1978).

are considered anomalous. In normal distributions, the standard deviation of normalized factor scores is 1.00 (Tripathi, 1979), and all values of factor scores above unity are considered anomalous. The mode and median are both equal to zero. The number of anomalous values are listed in Table 33. The Gaborone Subpopulation has been excluded in the calculation of factor scores.

Figure 26 indicates that the associations that occur in the Tletletsi Subpopulation also occur in the Gaborone Subpopulation. The main similarity between the two subpopulations is that Ti and Sn are not associated in the environment. The effect of Mn adsorption is much more clear in the Gaborone Subpopulation as is shown by the loadings of V, Mn, and Cr on Factor 1Q.

The factors for the Tletletsi Subpopulation are interpreted as follows:

Factor 1V (Cr-V)

The high mode of the factor scores over two standard deviations suggests a large number of anomalous values. The main control of the Cr-V association is lithological, and occurs mainly over diabase (Figure 27). The restriction to the mafic rock type indicates low chemical or clastic migration of one or both elements (as might occur if both are held in magnetite).

Factor 2V, 2Q (Ti-Mn)

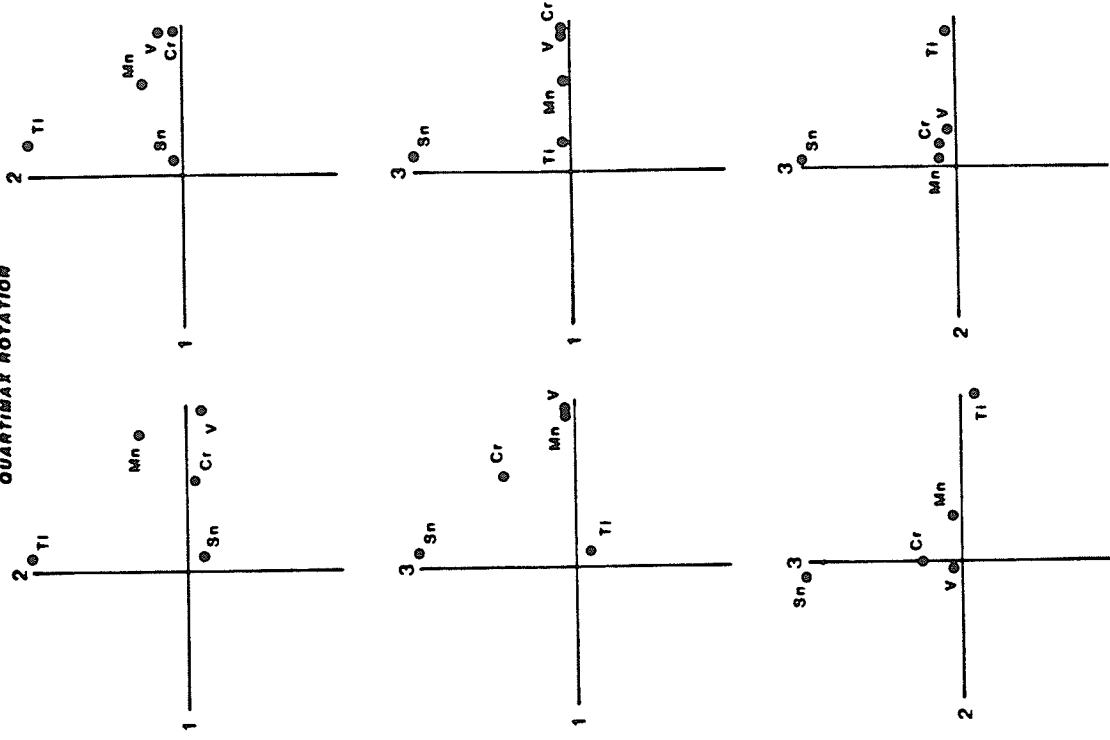
The statistical parameters of this factor indicate that the association has been "homogenized" in the Tletletsi Area. The difference between the mode and the median is the lowest (Table 33, 34) for the subpopulation. The standard deviation of the factor scores is also the closest to unity. Ti is not adsorbed by Fe or Mn compounds (Nowlan, 1976 and Siegel, 1974, p. 193) in the weathering environment. The anomalous contents

Figure 26. Factor Loadings for the Tletletsi and
Gaborone Area Stream Sediment Data
Data from Marengwa (1978).

GABORONE

TLETLETSI

QUARTIMAX ROTATION



GABORONE

TLETLETSI

VARIMAX ROTATION

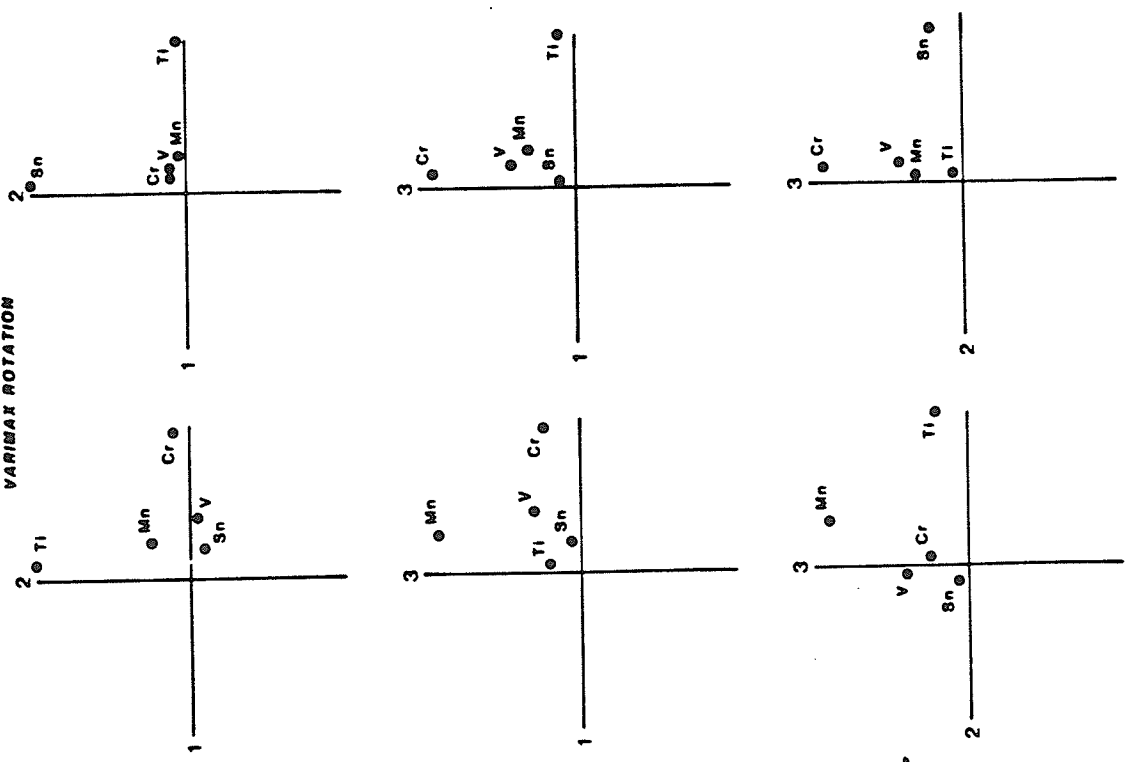
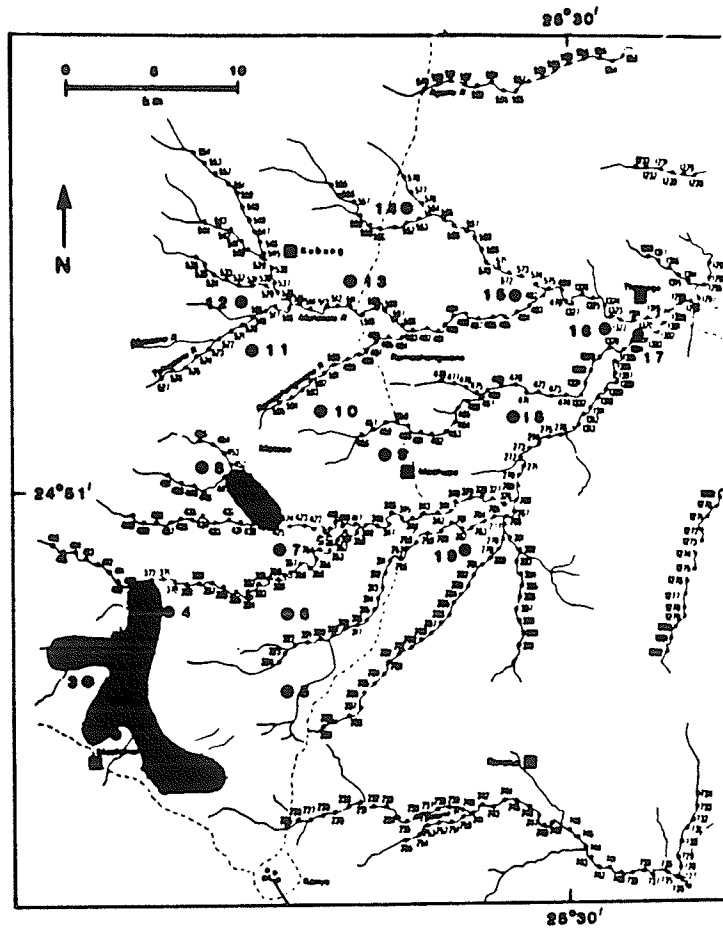


Figure 27. Distribution of Factor 1V. for Cr-V.

Factor Score $\geq 2\sigma$.

Data from Marengwa (1978).

TLETLESI AREA STREAM AND PROFILE SAMPLING LOCATIONS



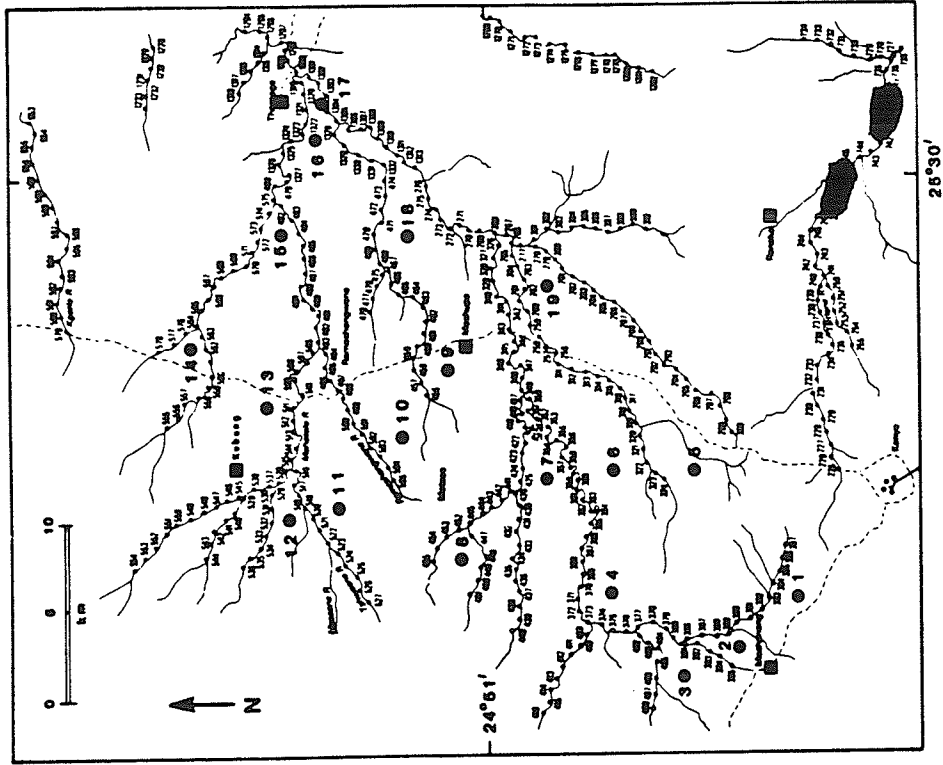
FACTOR 1V

Figure 28. Distribution of Factors 2V, 2Q for Ti-Mn.

Factor Score $> 2\sigma$.

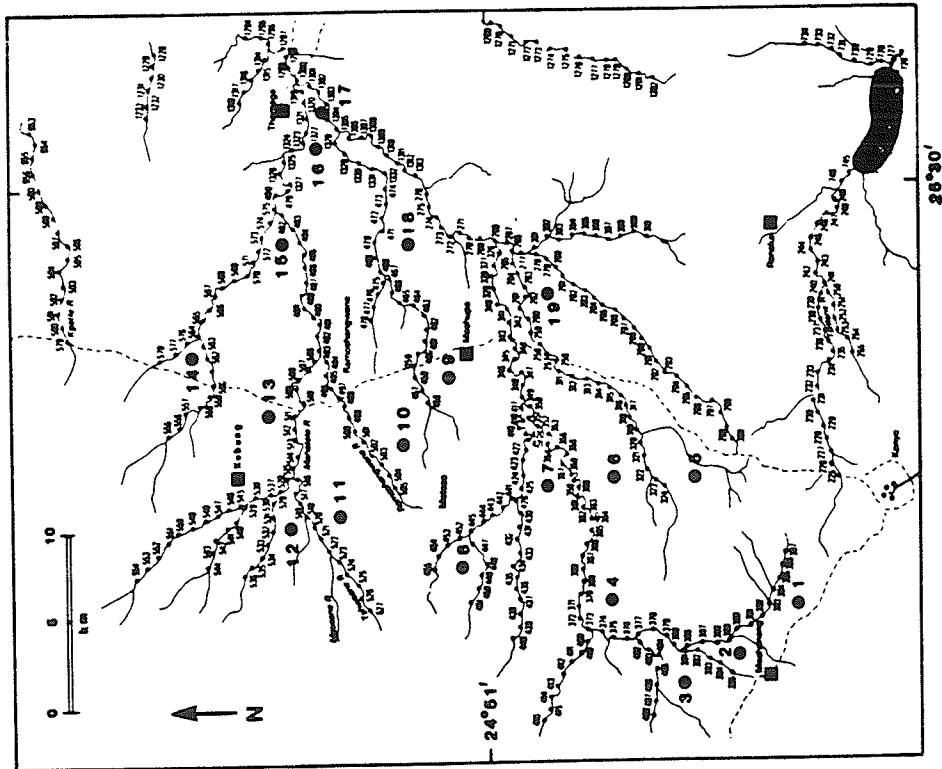
Data from Marengwa (1978).

TLETLESI AREA STREAM AND PROFILE SAMPLING LOCATIONS



FACTOR 2Q

TLETLESI AREA STREAM AND PROFILE SAMPLING LOCATIONS



FACTOR 2V

of Ti and Mn (Figure 28) occur in an area of known diabase outcrops. It is interesting to note that the diabases elsewhere do not score anomalously with respect to this association. It is suggested that this may be an indication of the presence of different diabases in the area.

Factor 3V (Mn-V), 1Q (V-Mn-Cr)

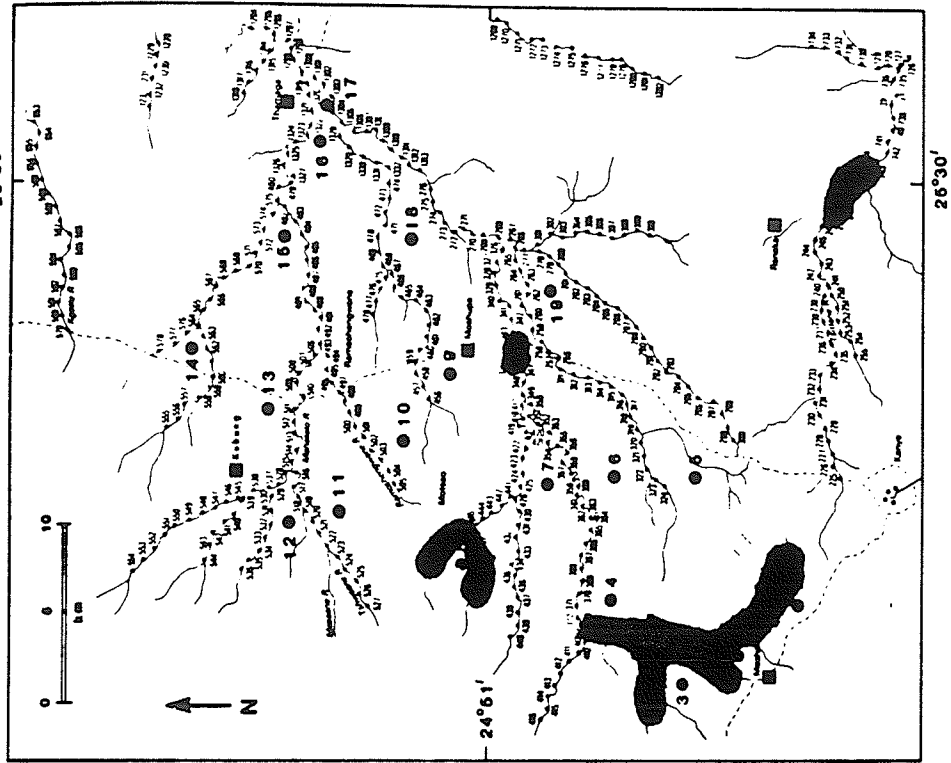
The association of Mn with V and/or Cr is a common occurrence in stream sediments and soils. The association has anomalous factor scores. It represents the adsorptive effects of Mn and in geochemical prospecting the anomalous values are merely geochemical 'noise'. The factor 3V and 1Q have the largest distribution in the area (Figure 29).

Factor 3Q (Sn)

The Sn factor has a near normal distribution as is indicated by the low mode and median (Table 33). The factor scores were found to have a kurtosis of 18.76 which supports the fact that the distribution is nearly normal and therefore most of the data is a single background rather than different aggregate subpopulations. The distribution of the anomalous values is shown in Figure 30. It is believed that the normal distribution of this factor indicates that Sn originates mostly from weathered Sn bearing minerals (possibly biotite) in the granite.

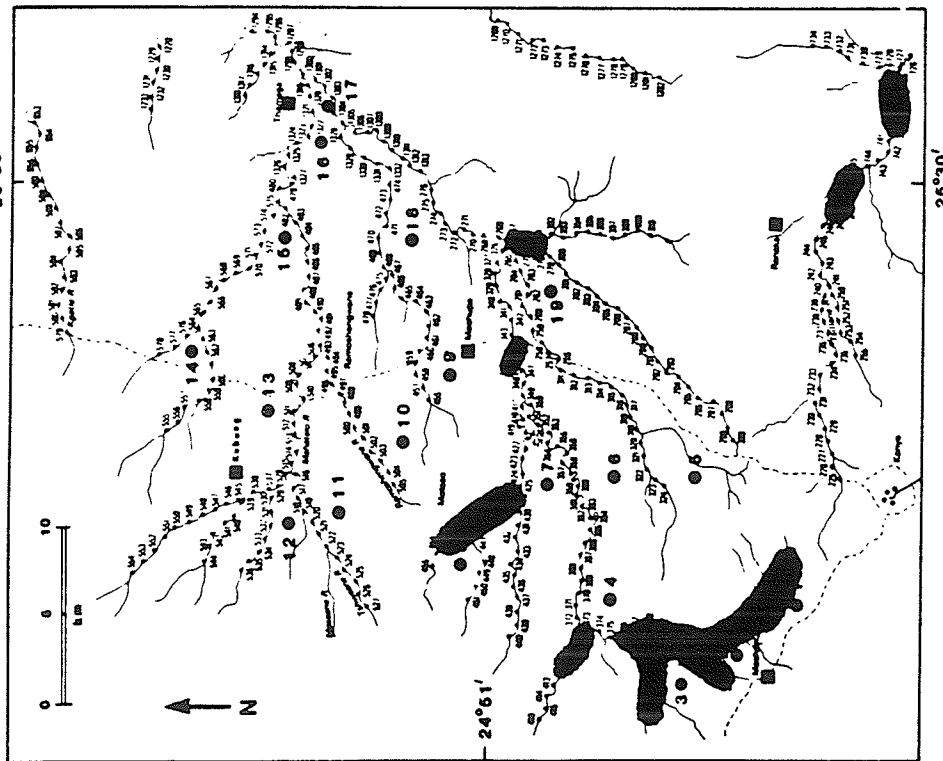
Figure 29. Distribution of Factors 3V (Mn-V), 1Q
(V-Mn-Cr). Factor Score $> 2\sigma$.
Data from Marengwa (1978).

TLETLESI AREA STREAM AND PROFILE SAMPLING LOCATIONS



FACTOR 1Q

TLETLESI AREA STREAM AND PROFILE SAMPLING LOCATIONS



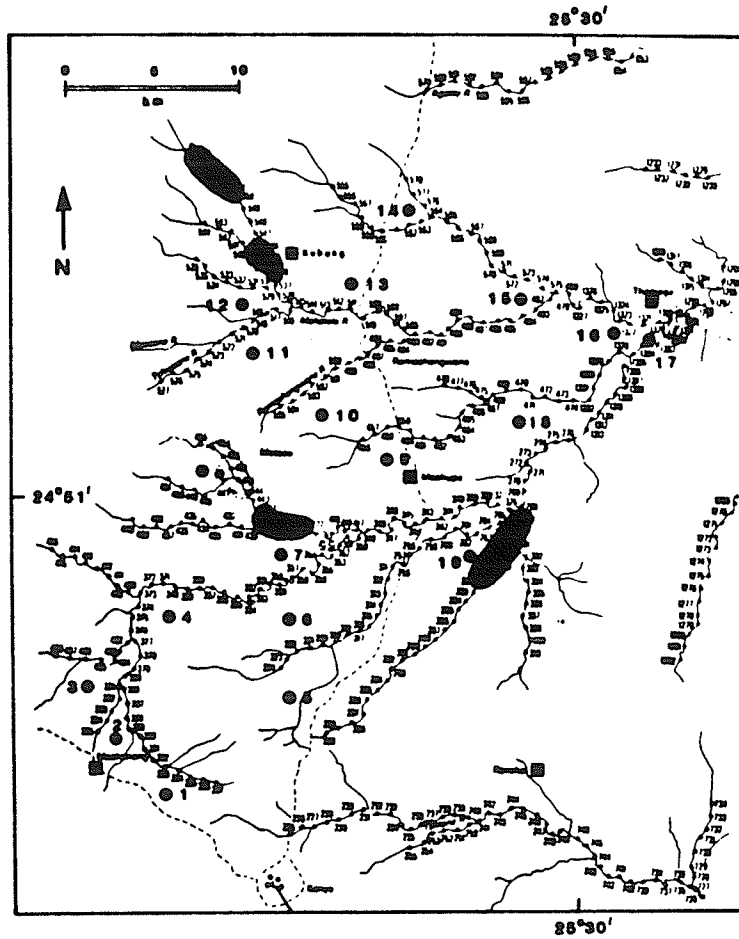
FACTOR 3V

Figure 30. Distribution of Factor 3Q (Sn).

Factor Score $> 2\sigma$.

Data from Marengwa (1978).

TLETLES! AREA STREAM AND PROFILE SAMPLING LOCATIONS



FACTOR 30

CHAPTER VI

CONCLUSIONS

The surface geochemistry of the Tletletsi Area, has been investigated by considering both the physical and chemical properties of soils. In addition, the stream sediment data from a separate study (Marengwa, 1978) has been examined in order to determine the relationships between selected elements. The conclusions reached in this study are as follows:

a) The Tletletsi Area is an environment of active physical and chemical weathering.

b) The products of weathering constitute two groups of soils; residual soils and transported soils. The residual soils are characterized by a sequence of subhorizons, which begins with the A subhorizons and ends with the partly decomposed bedrock. The transported soils have transportational features represented by alternations of coarse and fine to medium-grained material. The transported soils are also weathered to different extents unlike the more uniform weathering exhibited by the residual soils.

c) The geochemical dispersion of the different trace elements indicate that the residual soils tend to have higher element contents in specific subhorizons due to enrichment by downward migration. Transported soils generally have no accumulation of elements in any part of the profile.

The trace element contents in the soils can be correlated with the underlying rock type irrespective of whether the soil is transported or residual. Thus in a wider soil survey encompassing areas underlain by different rock types, the geochemical 'relief' would indicate the different rock types. Mineralization, which contains even higher levels of

trace elements, can be found using a soil survey. The relatively shallow overburden is an advantage because high trace element concentrations normally occur closer to the source.

d) pH can be used as a "rough indicator" of transported soils versus residual soils. The latter tend to have acidic or more acidic pH values than transported soils.

e) The concentrations of the elements Zn, Co, Ni, Pb and Cu in the Tletletsi Area soils are controlled to varying extents by Fe and Mn compounds. The comparative affinities for Fe and Mn are shown in Table 36. Fe exerts more control than Mn on all the elements except Co. The controls can be a possible source of false anomalies. The presence of carbonate will inhibit the migration of the elements by the formation of carbonate compounds.

f) The downprofile patterns of Mn suggest that it is mobile in the soils of the Tletletsi Area.

g) Organic matter affects the dispersion of Fe, Mn and Cu such that an optimum sampling depth will be below the A horizon or at least deeper than 60 cm.

h) An Fe and Mn determination should always be carried out irrespective of whatever elements are of interest in any geochemical survey. The use of different analytical extraction methods would be advantageous in a prospecting program because the effects of Fe and Mn on other elements can be determined and isolated.

i) Ti, Cr and V are redistributed by weathering. The magnetites found in this area contain significant amounts of Ti, Cr and V. The high contents of these elements in soils and stream sediment samples may be primarily due to weathering of magnetite.

Table 36. Comparitive affinities of Zn, Co, Ni, Pb
and Cu for Fe and Mn in the Tletletsí Area soils.

Element	Strength of Control
Zn	Fe > Mn
Co	Fe < Mn
Ni	Fe > Mn
Pb	Fe > Mn
Cu	Fe > Mn

j) Clastic magnetite of very fine grain size may be the cause of the anomalous Cr-V and Ti-Mn associations as indicated by factor analysis.

REFERENCES

- Armour-Brown, A. and Nichol, I., 1970. Regional geochemical reconnaissance and location of metallogenic provinces. *Econ. Geol.*, 65:312-330.
- Baas-Becking, L. G. M., Kaplan I. R. and Moore D., 1960 Limits of the natural environment in terms of pH and oxidation - reduction potentials. *J. of Geol.*, 68 (No. 3): 243-284.
- Bawden, M. G. and Stobbs, A. R., 1963. Land resources of Eastern Bechuanaland. Directorate of Overseas Surveys London. 75 pp.
- Boyle, R. W. and Dass, A. S., 1967. Geochemical prospecting - Use of the A horizon in soil survey. *Econ. Geol.*, 62:284-285.
- Bradshaw, P. M. D. and Thompson, I., 1979. The application of soil sampling to geochemical prospecting in non-glaciated regions of the world. in *Geophysics and Geochemistry in the search for metallic ores*. Geological Survey of Canada, Economic Geology Report 31:327-338.
- Chao, T. T., 1972. Selective dissolution of manganese oxides from soils and sediments with acidified hydroxylamine hydrochloride. *Soil Sci. Soc. Amer. Proc.*, 36:764-768.
- Cloke, P. L., 1965. The geochemical application of Eh-pH diagrams *J. of Geological Education*. Vol. XIV, (4):140-148.
- Closs, L. G. and Nichol, 1975. The role of factor and regression analysis in the interpretation of geochemical exploration data. *Canadian J. of Earth Sciences* 21:1316-1330.
- Crockett, R. N. 1972. A brief explanation of the Geology Sheet 2425C. *Geol. Surv. Dept.*, Botswana.
- Erickson, K. A. and Vos, R. G., 1979. A fluvial fan depositional model for Middle Proterozoic redbeds from the Waterberg Group, South Africa. *Precambrian Research*, 9:169-188. in Key R., 1979. *Memoirs on Gaborone Granite*. Geological Survey Department, Botswana.
- Farrah, H., Hatton, D. and Pickering, W. F., 1980. The affinity of metal ions for clay surfaces. *Chemical Geology*, 28:55-68.
- Garrels, R. M. and Christ, C. L. (1965). *Solutions, minerals and equilibria*. Harper and Row Publisher, N.Y. 450 pp.

- Gatehouse, S., Russell, D.W, and Van Moort, J, C., 1977. Sequential analysis in Exploration Geochemistry J. of Geochem, Expl., 8; 483-494.
- Gedeon, A. Z., Butt, C. R. M., Gardener, K. A. and Hart, M. K. 1977. The applicability of some geochemical analytical techniques in determining the "total" compositions of some laterized rocks. J. of Geochem. Expl. 8:283-303.
- Hamil, B. M. and Nackowski, M. P., 1971. Trace element distribution in accessory magnetite from quartz-monzonite intrusives and its relation to sulphide mineralization in the Basin and Range Province of Utah and Nevada Geochem. Expl., 11:331-333.
- Harriss, R. C. and Adams, J. A. S., Geochemical and mineralogical studies in the weathering of granitic rocks. American J. of Science, Vol. 264: 146-173.
- Horsnail, R. F. and Elliott, I. L., 1971. Some environmental influences on the secondary dispersion of molybdenum and copper in Western Canada. Geochem. Expl., 11:166-175.
- Howarth, R. J. and Martin I., 1979. Computer-based techniques in the compilation, mapping and interpretation of exploration geochemical data; in Geophysics and Geochemistry in search for metallic ores; Geological Survey of Canada. Economic Geology Report 31: 545-574.
- Jenne, E. A. 1968. Controls on Mn, Fe, Co, Ni, Cu and Zn Concentrations in soils and water: the significant role of hydrous Mn and Fe Oxides; in Trace Inorganics in water. Amer. Chem. Soc. Advances in Chemistry Series, No. 73: 337-380.
- Key, R. 1979. Memoirs on the Gaborone Granite. Unpublished. Geological Survey Department of Botswana.
- Krauskopf, K. B., 1979. Introduction to Geochemistry. McGraw-Hill Book Company, 617 pp.
- Levinson, A. A., 1974. Introduction to Exploration Geochemistry. 2nd Edition, Applied Publishing Co. Ltd. 924 pp.
- Mallick, D. I. J. and Habgood F. 1978. Notwani River Geology. Directorate of Overseas Surveys. London.
- Mann, A. W. and Deutscher, R. L. 1980. Solution geochemistry of lead and zinc in water containing carbonate, sulphate and chloride ions. Chemical Geology, 29:293-311.
- Marengwa, B. S. I. 1978. A Geochemical stream sediment survey of stream sediments derived from the Gaborone Granite, Kanye Metavolcanics and Adjacent Rocks. Bulletin 17, Geological Survey Department, Botswana, 51 pp.

- Meyer, W. I., Theobald, P. K. and Bloom, H. 1979. Stream sediment survey in Geochemistry; in Geophysics and Geochemistry in search for Metallic Ores; Pete J. Hood, Editor; Geological survey of Canada Economic Geology Report 31: 411-434.
- Mitchell, R. L. 1972. Trace elements in soils and factors that affect their availability. Geological Society of America Bulletin, v. 83: 1069-1076.
- Murray, J.W. 1975. The interaction of metal ions at the manganese dioxide-solution interphase. Geochimica et Cosmochimica Acta. 39: 505-519.
- Nichol, I., Garrett, R. G. and Webb, J. S. 1969. The Role of some statistical and mathematical methods in the interpretation of geochemical data. Econ. Geol., 64:204-220.
- Nie, N. M., Hull, C. H., Jenkins, G. J., Steinbrenner, K. and Bent, D. H. 1975 Statistical Package for the Social Sciences. 2nd Edition. McGraw-Hill Book Corp. 675 pp.
- Norton, A. S. 1973. Laterite and Bauxite formation. Econ. Geol., 68:353-361.
- Nowlan, G. A. 1976. Concretionary Mn-Fe oxides in streams and their usefulness as a sample medium for geochemical exploration. J. of Geochem. Expl. 6:163-210.
- Perel'man, A. I., 1967. Geochemistry of Epigenesis, Plenum Press, New York, 266 pp.
- Rankama, K. and Sahama Th. G., 1950. Geochemistry. The University of Chicago Press. 911 pp.
- Rose, A. W., Hawkes, H. E. and Webb, J. S., 1979. Geochemistry in Mineral Exploration. Academic Press. 657 pp.
- Siegel, F. R. 1974. Applied Geochemistry. John Wiley and Sons, Inc. 353 pp.
- Taylor, R. M. and McKenzie, R. M., 1965. The association of trace elements with manganese minerals in Australian soils. Austr. J. Soil. Res. 4:29-39.
- Tessier, A., Campbell. P. G.C. and Bisson, M. 1982. Particulate trace metal speciation in stream sediments and relationships with grain size: Implications for geochemical Exploration. J. of Geochem. Expl. 16, 77-104.
- Tripathi, V. S., 1979. Factor Analysis in Geochemical Exploration. J. of Geochem. Expl. 11:263-275.

- Wagner, G. H., Koning, R. H., Vogelpohl, S. and Jones, M. D. 1979. Base metals and other minor elements in the manganese deposits of West-Central Arkansas. *Chemical Geology*, 27:309-327.
- Whitney, P. R., 1981. Heavy metals and manganese oxides in the Genessee Watershed, N. Y. State: Effects of geology and land use. *J. of Geochem. Expl.* 14:95-117.
- Wright, E. P., 1961. Geology of the Gaborone District. Unpub. Ph. D. Thesis, Univ. of Oxford. in Key, R., 1979. Memoirs on the Gaborone Granite. Unpublished. Geological Survey Department of Botswana.
- Young, A., 1976. Tropical Soils and Soil Surveys. Cambridge University Press.

APPENDIX

CHEMICAL DATA FOR TLETLETSI AREA SOILS.

P_x = PARTIAL EXTRACTION.

T_x = TOTAL EXTRACTION.

Pit 14	Fe		Mn		Zn		Co		Ni		Pb		Cu		pH
	Px	Tx	Px	Tx	Px	Tx	Px	Tx	Px	Tx	Px	Tx	Px	Tx	
1	1.25	1.38	300	331	20.0	33.7	5.8	13.5	23.0	28.0	8.0	18.0	7.0	15.0	6.40
2	1.19	2.00	163	275	15.0	31.3	7.3	11.6	12.0	19.0	7.5	14.0	7.0	11.0	6.15
3	1.38	1.88	94	250	18.8	33.8	6.5	17.5	15.0	28.0	7.0	17.0	7.0	15.0	6.45
4	1.88	2.56	138	356	26.3	37.5	6.0	14.5	16.0	37.0	6.5	21.0	9.0	16.0	6.55
5	2.75	3.58	138	388	31.3	43.7	6.5	18.3	30.0	60.0	16.0	22.0	19.5	25.0	6.30
6	3.38	4.38	194	494	37.6	43.0	12.0	16.0	39.0	68.0	16.0	22.5	15.0	22.0	6.35
7	2.81	4.13	219	509	42.6	51.3	21.5	23.7	41.0	73.0	21.0	31.0	31.0	50.0	6.70
8	2.69	2.69													

Pit	Fe		Mn		Zn		Co		Ni		Pb		Cu		pH
	Px	Tx	Px	Tx	Px	Tx	Px	Tx	Px	Tx	Px	Tx	Px	Tx	
1	0.33	.63	110	300	10	16	7	10	8	11	14	14	7	46	8.00
2	1.00	1.18	320	320	18	19	5	5	15	17	14	15.1	11	25	7.65
3	1.25	1.25	230	250	18	20	10	10	13	19	15	24.1	11	24	9.25
4	1.25	1.33	220	330	18	24	7	7	13	22	13	29.0	12	27	9.55
5	1.55	2.13	220	370	19	26	7	11	13	21	16	28.2	13	26	9.60
6	2.13	2.28	220	370	25	31	3	13	14	22	18	37.13	26	44	9.60
7	2.00	2.28	230	360	21	29	7	14	25	25	15	44.9	14	33	9.55
8	2.00	2.05	300	340	25	31	7	7	25	25	17	48.8	31	31	9.45
9	2.00	1.55	280	400	26	39	10	15	22	25	18	50.6	26	29	9.45
10	1.45	1.48	230	370	37	37	3	15	19	23	14	55	25	31	9.25

Fe Mn Zn Co Ni Pb Cu pH

PIT 18	Fe		Mn		Zn		Co		Ni		Pb		Cu		pH
	Px	Tx	Px	Tx	Px	Tx									
1	1.00	1.05	750	1250	24.0	30.0	13.0	18.0	46.0	48.0	5.9	12.4	18.4	18.5	6.90
2	1.00	1.06	750	1100	21.0	26.5	12.0	14.0	44.0	48.0	9.4	13.3	16.0	18.5	6.45
3	1.08	1.08	500	790	27.5	33.0	12.0	12.0	44.0	50.0	8.3	10.5	12.0	25.0	6.75
4	1.38	1.48	200	250	26.5	35.0	8.0	8.0	13.0	18.0	22.5	25.7	10.5	20.0	6.90
5	1.83	2.23	1180	1425	32.0	43.0	24.0	50.0	86.0	97.0	26.5	54.7	24.0	32.0	6.80
6	2.75	3.75	1120	1480	25.0	33.0	34.0	34.0	99.0	108.0	14.5	37.7	28.5	34.0	6.80
7	2.33	2.68	200	300	24.0	33.0	12.0	12.0	64.0	76.0	16.0	20.9	24.0	34.0	6.90
PIT 12															
1	2.00	2.25	310	430	25.0	35.0	12.0	12.0	14.0	15.0	14.0	18.0	10.5	11.0	6.40
2	2.00	2.00	300	430	25.0	30.0	10.5	16.0	7.0	15.0	13.0	21.0	10.0	14.5	6.20
3	3.00	3.15	200	200	40.0	40.0	8.0	11.0	14.0	21.0	19.0	20.5	9.0	12.5	6.20
4	4.15	4.15	160	190	55.0	55.0	10.5	15.0	17.0	27.0	19.5	23.0	16.0	18.0	6.60
5	3.75	4.30	120	190	40.0	45.0	10.5	11.0	15.0	29.0	16.0	26.5	18.0	19.0	6.50
6	3.75	4.15	120	190	45.0	55.0	10.5	15.0	14.0	20.0	16.5	31.0	20.0	21.5	6.50
7	4.15	5.15	150	230	55.0	70.0	11.0	15.0	19.0	29.0	27.0	46.0	39.0	40.0	6.60
8	5.65	5.85	200	430	75.0	95.0	17.0	18.0	22.0	28.0	n.a.	41.0	n.a.	40.5	6.75

n.a. = no analysis

Fe Mn Zn Co Ni Pb Cu pH

PIT 11	Fe		Mn		Zn		Co		Ni		Pb		Cu		pH
	Px	Tx	Px	Tx	Px	Tx	Px	Tx	Px	Tx	Px	Tx	Px	Tx	
1	0.59	0.73	205	251	15.0	20.0	6.0	8.0	11.5	11.5	7.5	15.5	6.70		
2	0.56	0.76	175	190	14.0	16.0	5.0	6.0	10.0	16.0	8.5	19.5	6.75		
3	0.50	0.76	50	115	10.0	16.0	2.5	3.5	7.0	14.0	7.5	17.5	6.60		
4	0.73	0.87	75	140	15.0	18.0	8.0	12.5	13.0	13.0	8.5	17.0	6.40		
5	1.46	1.58	150	210	18.5	21.0	12.5	14.0	18.0	25.5	20.0	43.0	6.70		
6	1.21	1.21	70	250	20.0	22.0	9.5	9.5	23.5	23.5	17.5	18.0	6.60		
7	0.63	0.69	50	250	15.0	16.0	4.5	7.0	13.0	13.0	10.5	16.0	6.50		
8	0.49	0.59	75	165	10.5	17.0	10.5	11.5	8.0	8.0	8.0	21.0	6.50		
9	0.49	0.59	150	235	10.0	13.0	8.0	9.5	8.0	8.0	14.0	24.5	6.45		
PIT 9															
1	0.70	0.70	115	136	9.0	11.0	6.0	7.0	8.0	9.0	2.1	2.5	6.45		
2	0.88	0.90	106	125	14.0	16.0	4.0	4.0	10.0	14.0	7.6	13.5	6.45		
3	0.86	0.98	73	95	14.0	14.0	7.0	7.0	11.0	14.0	9.0	10.7	6.40		
4	0.97	1.04	73	105	15.0	16.0	4.0	4.0	13.0	17.0	11.9	13.0	6.40		
5	1.55	1.55	100	103	20.0	22.0	11.0	11.0	19.0	22.0	13.7	14.5	6.45		
6	1.73	1.88	168	168	20.0	23.0	19.0	20.0	15.0	23.0	8.0	14.8	6.45		

PIT 19	Fe		Mn		Zn		Co		Ni		Pb		Cu		pH		
	Px	Tx															
1	16.0	16.5	6.5	8.1	6.0	13.8	14.4	38.8	8.8	13.8	6.00	13.8	14.4	38.8	8.8	13.8	6.00
2	9.5	15.5	4.0	6.9	5.6	15.0	13.8	37.5	11.9	13.0	7.10	13.8	13.8	37.5	11.9	13.0	7.10
3	9.5	14.5	7.5	8.8	5.6	23.1	21.3	31.3	12.5	18.0	7.10	21.3	21.3	31.3	12.5	18.0	7.10
4	15.5	18.5	9.5	10.6	6.3	17.5	25.0	31.9	11.3	17.0	7.20	25.0	25.0	31.9	11.3	17.0	7.20
5	15.5	15.5	9.4	10.0	10.0	15.0	27.5	32.5	12.5	13.5	7.15	27.5	27.5	32.5	12.5	13.5	7.15
6	9.5	15.5	6.7	10.0	3.8	11.9	22.5	32.5	10.0	10.0	7.15	22.5	22.5	32.5	10.0	10.0	7.15
7	16.0	22.5	13.7	19.4	7.5	20.0	31.3	47.5	17.5	35.0	7.10	31.3	31.3	47.5	17.5	35.0	7.10
8	22.5	26.0	13.7	15.0	11.3	28.8	40.6	47.1	20.0	20.0	7.20	40.6	40.6	47.1	20.0	20.0	7.20
9	22.5	28.3	14.4	20.0	7.5	21.3	47.5	55.0	21.3	24.0	7.00	47.5	47.5	55.0	21.3	24.0	7.00
10	26.5	29.5	17.5	24.4	12.5	33.8	52.5	58.8	20.6	24.0	6.90	52.5	52.5	58.8	20.6	24.0	6.90
11	26.5	31.0	10.0	16.9	10.0	21.3	49.4	50.0	24.4	26.9	6.80	49.4	49.4	50.0	24.4	26.9	6.80
12	0.9	0.9	11.0	17.5	5.0	15.0	46.9	55.0	20.0	20.0	6.75	46.9	46.9	55.0	20.0	20.0	6.75

Fe Mn Zn Co Ni Pb Cu pH

PIT 8	Fe		Mn		Zn		Co		Ni		Pb		Cu		pH
	Px	Tx	Px	Tx	Px	Tx	Px	Tx	Px	Tx	Px	Tx	Px	Tx	
1	0.55	0.94	221	230	12	20	9	15	14	15	8.0	13.0			6.80
2	0.55	0.90	200	220	15	15	10	14	14	15	7	15			6.60
3	0.54	0.86	174	195	18	18	10	10	15	15	6.5	16.0			6.65
4	0.51	0.88	139	145	16	18	7	11	11	12	6.0	12.0			6.75
5	0.50	0.89	129	145	16	18	7	15	9	14	8.0	15.5			6.75
6	0.51	0.88	139	160	15	18	5	13	15	20	6.0	18.5			6.70
7	0.53	0.89	144	170	17	19	8	16	15	15	4.0	12.0			6.70
8	0.93	0.93	141	160	18	19	7	18	15	20	7.5	15.0			6.75
9	0.89	0.95	130	160	18	20	10	18	15	18	7.0	17.5			6.70
10	0.93	0.95	136	160	18	20	10	13	15	17	9.5	22.0			6.75
11	1.01	1.01	131	145	20	21	11	18	18	20	12.0	19.5			6.75
12	1.00	1.00	100	106	19	19	9	18	12	17	10.5	18.0			6.80
13	0.89	0.90	86	100	17	18	10	18	11	18	9.0	17.0			6.80
14	0.78	0.94	68	100	17	18	7	17	9	18	8.0	16.0			6.80
15	0.70	n.a.	71	n.a.	16	n.a.	7	n.a.	9	18	8.5	n.a.			6.80

163

n.a. = no analysis

PIT 7	Fe		Mn		Zn		Co		Ni		Pb		Cu		pH
	Px	Tx	Px	Tx	Px	Tx	Px	Tx	Px	Tx	Px	Tx	Px	Tx	
1	.28	.29	300	375	22.0	22.0	10.0	10.0	18.0	20.0	13.0	12.0	13.0	13.0	7.75
2	.23	.25	230	260	15.0	15.0	5.0	12.0	15.0	15.0	10.0	8.0	12.0	12.0	7.50
3	.24	.27	190	230	15.0	17.0	9.0	12.0	13.0	18.0	8.5	11.0	16.0	16.0	7.60
4	.28	.35	300	335	18.0	21.0	10.0	14.0	16.0	25.0	14.2	13.0	19.5	19.5	
5	.25	.34	280	400	17.0	20.0	10.0	11.0	15.0	25.0	8.3	12.0	19.0	19.0	8.10
6	.21	.40	250	280	13.0	22.0	8.0	12.5	6.5	12.0	8.2	9.0	10.0	10.0	8.10
7	.24	.38	240	400	17.0	20.0	8.0	10.0	8.0	10.0	11.2	10.0	10.0	10.0	8.10
8	.19	.28	200	360	12.0	16.0	8.0	12.0	8.0	13.5	11.1	9.5	11.0	11.0	8.10
9	.23	.43	270	555	13.0	22.0	10.0	18.0	10.0	15.0	8.9	8.0	8.0	8.0	8.25
10	.42	.87	580	850	20.0	38.0	8.0	20.0	12.0	18.0	11.5	12.0	12.0	12.0	8.25
11	.34	.73	450	950	20.0	40.0	9.0	16.0	8.5	16.5	11.6	13.0	13.0	13.0	8.20
12	.24	.38	315	810	17.0	23.0	9.0	16.0	6.5	12.0	11.9	11.0	13.0	13.0	8.20
13	.20	.32	240	445	16.0	24.0	9.0	12.5	8.5	10.0	9.9	11.0	12.0	12.0	8.30
14	.21	.42	260	820	12.0	23.0	9.0	11.5	8.5	15.0	10.2	8.5	13.0	13.0	8.30
15	.20	.50	260	840	12.0	n.a.	10.0	12.0	13.0	15.0	9.4	11.0	11.0	11.0	8.25

n.a. = no analysis

Fe Mn Zn Co Ni Pb Cu PH

PIT 6	Px	Tx	Px	Tx	Px	Tx	Px	Tx	Px	Tx	Px	Tx	Px	Tx
1	n.a.	0.54	78	91	1.5	3.0	4.5	11.0	n.a.	22.0	4.5	6.5	7.00	
2	0.58	0.58	55	78	3.0	4.5	9.5	11.0	13.0	21.5	6.5	8.5	6.55	
3	0.35	0.46	23	75	4.5	6.5	3.0	8.0	10.5	20.0	4.5	10.5	6.10	
4	0.41	0.41	31	73	4.5	8	4.5	11.0	13.0	19.5	6.5	8.5	6.15	
5	0.39	0.40	33	55	4.5	8.5	4.5	8.0	9.5	22.0	6.5	6.5	6.90	
6	0.49	0.51	36	71	4.5	6.5	4.5	6.5	13.0	13.5	7.0	7.0	6.70	
7	0.40	0.44	31	75	4.5	8	3.0	4.5	7.5	17.0	5.5	8.0	6.80	
8	0.49	0.51	39	78	4.5	8.5	3.0	4.5	12.0	12.0	6.5	6.5	6.85	
9	0.33	0.33	41	71	1.5	4.5	3.0	4.5	8.5	14.5	5.5	7.0	7.50	
10	0.40	0.40	46	71	3.0	3.0	3.0	4.5	5.5	15.5	7.0	7.0	7.10	
11	0.39	0.46	41	86	4.5	6.5	4.5	4.5	4.5	17.5	9.5	9.5	7.05	
12	0.35	0.40	50	75	1.5	3.0	4.5	8.0	4.0	16.5	8.5	8.5	7.00	
PIT 5														
1	1.10	1.10	120	150	5.0	7.0	4.0	5.0	18	20.0	5.5	7.0	7.00	
2	1.20	1.20	120	160	5.0	7.0	4.0	5.0	20	23.0	6.5	7.5	7.30	
3	1.15	1.20	100	120	5.0	7.0	4.0	7.0	21	24.0	6.5	7.5	6.40	

Fe Mn Zn Co Ni Pb Cu PH

PIT 3	Fe		Mn		Zn		Co		Ni		Pb		Cu		PH
	Px	Tx	Px	Tx	Px	Tx	Px	Tx	Px	Tx	Px	Tx	Px	Tx	
1			32.5	35.0	61.0	111.5	18	28.0	12.5	15.0	30.5	43.0	7.35		
2			35.0	47.5	65.0	122.0	27	45.5	21.0	22.0	35.0	40.0	7.05		
3			32.5	42.5	77.5	131.0	34	45.0	16.8	22.8	36.0	60.0	7.70		
4			32.5	50.5	74.5	122.5	27	43.0	24.0	30.4	38.0	62.5	7.45		
5			47.5	50.0	89.0	110.0	37	45.5	25.0	29.1	38.0	62.5	7.50		
PIT 2															
<u>Cr</u>															
1	n.a.	n.a.	n.a.	n.a.	n.a.	n.a.	n.a.	n.a.	n.a.	n.a.	n.a.	n.a.	n.a.	n.a.	n.a.
2	6.10	7.50	1400	1450	35	35	80	95	70.0	92.0	70.0	105.0	7.20		
3	6.76	7.50	n.a.	n.a.	33	55	86	103	90.0	95.0	75.0	118.0	7.10		
4	7.26	7.50	1800	1850	40	60	45	110	98.0	98.0	80.0	130.0	7.05		
5	6.10	6.56	1550	2350	50	70	45	115	132.0	148.0	95.0	120.0	7.15		
6	5.36	6.30	1500	3000	40	45	135	135	126.0	132.0	70.0	90.0	7.50		
7	5.56	6.56	1950	3350	40	50	130	130	138.0	148.0	90.0	105.0	7.65		
8	4.90	6.80	2250	3100	40	70	200	215	188.0	132.0	55.0	85.0	7.90		
9	5.20	6.80	1550	3250	35	70	158	200	266.0	276.0	35.0	35.0	7.70		
10	n.a.	n.a.	1450	2550	50	70	65	85	232.0	292.0	35.0	60.0	7.70		

n.a. = no analysis

Fe Mn Zn Co Ni Pb Cu pH

PIT 1	Fe		Mn		Zn		Co		Ni		Pb		Cu		pH
	Px	Tx	Px	Tx	Px	Tx	Px	Tx	Px	Tx	Px	Tx	Px	Tx	
1	1.96	2.20	465	480	16	36	13.5	14.0	18.0	25.5	33.9	39.1	26	80.0	7.40
2	1.25	2.30	425	480	37	45	9.0	15.5	22.5	36.5	37.6	44.6	45.5	115.0	7.55
3	2.25	4.10	250	495	29	36	13.0	15.5	29.0	34.0	12.0	45.5	34.5	376.0	7.50
4	4.66	4.80	510	510	40	44	14.0	19.0	28.0	38.5	38.1	48.8	42.5	44.5	7.65
5	4.90	5.00	550	550	40	45	14.0	19.0	25.5	38.5	36.8	41.6	27.5	47.5	7.90
6	4.60	5.76	580	580	44	44	11.5	16.0	27.5	36.0	37.7	44.2	43.5	60.0	8.00
7	5.30	5.40	700	735	40	44	13.5	14.0	41.0	49.0	51.7	56.5	44	70	8.00
8	5.80	5.90	780	800	44	48	15.5	16.0	37.5	44.0	50.6	50.6	47.5	75.0	8.05
9	3.60	5.66	750	800	44	45	19.5	21.2	30.5	47.0	44.8	54.1	47.0	68.8	8.10
10	3.80	5.00	960	1040	23	24	18.0	18.0	29.0	36.5	39.6	52.8	37.0	81.2	8.10
11	3.20	5.26	900	905	36	41	17.2	17.2	36.5	39.0	44.7	52.2	37.5	81.5	8.10
12	5.10	5.10	900	928	40	41	15.5	19.5	38.0	43.5	41.3	41.2	37.5	77.5	8.10
13	5.40	6.10	610	625	23	48	16.5	19.0	37.0	43.5	45.9	52.4	50.0	62.5	8.20

Cr

1.	20	38	5.	23	45	9.	25	55	13.	35	70
2.	29	49	6.	34	55	10.	23	85			
3.	26	41	7.	33	61	11.	25	85			
4.	19	39	8.	25	75	12.	30	75			

Fe Mn Zn Co Ni Pb Cu pH

PIT 13	Fe		Mn		Zn		Co		Ni		Pb		Cu		pH
	Px	Tx	Px	Tx	Px	Tx	Px	Tx	Px	Tx	Px	Tx	Px	Tx	
1	0.017	0.140	356	525	22.5	26.3	13.5	8.0	8.0	9.25	13.4	4.0	8.5	6.99	
2	n.a.	n.a.	n.a.	n.a.	n.a.	n.a.	n.a.	n.a.	n.a.	n.a.	n.a.	n.a.	n.a.	7.05	
3	0.150	0.330	331	437	22.5	27.5	11.3	13.0	15.0	12.00	15.3	8.0	8.0	6.95	
4	0.169	0.220	300	463	20.0	33.7	6.5	18.0	18.0	12.50	14.9	8.0	11.0	6.95	
5	0.229	0.250	331	463	33.72	39.7	6.0	26.0	30.5	13.00	15.4	10.0	12.0	7.05	
6	0.253	0.320	331	525	36.26	45.0	17.5	24.3	38.5	8.50	18.8	9.0	25.0	6.90	
7	0.313	0.520	412	938	36.26	75.0	23.8	24.3	60.0	12.00	33.5	10.0	13.5	6.85	
8	0.438	0.440	432	613	33.76	49.0	19.0	23.3	55.0	16.00	25.8	n.a.	20.0	6.90	

168

n.a. = no analysis